DISSERTATION

submitted to the

Combined Faculty of Mathematics, Engineering and Natural Sciences
of Heidelberg University, Germany

for the degree of

Doctor of Natural Sciences

Put forward by

Thede de Boer

born in: Leer, Germany

Oral examination: 09. Juli 2025

Scale invariance and the hierarchy problem: From dynamical symmetry breaking to a pseudo-Goldstone Higgs boson

Referees: Prof. Dr. Dr. h.c. Manfred Lindner
Prof. Dr. Joerg Jaeckel

Abstract

In the Standard Model of particle physics, the masses of fermions and gauge bosons are generated by the Higgs mechanism at the classical level. The Higgs boson is an elementary scalar field and its mass is not protected against quantum correction from new scales thereby giving rise to the hierarchy problem. In this thesis, we explore classical scale invariance as a potential solution to the hierarchy problem. Our main result is the proposal of Custodial Naturalness, which is based on a combination of classical scale invariance and an enhanced custodial symmetry in the scalar sector, imposed at some high scale. Both symmetries are radiatively broken, and dimensional transmutation generates an intermediate scale that spontaneously breaks the enhanced custodial symmetry. The Standard Model Higgs boson arises as a pseudo-Nambu-Goldstone-boson associated with this breaking. We present several models in which Custodial Naturalness is realized. The number of free parameters in the minimal model is the same as in the Standard Model, and extensions can populate the neutrino portal or introduce dark matter candidates. Further, we also discuss outer automorphisms. The transformations of fields under outer automorphisms are not symmetries of the Lagrangian. We show that they can be thought of as symmetries of the beta functions. Further, we explore connections to naturalness and discuss scale transformations as outer automorphisms.

Zusammenfassung

Im Standardmodell der Teilchenphysik werden die Massen von Fermionen und Eichbosonen auf der klassischen Ebene durch den Higgs-Mechanismus erzeugt. Das Higgs-Boson ist ein elementares skalares Feld und seine Masse ist nicht beschützt gegen Quantenkorrekturen von neuen Skalen. Dies führt zu dem Hierarchieproblem. In dieser Arbeit untersuchen wir die klassische Skaleninvarianz als mögliche Lösung für das Hierarchieproblem. Das Hauptergebnis dieser Arbeit ist der Vorschlag von Custodial Naturalness, welcher auf einer Kombination der klassischen Skaleninvarianz und einer Erweiterung der custodialen Symmetrie im skalaren Sektor beruht, welche bei einer hohen Skala realisiert werden. Beide Symmetrien werden durch Quantenkorrekturen gebrochen, und dimensionale Transmutation erzeugt eine Zwischenskala, welche spontan die erweiterte custodiale Symmetrie bricht. Das Higgs-Boson des Standardmodells ist ein Pseudo-Nambu-Goldstone-Boson, welches mit dieser Brechung assoziiert ist. Wir präsentieren mehrere Modelle, in denen Custodial Naturalness realisiert ist. Die Anzahl der freien Parameter im minimalen Modell ist die gleiche wie im Standardmodell während Erweiterungen das Neutrinoportal erzeugen oder Kandidaten für dunkle Materie einführen können. In dieser Arbeit diskutieren wir zudem äußere Automorphismen. Die Transformationen von Feldern unter äußeren Automorphismen sind keine Symmetrien der Lagrangedichte. Wir zeigen, dass diese als Symmetrien der Beta-Funktionen betrachtet werden können. Außerdem untersuchen wir Verbindungen zu Naturalness und diskutieren Skalentransformationen als äußere Automorphismen.

Contents

Chapter 1

Introduction

The Standard Model (SM) of particle physics is remarkably successful in describing the known particles and their interactions. Central for the description of interactions are gauge symmetries. The gauge group of the SM is given by $\mathrm{SU}(3)_c \times \mathrm{SU}(2)_L \times \mathrm{U}(1)_Y$. The electroweak sector is spontaneously broken to electromagnetism as $\mathrm{SU}(2)_L \times \mathrm{U}(1)_Y \to \mathrm{U}(1)_{em}$ by the Higgs mechanism [5–7]. The discovery of the Higgs boson with a mass of 125 GeV confirmed this final piece of the SM [8, 9]. The value of 125 GeV for the Higgs mass allows for the SM to be valid up to the Planck scale fulfilling constraints from triviality [10] and vacuum stability [11–13]. It turns out that the Higgs potential is metastable and the quartic coupling is close to zero at the Planck scale [14–16].

In the SM, the Higgs boson stands out as it is the only elementary scalar field. While gauge bosons are required to be massless due to unitarity and fermion masses are protected by chiral symmetry, the mass terms of elementary scalar fields are not protected by any internal symmetry. If there was a new mass scale Λ, then there would be loop corrections to the Higgs mass $\propto \Lambda^2$. Naively, one expects that the Higgs mass is close to Λ unless there is a very precise cancellation of the different contributions to the Higgs mass. This is known as the hierarchy problem.

The classical action of the SM has only one dimensionful coupling which is the Higgs mass parameter. All other couplings are marginal. It turns out that an action with only dimensionless couplings is scale invariant.[1] In case of the

[1] In this thesis, we often use the terms scale invariance and conformal for classical scale invariance. Occasionally, we also discuss the case where these symmetries hold at the quantum level. It should be clear from context, whether we refer to the symmetry of the classical action or the symmetry that holds at the quantum level.

SM, this scale invariance is explicitly broken by the Higgs mass parameter. In the context of Quantum Field Theory (QFT), there is a second source of explicit breaking of scale invariance given by the scale anomaly. Quantum corrections generate a scale dependence of the couplings which manifests in the non-vanishing beta functions. In Ref. [17], Bardeen argued that, if there is no mass scale other than the electroweak (EW) scale, then the anomalous breaking of scale invariance will not give divergent contributions to the Higgs mass parameter and the SM does not have a hierarchy problem. The hierarchy problem manifests itself when new physics and therefore additional scales are introduced.

A natural step is to consider scenarios where the approximate scale invariance of the SM is promoted to an exact symmetry of the classical action.[2] Coleman and Weinberg showed that in classically scale invariant theories, dimensional transmutation in the weak coupling regime can generate a scale [22]. The simplest incarnation, i.e. the SM without a Higgs mass term, is excluded as it requires a light top quark and a Higgs mass below 10 GeV [22–24]. In models with additional scalar fields, symmetry breaking via the Coleman-Weinberg mechanism can successfully be realized, for example in minimal realizations [25–34], including dark matter (DM) [35–42] and $B - L$ gauge symmetry [43–47]. Left-right symmetric models have been considered in Ref. [48] and the generation of neutrino masses in scale invariant models is realized in Refs. [49–54].

In these scale invariant extensions of the SM, a large separation between the EW scale and the Planck scale is naturally achieved by dimensional transmutation. The classical action has only dimensionless couplings which have a logarithmic dependence on the renormalization scale. Due to this logarithmic running, it typically takes many orders of magnitude for the couplings to reach the critical values where spontaneous symmetry breaking occurs and an intermediate scale is generated. The Higgs doublet obtains a mass term via the scalar portal coupling. Typically, new particles gain masses of order of the intermediate scale and, due to experimental constraints, these new particles are required to be heavy giving rise to the little hierarchy problem.

The little hierarchy problem is often addressed by the idea that the Higgs boson might be a pseudo Nambu Goldstone boson (pNGB) of a spontaneously broken global symmetry. It can be realized for example in composite Higgs models [55–58], little Higgs models [59–64] and twin Higgs models [65–67]. Goldstones theorem [68–70] implies that for any global continuous symmetry which is sponta-

[2]Scale invariance can be imposed as a symmetry of the classical action. It might also originate, for example, via the resurgence mechanism [18–21] in the context of asymptotic safety.

neously broken, there is a massless scalar field. This so called Goldstone boson π has shift symmetry, i.e. the action is invariant under $\pi(x) \to \pi(x) + \theta$ where θ is a constant. Shift symmetry requires that the Goldstone boson has only derivative interactions while mass terms and quartic interactions of the Goldstone boson violate shift symmetry. If the global symmetry is approximate, then we will expect contributions to the mass of the pNGB proportional to the amount of explicit symmetry violation and the scale of spontaneous symmetry breaking. In the SM, shift symmetry of the Higgs boson is badly violated by the top Yukawa interaction and, to a lesser extent, by the electroweak gauge interactions and the scalar quartic term in the potential. Naively, one expects the scale where the approximate global symmetry is spontaneously broken, to be close to the EW scale. Alternatively, there could be a top partner which, together with the SM top quark, forms a multiplet under the global symmetry. Regardless one expects new physics at $\sim 1\,\text{TeV}$.

One of the main results of this thesis is the concept called Custodial Naturalness [1, 2]. This concept combines classical scale invariance with an enhanced custodial symmetry in the scalar sector. The Higgs boson is assumed to be the pNGB associated with the spontaneous breaking of the enhanced custodial symmetry. The Higgs field is a fundamental scalar field and the top Yukawa coupling is a marginal coupling, just as in the SM. By similar reasoning to Bardeen's argument, there are no large contributions to the Higgs mass from the top quark loop. This is in contrast to strongly coupled models where the top Yukawa interaction is generated at the intermediate scale. In models realizing Custodial Naturalness the top Yukawa interaction violates the global symmetry explicitly and no top partner is introduced. However, it can be shown that the contributions to the Higgs mass associated with this explicit symmetry violation are small due to the nature of the top Yukawa coupling as a marginal coupling. Previous work on an elementary Goldstone Higgs boson [71, 72] also finds that a top partner is not necessary.

Custodial Naturalness is based on the combination of conformal and enhanced custodial symmetry. The scalar sector consists of the Higgs doublet and an additional complex scalar field. At some high scale such as the Planck scale, the potential has a SO(6) custodial symmetry and is scale invariant. Both symmetries are radiatively broken and at an intermediate scale the Coleman-Weinberg potential has a non trivial minimum such that SO(6) custodial symmetry is spontaneously broken. The Higgs boson is much lighter than the intermediate scale as it is a pNGB associated with this spontaneous breaking of SO(6) custodial symmetry. The charge assignment and particle content of the minimal realization of Custodial Naturalness are very similar to the conformal version [43, 44] of the minimal $B - L$ model [73–79].

Solutions to the hierarchy problem where the Higgs boson is a pNGB rely on symmetries which are explicitly broken. Explicitly broken symmetries are closely connected to t'Hoofts understanding of naturalness [80] which states that dimensionless parameters will be naturally small if, by setting them to zero, the symmetry of the model is enhanced. This concept of naturalness relies on the behaviour of the beta functions under the symmetry transformations of the explicitly broken symmetry. It turns out that such explicitly broken symmetries are often connected to so called outer automorphisms. Mathematically, outer automorphisms are maps from the symmetry group to itself. We can define how fields transform under outer automorphisms. These transformations are not symmetries but they can be absorbed into the couplings of the theory. Outer automorphisms can play an important role in understanding features of a model. For example they map redundant parts of the parameter space onto each other. Some aspects of outer automorphisms in particle physics have been studied for example in Refs. [81–91]. In this work we show that outer automorphism transformations can be understood as symmetries of the beta functions, i.e. the beta functions transform covariantly. This then implies the underlying argument of t'Hooft naturalness, i.e. the beta function of a small coupling is small if by setting this coupling to zero a symmetry in enhanced. Scale transformations (dilations) are an outer automorphism of the Poincarè group. Due to the scale anomaly, dilations serve as an important example to understand anomalies of outer automorphisms.

This thesis is structured as follows: In Chapter 2 we introduce scale symmetry and discuss the scale anomaly and in Chapter 3 we review die hierarchy problem and various approaches that address the hierarchy problem. The effective potential, which is essential to understand the vacuum structure of scale invariant models, is introduced in Chapter. 4. Chapter 5 discusses the relation of the effective potential to the beta functions and we present calculations that illustrate how a pNGB obtains a mass in scale invariant settings. In Chapter 6 we introduce the concept of Custodial Naturalness. We also discuss different models that realize Custodial Naturalness and the experimental signatures. Chapter 7 introduces outer automorphisms and we discuss the transformation properties of beta functions. We also provide several examples. In Chapter 8 we draw our conclusions.

Chapter 2

Scale invariance and scale anomaly

In this chapter we introduce scale transformations and discuss how fields and the action transform. The Noether current for scale transformations can be expressed in terms of the modified energy momentum tensor. Scale invariance of the classical action does not imply scale invariance at the quantum level. In QFT, scale symmetry is typically anomalous and we discuss the origin and consequences of the anomaly.

2.1 Scale transformations in classical field theory

2.1.1 Scale transformations

Scale transformations (also called dilations) are space-time transformations that act on a space-time point x_μ as

$$x_\mu \to x'_\mu = e^\sigma x_\mu, \tag{2.1}$$

where σ is a real number. The fields transform as

$$\phi(x) \to \phi'(x) = e^{d\sigma}\phi(e^\sigma x), \tag{2.2}$$

where $d = 1$ for bosons and $d = \frac{3}{2}$ for fermions. For infinitesimal σ, we have

$$\phi'(x) = \phi(x) + \sigma(d + x^\nu \partial_\nu)\phi(x). \tag{2.3}$$

The transformation of the action is found by

$$\begin{aligned}S[\phi'] =& \int d^4x\, \mathcal{L}[\phi'(x), \partial_\mu \phi'(x)] \\ =& \int d^4x\, \mathcal{L}[\phi(x), \partial_\mu \phi(x)] + \\ & \qquad + \sigma \left(\frac{\delta \mathcal{L}}{\delta \phi}(d + x^\nu \partial_\nu)\phi(x) + \frac{\delta \mathcal{L}}{\delta\, \partial_\mu \phi}(d + 1 + x^\nu \partial_\nu)\partial_\mu \phi(x) \right) \\ =& S[\phi] + \sigma \int d^4x \left(\partial_\nu \left(x^\nu \mathcal{L}\right) + d\frac{\delta \mathcal{L}}{\delta \phi}\phi(x) + (d+1)\frac{\delta \mathcal{L}}{\delta\, \partial_\mu \phi}\partial_\mu \phi(x) - 4\mathcal{L} \right).\end{aligned} \tag{2.4}$$

The action will be symmetric under dilations if $S[\phi'] = S[\phi]$. This requires that the integrand vanishes up to total derivatives and therefore scale invariance implies

$$d\frac{\delta \mathcal{L}}{\delta \phi}\phi(x) + (d+1)\frac{\delta \mathcal{L}}{\delta\, \partial_\mu \phi}\partial_\mu \phi(x) - 4\mathcal{L} = 0. \tag{2.5}$$

Since d is equal to the mass dimension of the field ϕ, for any dimension four operator the contributions cancel. Thus Eq. (2.5) implies that there are no dimensionful couplings in the Lagrangian.

For a scale invariant action, we find that the Lagrangian transforms as

$$\delta \mathcal{L} = \partial_\nu (x^\nu \mathcal{L}), \tag{2.6}$$

and the Noether current [92] for scale transformations is given by

$$D^\mu(x) = \frac{\delta \mathcal{L}}{\delta(\partial_\mu \phi_a(x))}(d + x^\nu \partial_\nu)\phi_a(x) - x^\mu \mathcal{L}. \tag{2.7}$$

2.1.2 Modified energy momentum tensor

The Noether currents for space-time translations and Lorentz transformations can all be expressed in terms of the energy momentum tensor, which is given by

$$T^\mu{}_\nu = \frac{\delta \mathcal{L}}{\delta \partial_\mu \phi}\partial_\nu \phi - g^\mu{}_\nu \mathcal{L}. \tag{2.8}$$

For example, translation invariance implies

$$\partial_\mu T^\mu{}_\nu = 0. \tag{2.9}$$

Ref. [93] showed that it is possible to define a new energy momentum tensor as

$$\Theta^{\mu\nu} = T^{\mu\nu} + \partial_\lambda \Sigma^{\mu\nu\lambda}, \tag{2.10}$$

where $\Sigma^{\mu\nu\lambda} = -\Sigma^{\lambda\nu\mu}$. One can easily check that, due to translation invariance,

$$\partial_\mu \Theta^{\mu\nu} = 0. \tag{2.11}$$

Ref. [93] showed that this modified energy momentum tensor is connected to the Noether current of scale transformations (see Eq. (2.7)) via

$$D^\mu = x_\nu \Theta^{\mu\nu}, \tag{2.12}$$

and therefore scale invariance implies

$$\partial_\mu D^\mu = \Theta^\mu_{\ \mu} = 0. \tag{2.13}$$

For illustration, consider a real scalar field ϕ with the following Lagrangian

$$\mathcal{L} = \frac{1}{2}\partial_\mu \phi \partial^\mu \phi - \frac{1}{2}m^2\phi^2 - \frac{\lambda}{4!}\phi^4. \tag{2.14}$$

The modified energy momentum tensor is given by [93]

$$\Theta_{\mu\nu} = T_{\mu\nu} - \frac{1}{6}\left(\partial_\mu \partial_\nu - g_{\mu\nu}\Box^2\right)\phi^2, \tag{2.15}$$

and the equations of motion imply that

$$\partial_\mu D^\mu = \Theta^\mu_{\ \mu} = m^2\phi^2, \tag{2.16}$$

which is in line with the observation in Eq. (2.5) that dimensionful couplings violate scale invariance.

2.1.3 Conformal symmetry

Scale invariance is closely related to conformal symmetry. The conformal group is generated by Lorentz transformations, translations, dilations (see Eq. (2.1)) and by the so called special conformal transformations. The latter act in space-time points as

$$x^\mu \to \frac{x^\mu - b^\mu x^2}{1 - 2b\cdot x + b^2x^2} = x^\mu + 2(b\cdot x)x^\mu - b^\mu x^2, \tag{2.17}$$

where we expanded for infinitesimal transformations in the second step. In four space-time dimension, the conformal group is isomorphic to SO(4, 2) and has 15 generators. By definition, conformal invariance implies scale invariance.

Under specific circumstances, the converse is also true. For example, consider a classical field theory in four dimensions, which is Poincarè invariant, and has renormalizable interactions. Then scale invariance implies conformal invariance of the classical action [93–95] (see also Refs. [96, 97]).[1]

In QFT the analogue question is more involved. Whether a theory, which is invariant under dilations even at the quantum level, is also conformally invariant is not conclusively answered. In two space-time dimensions there is a proof that scale invariant QFTs necessarily posses conformal invariance. In four space-time dimensions, there is no such proof. Under certain assumptions (such as unitary and causality) there is a perturbative proof of the enhancement of scale invariance to conformal invariance [97, 99].

2.2 Scale anomaly

Scale invariance of the classical action does not imply scale invariance of the corresponding QFT. Quantum effects generate the running of couplings which violates scale symmetry explicitly. In the path integral formulation of QFT, the anomaly must come from the transformation of the path integral measure since the classical action is assumed to be invariant.

2.2.1 Scale anomaly from path integral measure

Consider the generating functional

$$\begin{aligned} Z[J] &= \int \mathcal{D}\phi \; \exp\left(iS[\phi] + i \int d^4x \, J(x)\phi(x) \right) \\ &= \int \mathcal{D}\phi' \; \exp\left(iS[\phi'] + i \int d^4x \, J(x)\phi'(x) \right), \end{aligned} \tag{2.18}$$

[1] There are examples where scale invariance does not imply conformal invariance of the classical action. For example, the free Maxwell theory in $d \neq 4$ is scale invariant but not conformal invariant [98].

where in the second equality we substitute the integration variable. In order to express the measure $\mathcal{D}\phi'$ in terms of $\mathcal{D}\phi$ we use the Fujikawa trick [100] by writing $\phi = \sum_n a_n \phi_n$ for some orthogonal basis ϕ_n. Then we have

$$\mathcal{D}\phi = \prod_n da_n. \tag{2.19}$$

The transformed measure $\mathcal{D}\phi'$ can be written as

$$\mathcal{D}\phi' = \prod_n da'_n = \prod_n da_n \det(J) = \prod_n da_n \, e^{\mathrm{Tr}\log J} = \mathcal{D}\phi \, e^{\mathrm{Tr}\log J}, \tag{2.20}$$

where $J_{nm} := \frac{\partial a'_n}{\partial a_m}$ is the Jacobian matrix. For an infinitesimal transformation $\phi'(x) = \phi(x) + \delta\phi(x)$, we have

$$a'_n = a_n + \int d^4x \; \delta\phi(x)\phi_n(x), \tag{2.21}$$

and therefore

$$\mathcal{D}\phi' = \prod_n da_n \; \left(1 + \mathrm{Tr}\int d^4x \, \frac{\partial}{\partial a_m}\delta\phi(x)\phi_n(x)\right). \tag{2.22}$$

If we expand Eq. (2.18) for infinitesimal transformations and set the source $J(x) = 0$, we will find

$$0 = \int \mathcal{D}\phi \; \left(\mathrm{Tr}\int d^4x \, \frac{\partial}{\partial a_m}\delta\phi(x)\phi_n(x) + \delta S\right) e^{iS} =: \int \mathcal{D}\phi \; \left(\mathcal{A} + \delta S\right) e^{iS}. \tag{2.23}$$

For the scale transformation $\delta\phi = (d + x^\nu\partial_\nu)\phi$, we have

$$\mathcal{A} = \mathrm{Tr}\int d^4x \, \frac{\partial}{\partial a_m}\delta\phi(x)\phi_n(x) = \mathrm{Tr}\int d^4x \, \phi_n(x)(d + x^\nu\partial_\nu)\phi_m(x). \tag{2.24}$$

We might try to use partial integration and calculate

$$\mathcal{A} = (d-2)\mathrm{Tr}\int d^4x \, \phi_n(x)\phi_m(x) = (d-2)\mathrm{Tr}\,\delta_{nm} = (d-2)\sum_n \delta_{nn}, \tag{2.25}$$

where we used that ϕ_n is an orthogonal basis. This expression diverges and therefore we need to use a regulator.

As an example, we sketch this calculation for the massless ϕ^4 theory (i.e. Eq. (2.14) with $m^2 = 0$) following Ref. [101]. We introduce a regulator function $f\left(\lambda_n^2/M^2\right)$ as

$$\mathcal{A} = \mathrm{Tr}\int d^4x \, \phi_n(x)(1 + x^\nu\partial_\nu) f\left(\lambda_n^2/M^2\right)\phi_m(x), \tag{2.26}$$

where λ_n are the eigenvalues defined by the equation $\left(\partial_\mu \partial^\mu + \frac{\lambda}{2}\phi^2\right)\phi_n = \lambda_n \phi_n$ and

$$f\left(\frac{\lambda_n^2}{M^2}\right) = \frac{1}{1-\left(\frac{\lambda_n}{M}\right)^4}. \tag{2.27}$$

Ref. [101] explicitly calculates the anomaly $\mathcal{A}$ and the result is given by[2]

$$\mathcal{A} = \int d^4x \, \frac{1}{32\pi^2}\left(\frac{\lambda}{2}\phi^2\right) = \int d^4x \, \frac{\beta_\lambda}{4!}\phi^4. \tag{2.28}$$

Therefore the scale anomaly is simply given by the non-vanishing beta function. Eq. (2.23) suggests that

$$\mathcal{A} = -\delta S, \tag{2.29}$$

which justifies the statement that, under scale transformations, the couplings transform as $\lambda \to \lambda - \sigma\beta_\lambda$.

2.2.2 Scale anomaly from loop calculations

We have shown how the scale anomaly can be derived from the transformation of the path integral measure. This is not the only way to see that an anomaly is present. The violation of the symmetry by quantum effects also shows up in the calculation of loop diagrams. The following argument does hold for any anomalous symmetry.

The Feynman rules are obtained from the classical Lagrangian which is invariant under the symmetry. Therefore, in any Feynman diagram, every vertex and every propagator transforms covariantly. Superficially it seems that there is no way that the symmetry is broken. However, in loop diagrams we need to regularize the divergences in order to make predictions. If there is an anomaly present, the regulator will break the symmetry. One needs to be careful since the converse statement is not correct. For example, in QED with cutoff regularization, the cutoff breaks gauge invariance, however gauge invariance is not anomalous.[3] In different regularisation schemes, such as dimensional regularization, gauge invariance is never broken. We should make the more precise statement: If a symmetry is anomalous, then every regulator will break the symmetry.

[2] There are some subtleties in this calculation. There is an infinity which occurs even for the free theory known to be scale invariant. Therefore this infinity needs to be subtracted. There is also the usual quadratic divergence which is canceled by the counterterm. Further ϕ_n are obtained by assuming fluctuations around a saddle point truncated at leading order. The beta function found by this procedure only includes the one-loop contribution.

[3] Gauge symmetries are required to be anomaly free, as otherwise unitarity is violated.

Scale symmetry is anomalous, unless the beta functions vanish, i.e. the theory lives at a fixed point. In cutoff regularization, the cutoff scale Λ breaks scale invariance. In dimensional regularization, the scale μ is introduced to keep the marginal couplings dimensionless. This scale then breaks scale invariance.

At this point we comment on an idea to regularize the divergence without breaking scale invariance [102] (see also [103–107]). Suppose in dimensional regularization, the scale μ is replaced by $\mu^{2\epsilon} \to (\omega^2)^{\epsilon/(1-\epsilon)}$ where ω is a dynamical field with non-zero expectation value. Since ω transforms covariantly under scale transformations, the regularization process does not break scale invariance and there is no scale anomaly. In the broken phase, where we expand around the VEV of ω, this regularization scheme gives very similar results to traditional regularization schemes. However new interactions involving ω are present. In the unbroken phase the theory is non-renormalizable due to the interactions involving $(\omega^2)^{\epsilon/(1-\epsilon)}$ and it is unclear whether this is a well defined theory. It should also be noted that scale invariant renormalization is not simply a new regularization scheme. It does introduce new interactions and therefore the theory is altered compared to other regularization schemes.

Chapter 3

Hierarchy problem

The particle content of the SM includes an elementary scalar field given by the Higgs boson. The masses of scalar fields are sensitive to new scales giving rise to the hierarchy problem [108–112]. In case of a single scale system, the quadratic divergences are an artifact of renormalization and such a system does not have a hierarchy problem. The hierarchy problem manifests if there are two or more mass scales present. In this chapter, we discuss the different aspects of the hierarchy problem and present some popular approaches to address the hierarchy problem.

To some degree, the hierarchy problem is connected to the understanding of renormalization. However, the discussion in this chapter should no be seen as a review of renormalization. We only mention those aspects of renormalization relevant to understanding the hierarchy problem and do not provide any more details on renormalization than necessary.

3.1 Quadratic divergence

Consider a toy model which consists of a single real scalar field ϕ with a Lagrangian given by

$$\mathcal{L} = -\frac{1}{2}\phi\,\Box\,\phi - \frac{m^2}{2}\phi^2 - \frac{\lambda}{4!}\phi^4. \tag{3.1}$$

Now, we consider the two-point functions in order to figure out how the mass term is renormalized. The two-point function is given by the geometric series

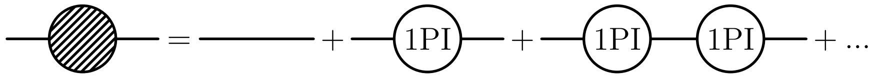

$$= \frac{i}{p^2 - m^2 + \Sigma(p^2)}, \tag{3.2}$$

where Σ is given by the sum of all 1PI graphs, i.e.

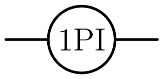

$$= i\Sigma(p^2). \tag{3.3}$$

In the previous equation, we dropped the in- and outgoing propagators. It is important to realize that the mass of ϕ is not simply given by the bare mass m. The parameter m^2 should be thought of as a parameter in the Lagrangian which needs to be fixed by a measurement. Typically a measurement fixes the pole mass m_P of ϕ. The pole of the propagator in Eq. (3.2) is given at

$$\left(p^2 - m^2 + \Sigma(p^2)\right)_{p^2=m_P^2} = 0. \tag{3.4}$$

This condition can be used to fix the mass parameter m^2.[1]

The leading order contribution to Σ is given by

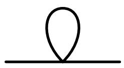

$$= -\frac{i\lambda}{2}\int \frac{d^4k}{(2\pi)^4}\frac{i}{k^2 - m^2}. \tag{3.5}$$

This integral is quadratically divergent. Wick rotating and evaluating the integral over the angular coordinates gives

$$-\frac{i\lambda}{2}\int \frac{d^4k}{(2\pi)^4}\frac{i}{k^2 - m^2} = -\frac{i\lambda}{16\pi^2}\int_0^\infty dk_E \frac{k_E^3}{k_E^2 + m^2}. \tag{3.6}$$

Introducing a cutoff Λ, we find

$$-\frac{i\lambda}{16\pi^2}\int_0^\Lambda dk_E \frac{k_E^3}{k_E^2 + m^2} = -\frac{i\lambda}{32\pi^2}\left(\Lambda^2 + m^2 \ln\left(\frac{m^2}{m^2+\Lambda^2}\right)\right). \tag{3.7}$$

From Eq. (3.4) we find the one-loop result

$$m_P^2 = m^2 - \frac{\lambda}{32\pi^2}\left(\Lambda^2 + m^2 \ln\left(\frac{m^2}{m^2+\Lambda^2}\right)\right). \tag{3.8}$$

Introducing a counterterm $m^2 = m_P^2 + \delta_m$, where δ_m is formally at one-loop order, gives

$$\delta_m = \frac{\lambda}{32\pi^2}\left(\Lambda^2 + m_P^2 \ln\left(\frac{m_P^2}{m_P^2+\Lambda^2}\right)\right). \tag{3.9}$$

[1] There is a second renormalization condition connected to the residue of the pole. We do not discuss this further as in this section we only consider scalar diagrams at one-loop level where the wave function renormalization is trivial.

Sometimes the hierarchy problem is formulated as follows: Why is there an almost exact cancellation between the bare mass term m^2 and Λ^2? This formulation of the hierarchy problem fails to fully capture the essence of the hierarchy problem. The reason is that Λ is just an unphysical regulator introduced, to allow us to deal with the divergence of the loop integral. We can just a well choose a different regularisation scheme. For example in dimensional regularisation we find

$$-\frac{i\lambda}{2}\int\frac{d^4k}{(2\pi)^4}\frac{i}{k^2-m^2}\to-\frac{i\lambda\mu^{4-d}}{2}\int\frac{d^dk}{(2\pi)^d}\frac{i}{k^2-m^2} \\ =\frac{-i\lambda\mu^{4-d}}{2(4\pi)^{d/2}}\left(\frac{1}{m^2}\right)^{1-d/2}\Gamma\left(1-\frac{d}{2}\right), \tag{3.10}$$

where μ is the usual renormalization scale and Γ is the Gamma function, i.e. the analytical continuation of the factorial. Expanding for $d=4-\epsilon$ we find

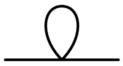

$$=\frac{-i\lambda}{32\pi^2}m^2\left(-\frac{2}{\epsilon}-1+\ln\left(\frac{m^2}{\mu^2 4\pi e^{-\gamma_E}}\right)\right), \tag{3.11}$$

where γ_E is the Euler-Mascheroni constant. Using the on-shell renormalization condition Eq. (3.4) and introducing a counterterm as $m^2=m_P^2+\delta_m$, we find

$$\delta_m=\frac{\lambda}{32\pi^2}m_P^2\left(-\frac{2}{\epsilon}-1+\ln\left(\frac{m_P^2}{\mu^2 4\pi e^{-\gamma_E}}\right)\right). \tag{3.12}$$

In dimensional regularisation, there still is a divergence that is canceled by the counterterm. In four dimensions this divergence is no worse than the divergence for marginal couplings and there is no reason to assume that there is anything wrong with with a small mass term in this toy model.[2]

We have seen that the appearance of the quadratic divergence depends on the renormalization scheme (more precisely the regularization scheme). Should we therefore conclude that the quadratic divergence is unphysical? In QFT, we do not expect any renormalization scheme to be "better" than any other.[3] All physical predictions should be scheme independent. Therefore, we conclude that the quadratic divergence is unphysical. For a discussion of scheme dependence in the Wilsonian approach to renormalization, we refer to Refs. [113, 114].

[2]To be precise, in dimensional regularisation we cannot even say if the mass term is small as there is no other scale, to which we can compare.

[3]It is however conceivable that at some UV scale, QFT is embedded, for example into string theory, in which case the UV completion might determine the "correct" renormalization scheme.

3.2 Scale symmetry and Bardeen argument

We have calculated the loop integral Eq. (3.5) in cutoff regularisation and dimension regularisation. The difference between the two result is even more profound, if we take the limit $m^2 \to 0$. We find

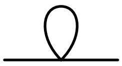

$$= \begin{cases} 0 & \text{in dimensional regularisation,} \\ -\frac{i\lambda}{32\pi^2}\Lambda^2 & \text{in cutoff regularisation.} \end{cases} \tag{3.13}$$

In dimensional regularisation, we can safely set the mass m^2 to zero. It will not be introduced by loop corrections. In cutoff regularisation, for $m^2 = 0$ the counterterm δ_m is still required to cancel the quadratic divergence.

The theory described by the Lagrangian in Eq. (3.1) with $m^2 = 0$ is invariant under scale transformations ($x \to \lambda x$). For non-zero λ this scale symmetry is anomalous, i.e. broken by quantum corrections in form of non-vanishing beta functions (see Chap. 2). Since scale symmetry is anomalous, the regularisation procedure always violates scale invariance. A crucial difference between cutoff regularization and dimensional regularisation lies in the way scale symmetry is broken. In cutoff regularisation the cutoff Λ breaks scale symmetry, and in the limit $\Lambda \to \infty$ scale symmetry violation is maximized. In contrast, in dimensional regularization, the only source of scale symmetry violation is μ^{4-d}. This scale μ only show up in logarithms and μ should not be taken to infinity. Even though dimensional regularisation also explicitly breaks scale symmetry, it does so in a minimal way and m^2 is protected from loop corrections by scale invariance.

The idea that scale symmetry protects the scalar mass term has been proposed in Ref. [17]. This so called Bardeen's argument has originally been formulated for the SM and also holds for any other single scale system such as our toy model Eq. (3.1). In the following we sketch the arguments formulated for the SM Higgs boson.

The Lagrangian of the SM is approximately scale invariant and the Higgs mass term m_H^2 explicitly breaks scale invariance. This explicit symmetry breaking can be seen from Noether current of dilations D^μ. Similar to our discussion in Chap. 2, we have $\partial_\mu D^\mu = 2m_H^2 H^\dagger H$. The Dilation current is related to the modified energy momentum tensor $\Theta^\mu_{\ \nu}$, and we have $\partial_\mu D^\mu = \Theta^\mu_{\ \mu}$. Therefore

$$\Theta^\mu_{\ \mu}\Big|_{\text{classical}} = 2m_H^2 H^\dagger H. \tag{3.14}$$

At one-loop, we have the additional anomalous contributions

$$\Theta^{\mu}_{\ \mu}\Big|_{\text{one-loop}} = 2\Delta m_H^2 H^\dagger H + \sum_i \beta_{\lambda_i} \mathcal{O}_i, \tag{3.15}$$

where $\mathcal{O}_i$ are dimension four operators and β_{λ_i} are the corresponding beta functions. The second term reflects the anomalous breaking of scale symmetry via the running of couplings. The term $2\Delta m_H^2 H^\dagger H$ describes the corrections to the Higgs mass with $\Delta m_H^2 \propto m_H^2$ and not $\propto \Lambda^2$. The quadratic divergences $\propto \Lambda^2$ explicitly violate scale invariance and are not consistent with the Ward identities Eqs. (3.14) and (3.15).

The findings in this section can be summarized in the simple statement: The SM does not have a hierarchy problem. Or more general: Any model with a single mass scale does not have a hierarchy problem.

3.3 Hierarchy problem

The hierarchy problem manifests itself, if there are two physical scales present. In order to see this, we consider a simple toy model consisting of two real scalar fields ϕ and Φ with a Lagrangian given by

$$\mathcal{L} = -\frac{1}{2}\Phi\,\Box\,\Phi - \frac{1}{2}\phi\,\Box\,\phi - \frac{M^2}{2}\Phi^2 - \frac{m^2}{2}\phi^2 - \frac{\lambda_\Phi}{4!}\Phi^4 - \frac{\lambda_p}{4}\Phi^2\phi^2 - \frac{\lambda_\phi}{4!}\phi^4. \tag{3.16}$$

The hierarchy problem occurs, if two physical scale are widely separated, so we assume $m^2 \ll M^2$. We now compute the contribution to the two point function of ϕ with Φ running in the loop. The one-loop contribution to Σ is given by

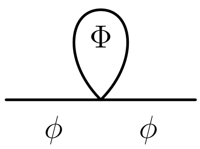

$$= -\frac{i\lambda_p}{2}\int \frac{d^4k}{(2\pi)^4}\frac{i}{k^2 - M^2}$$

$$= \begin{cases} \frac{-i\lambda_p}{32\pi^2} M^2 \left(-\frac{2}{\epsilon} - 1 + \ln\left(\frac{M^2}{\mu^2 4\pi e^{-\gamma_E}}\right)\right) & \text{in dimensional reg.} \\ \frac{-i\lambda_p}{32\pi^2}\left(\Lambda^2 + M^2 \ln\left(\frac{M^2}{M^2+\Lambda^2}\right)\right) & \text{in cutoff reg.} \end{cases} \tag{3.17}$$

For cutoff regularization there is the same quadratic divergence as in the single scalar system. However, in the two scalar system in dimensional regularization, there is also a large correction to m^2 given by $\sim \frac{\lambda_p}{32\pi^2}M^2$. The appearance of these quadratic corrections to the mass of the light scalar is quite generic. For any new physics with a heavy scale $\Lambda_{\rm NP}$ that has interactions with the light scalar ϕ, there are correction to m^2 given by $\Delta m^2 \propto \Lambda_{\rm NP}^2$.[4] The hierarchy problem is then: Why do the different contributions to the mass of the light scalar field cancel very precisely. This is a problem of fine tuning between the bare mass and the loop corrections.

The situation in Eq. (3.16) is qualitative very different to the situation in Eq. (3.1). Scale invariance is badly violated by the large mass term M^2 and therefore the limit $m^2 \to 0$ does not restore scale invariance. There is no symmetry protecting the mass term m^2 from large corrections.

An important insight is that the hierarchy problem does not make a theory inconsistent. Fore example, using the on-shell subtraction scheme, we find with $m^2 = m_P^2 + \delta_m$,

$$\delta_m = \begin{cases} \frac{\lambda_p}{32\pi^2} M^2 \left(-\frac{2}{\epsilon} - 1 + \ln\left(\frac{M^2}{\mu^2 4\pi e^{-\gamma_E}}\right)\right) & \text{in dimensional reg.} \\ \frac{\lambda_p}{32\pi^2} \left(\Lambda^2 + M^2 \ln\left(\frac{M^2}{M^2+\Lambda^2}\right)\right) & \text{in cutoff reg.} \end{cases} \tag{3.18}$$

Nothing is wrong with fixing our bare mass parameter is such a way that the pole mass is small (i.e. $m_P^2 \ll M^2$) as long as we accept the tuning. The hierarchy problem is not observable.[5]

Up to this point we encountered the hierarchy problem as a fine tuning problem where the bare mass and loop corrections to the scalar mass cancel very precisely. Under certain circumstances, the hierarchy problem already occurs at tree level. In the following we present a simple example where tree level contributions to the scalar mass are generated. In this case it is very obvious why there must be a fine tuning and there are no subtleties from the different renormalization schemes.

[4] There is some controversy, whether the quadratic corrections discussed in this section are physical. Refs. [115–118] present a renormalization scheme where the quadratic correction to scalar mass terms from physical scales are absent. If correct, this would imply that these corrections are scheme dependent and therefore unphysical, and there would be no hierarchy problem. There is however no consensus on the validity of this result. For example Ref. [119] claims that divergences are implicitly subtracted and this renormalization scheme is equivalent to the usual procedure.

[5] Ref. [120] claims that the hierarchy problem is unphysical since it is not observable. However, this interpretation does not explain the tuning of the parameters in the Lagrangian.

Consider Eq. (3.16) with a negative mass term for Φ, i.e. $M^2 < 0$. Φ obtains a VEV given by $\langle\Phi\rangle = \sqrt{\frac{-6M^2}{\lambda_\Phi}}$ and expanding around as $\Phi = \langle\Phi\rangle + \hat{\Phi}$ gives for the scalar potential

$$V = -M^2\hat{\Phi}^2 + \frac{1}{2}\left(m^2 - 3\frac{\lambda_p}{\lambda_\Phi}M^2\right)\phi^2 + \text{interaction terms}. \tag{3.19}$$

In order for ϕ to have a small mass term, we require $m^2 - 3\frac{\lambda_p}{\lambda_\Phi}M^2 \ll \frac{-6M^2}{\lambda_\Phi}$. Unless $\lambda_p \ll 1$,[6] there needs to be a very precise cancellation of m^2 and $3\frac{\lambda_p}{\lambda_\Phi}M^2$ which is again a question of fine tuning.

3.4 Solutions to the hierarchy problem

There are a number of different approaches that address the hierarchy problem. In this section, we briefly introduce some of these approaches and sketch how the hierarchy problem is solved. We first discuss approaches that explain why the Higgs boson does not receive quadratic correction from new physics between the EW and the Planck scale. These approaches often come with new physics at the $\mathcal{O}(\text{TeV})$ scale. The increasingly stringent collider bounds push the scale of the new physics higher, which typically gives a new tuning problem of the Higgs mass. This is known as the little hierarchy problem. We first discuss approaches that allow for large scale separations such as the separation of the EW scale and the Planck scale in Sec. 3.4.1. We then discuss approaches to the little Hierarchy problem in Sec. 3.4.2.

3.4.1 Separation of EW and Planck scale

Supersymmetry

Supersymmetry is a classic solution to the hierarchy problem. Space-time symmetry is extended by fermionic operators [123] which transform bosons into fermions and vice versa. For a review of supersymmetry we refer to Ref. [124].

[6] Small values of the portal coupling can be technically natural, if $\lambda_p = 0$ leads to a double Poincaré symmetry [121, 122].

In order to illustrate how supersymmetry addresses the hierarchy problem, we consider a simple supersymmetric Lagrangian, the Wess-Zumino model [125]. The Lagrangian is given by

$$\begin{aligned}\mathcal{L} = & i\bar{\psi}\bar{\sigma}^{\mu}\partial_{\mu}\psi - \frac{m}{2}(\psi\psi + \bar{\psi}\bar{\psi}) + |\partial_{\mu}\phi|^2 - m^2|\phi|^2 \\ & - y(\phi\psi\psi + \text{h.c.}) - ym\left(\phi^2\phi^* + \text{h.c.}\right) - y^2|\phi^4|,\end{aligned} \tag{3.20}$$

where ψ is a Weyl spinor with a Majorana mass term and ϕ is a complex scalar field. y is assumed to be real. We now calculate the one-loop corrections to the Higgs mass term. Ignoring external momenta[7] and evaluating the trace over the gamma matrices, we find

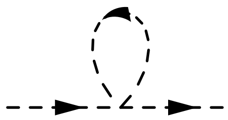

$$= y^2 \int \frac{d^4k}{(2\pi)^4} \frac{1}{k^2 - m^2}, \tag{3.21}$$

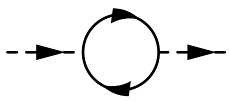

$$= (-1)y^2 \int \frac{d^4k}{(2\pi)^4} \frac{\text{Tr}[\sigma_{\mu}k^{\mu}\bar{\sigma}_{\nu}k^{\nu}]}{[k^2 - m^2]^2} = (-1)y^2 \int \frac{d^4k}{(2\pi)^4} \frac{k^2}{[k^2 - m^2]^2}, \tag{3.22}$$

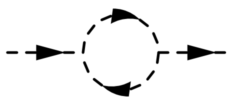

$$= m^2y^2 \int \frac{d^4k}{(2\pi)^4} \frac{1}{[k^2 - m^2]^2}. \tag{3.23}$$

The fermion loop has an additional factor of (-1) due to the different spin-statistics. Summing all three contributions simply gives zero and therefore the mass of ϕ does not receive corrections.

Exact supersymmetry predicts that for every SM field there is a mass degenerate superpartner with the same quantum numbers. None of these superpartner have been observed and supersymmetry needs to be broken. In order for supersymmetry to remain a solution to the hierarchy problem, the supersymmetry breaking scale, cannot be too large. The largest contribution to the Higgs mass stems from the top quark loop which is canceled by the superpartner of the top quark, the stop. With no experimental evidence, the limits on the stop mass require some fine tuning in supersymmetric models. For a review of the current status of fine tuning we refer to Ref. [126].

[7] Momentum dependence is only important for the wave function renormalization.

Dimensional transmutation

EWSB is not the only mechanism of scale generation in the SM. The QCD scale is generated by a mechanism called dimensional transmutation. At the classical level, the QCD Lagrangian is scale invariant. The scale anomaly induces a scale dependence which manifests in the running of couplings. Along the RG flow, the QCD gauge coupling g_3 reaches a critical value at which perturbation theory breaks down. This leads to a formation of quark and gluon condensates and chiral symmetry is spontaneously broken. Large scale separations can occur naturally since the logarithmic running usually spans many orders of magnitude before the critical value is reached.

Technicolor is based on the idea that electroweak symmetry is broken in a similar fashion to QCD [108,111,127–129]. The electroweak gauge group is embedded into a larger group G as a weakly gauged subgroup. "Technifermions" with electroweak charges form a condensate similar to QCD and this condensate breaks electroweak symmetry. Technicolor models suffer from a number of shortcomings. They typically lead to large corrections to EW precision observables [130–133] and it is hard to include fermion masses [130, 131]. Further and maybe most importantly, technicolor models do not explain the presence of the 125 GeV Higgs boson. The idea of EWSB by a strongly coupled sector is revived in composite Higgs models where confinement scale is larger than EW scale and vacuum misalignment breaks the electroweak gauge symmetry. We will discuss composite Higgs models in the next section. For a review on technicolor models, we refer to Ref. [134].

Dimensional transmutation can also occur in the weak coupling regime. In Ref. [22], Coleman and Weinberg showed that in scalar massless electrodynamics, the scalar field obtains a VEV and the scale of spontaneous symmetry breaking is roughly given by the scale where the scalar quartic coupling turns negative. Such classically scale invariant Coleman-Weinberg type models are the main topic of this thesis. The original setup is discussed in more detail in Chap. 4. Chapters 5 and 6 also cover classically scale invariant models.

Extra dimensions

Originally, extra dimensions were introduced in an attempts to unify electromagnetism and gravity [135,136]. In such Kaluza-Klein (KK) models, a 5th space-time dimension, which is compact, is introduced. Fields propagate in all 5 dimensions and excitations in the 5th dimension lead to a tower of 4d particles with masses

$\sim n/R$, where n is an integer number and R is the radius of the extra dimension. The gravitational coupling in five dimensions $M_5 =: M_*$, which is the 5d analogue of the Planck mass, is connected to the 4d Planck mass by

$$M_{\rm Pl}^2 = 2\pi R M_*^3. \tag{3.24}$$

On large distances the extra dimension is inaccessible and in four dimensions we get the usual predictions for gravity. In KK models one typically has $M_* \sim M_{\rm Pl}$ and not much is gained for the hierarchy problem.

Lowering the Planck scale is more successfully realized in models with large extra dimensions. Suppose the SM fields are trapped in a $(3+1)$-dimensional subspace of a higher dimensional space-time [137]. This subspace is usually called the brane. Gravity is assumed to propagate in all d dimension (often said to "'live in the bulk"). The extra dimensions are compact, however their size can be larger than the weak scale [138]. The coupling constant of gravity in d dimensions $M_d =: M_*$ is then the fundamental scale. It is related to the Planck scale by

$$M_{\rm Pl}^2 = M_*^{d-2} V_{d-4} \sim M_*^{d-2} R^{d-4}, \tag{3.25}$$

where V_{d-4} is the volume of the extra dimension and R is the size of the extra dimension. There is no hierarchy problem if $M_* \sim \mathcal{O}(\text{TeV})$. From Eq. (3.25) we find for $M_* \sim \mathcal{O}(\text{TeV})$ that $R \sim 10^{32/(d-4)}\,\text{TeV}^{-1}$, and for $d = 5$, we find $R \sim 10^{15}\,\text{cm}$. At scales smaller than R, the gravitational coupling is modified as gravity propagates in d dimensions rather than four dimensions. The case $d = 5$ is quickly excluded and Cavendish experiments pose constraints on the $d = 6$ case [139]. At first glace, it seems that with $M_* \sim \mathcal{O}(\text{TeV})$ and $d \geq 6$, the hierarchy problem is solved. However, in practice we swapped the hierarchy problem to a problem called radius stabilization. M_* and $1/R$ are vastly different without a good reason.

The Randall-Sundrum model [140] for a warped extra dimension is an interesting possibility to address the hierarchy problem. In this model, we have a 5-dimensional space-time with an anti-de Sitter metric

$$ds^2 = \left(\frac{R}{z}\right)(\eta_{\mu\nu} dx^\mu dx^\nu - dz^2). \tag{3.26}$$

The SM lives in the IR brane localized at $z = R' \gg R$ and the Higgs VEV is warped down from its natural value $v \sim \frac{1}{R}$ to $\frac{vR}{R'} \sim \frac{1}{R'}$. The Planck scale is not warped down and $M_{\rm Pl} \sim \frac{1}{R}$.

Other approaches

In models of cosmological relaxation [141], the quadratic correction to the Higgs mass are not suppressed and the mass parameter of the Higgs boson m_H^2 close to the cutoff. During inflation in the early universe, a new field ϕ will scan many different field values. A portal term $g|H|^2\phi$, with a dimensionful coupling g, induces corrections to the Higgs mass which depend on the field value of ϕ. ϕ naturally settles at a value where m_H^2 and $g\phi$ cancel and the Higgs mass is small.

Historical solutions such as Nnaturalness introduce many copies of the SM [142]. For $N \sim \Lambda^2/m_H^2$ copies, where Λ is the cutoff, we expect that by chance one copy has a light Higgs boson. A difficulty in this approach is that one needs to ensure that reheating only reheats the lightest sector.

A large number ($N \sim 10^{32}$) of new fields might also lower the scale where gravity becomes strong down to $M_* = M_{\rm Pl}/\sqrt{N}$ [143, 144]. This essentially lowers the cutoff down to $\sim$ TeV scales.

There also are anthropic arguments worth pointing out. For example, Ref. [145] argues that the closeness of the QCD scale and the EW scale is required as otherwise baryons are unstable or complex elements would not exist.

3.4.2 Little hierarchy problem

Composite Higgs

Composite Higgs models [55–58] introduce the Higgs boson as a composite scalar field originating from a strongly coupled sector. This can be used to address the issues of technicolor models. The strongly coupled sector generates a scale $f > v_{\rm EW}$ via dimensional transformations which spontaneously breaks a global symmetry of the Lagrangian. In the minimal composite Higgs model, the breaking pattern is given by SO(5) $\to$ SO(4) [146]. The SU(2)$_L$ gauge group is embedded into the SO(4) group and the Higgs boson is a pNGB associated with the breaking SO(5) $\to$ SO(4). Electroweak symmetry is broken by the misalignment mechanism [56, 58], where the direction of the VEV is shifted away from the EW preserving value effectively introducing a VEV for the (composite) Higgs doublet. Generating the Higgs couplings, especially the top Yukawa coupling, inevitably breaks the shift symmetry which protects the Higgs boson from quadratic corrections and typically some tuning is required in these models.

Little Higgs

Similar to composite Higgs models, little Higgs models realize the idea of the Higgs boson as a pNGB of a spontaneously broken global symmetry. The global symmetry is explicitly broken, however only collectively [59–64] which allows for an additional protection of the Higgs mass. Collective symmetry breaking means that the symmetry is explicitly broken only if two or more couplings in the Lagrangian are non-zero. If only only one coupling of these couplings is non-zero, then the Higgs boson is a massless Goldstone boson.

Twin Higgs

Twin Higgs models [65–67, 147–152] assume that there is a copy of the SM. The SM Higgs H and the Higgs boson from the copy H' have a potential that has an approximate SU(4) symmetry. A parity symmetry, i.e. the exchange symmetry of the SM and the copied SM, ensures that the quantum corrections to the scalar mass terms are always symmetric under the global SU(4) symmetry. Corrections to the quartic couplings are not SU(4) symmetric, however these corrections are only logarithmically divergent. The parity (exchange) symmetry is spontaneously broken together with the SU(4) symmetry and the mirror sector obtains a mass. The Higgs field is the pNGB associated with this spontaneous breaking and therefore the Higgs mass is suppressed compared to the parity breaking scale. Due to light new degrees of freedom in the hidden sector, twin Higgs models often suffer from cosmological constraints [153–156].

Chapter 4

Effective Potential

Scale invariant theories are on the boundary between the symmetry preserving and the symmetry breaking phase. Small perturbations in form of loop corrections decide whether the vacuum of the theory breaks the symmetry. The effective potential takes these loop corrections to the potential into account. In this chapter we sketch the derivation of the effective action and the effective potential. We then discuss the Coleman-Weinberg potential which serves as an example of spontaneous symmetry breaking in a scale invariant theory.

4.1 Effective action

We start by introducing the effective action, where we somewhat follow the derivation given in Ref. [157]. Many steps of the derivation are also found in the original Coleman-Weinberg paper [22].

A QFT can be studied using the canonical quantization approach or the path integral formulation. For the derivation of effective potentials the latter is most convenient. The generating functional is defined by

$$Z[J] = \int \mathcal{D}\phi \, e^{iS[\phi]+i\int d^4x\, J(x)\phi(x)}, \tag{4.1}$$

where $S[\phi]$ is the classical action and $\mathcal{D}\phi$ should be understood as integrating over all possible field configurations. This generating functional contains all the information about the QFT. For example time-ordered products are obtained by

$$\langle\Omega|\mathcal{T}\{\phi(x_1)...\phi(x_n)\}|\Omega\rangle = (-i)^n \frac{1}{Z[0]} \left.\frac{\delta^n Z}{\delta J(x_1)...\delta J(x_n)}\right|_{J=0}. \tag{4.2}$$

We can define the functional $W[J] = -i \ln Z[J]$. As a consequence, $W[J]$ generates the connected Feynman diagrams, i.e.

$$\langle\Omega|\mathcal{T}\{\phi(x_1)...\phi(x_n)\}|\Omega\rangle_{\text{connected}} = (-i)^n \left.\frac{\delta^n W[J]}{\delta J(x_1)...\delta J(x_n)}\right|_{J=0}. \tag{4.3}$$

We define the classical field φ_{cl} as the weighted average over all possible field configurations of the field ϕ in the presence of the source J. It is obtained from the generating functional by

$$\varphi_{\text{cl}}(x) = \langle J|\phi(x)|J\rangle = \frac{\delta W[J]}{\delta J(x)}. \tag{4.4}$$

The effective action $\Gamma[\varphi_{\text{cl}}]$ is then defined as the Legendre transform of $W[J]$, explicitly

$$\Gamma[\varphi_{\text{cl}}] = W[J_\varphi] - \int d^4x\, J_\varphi(x)\varphi_{\text{cl}}(x), \tag{4.5}$$

where J_φ is obtained by solving Eq. (4.4) at $J = J_\varphi$.

The effective action is a powerful object. It allows us to find the vacuum configurations and directly gives the one-particle irreducible (1PI) n-point functions by taking derivatives of the effective action. The first derivative of $\Gamma[\varphi_{\text{cl}}]$ is evaluated to

$$\frac{\delta\Gamma[\varphi_{\text{cl}}]}{\delta\varphi_{\text{cl}}(x)} = -J_\varphi(x). \tag{4.6}$$

The field configuration φ_0 is defined by $J_{\varphi_0} = 0$. Thus we simply have

$$\left.\frac{\delta\Gamma[\varphi_{\text{cl}}]}{\delta\varphi_{\text{cl}}(x)}\right|_{\varphi_{\text{cl}}=\varphi_0} = 0. \tag{4.7}$$

This equation is the analogue to the equations of motion in classical field theory, obtained from $\frac{\delta S}{\delta\phi} = 0$. The field φ_0 fulfills the classical equations of motion with the classical action replaced by the effective action. In Eq. (4.4), we defined φ_{cl} as the expectation value in the presences of the source J and therefore φ_0 is the expectation value for ϕ at the true vacuum of the theory.

The second derivative of $\Gamma[\varphi_{\text{cl}}]$ turns out to be the inverse propagator

$$\left.\frac{\delta^2\Gamma[\varphi_{\text{cl}}]}{\delta\varphi_{\text{cl}}(x)\delta\varphi_{\text{cl}}(y)}\right|_{\varphi_{\text{cl}}=\varphi_0} = iG(x,y)^{-1} = i\Big[\langle\Omega|\mathcal{T}\{\phi(x)\phi(y)\}|\Omega\rangle_{\text{connected}}\Big]^{-1}. \tag{4.8}$$

Any higher derivative yields the 1PI n-point function, i.e. for $n \geq 3$ we have

$$\left.\frac{\delta^n\Gamma[\varphi_{\text{cl}}]}{\delta\varphi_{\text{cl}}(x_1)...\delta\varphi_{\text{cl}}(x_n)}\right|_{\varphi_{\text{cl}}=\varphi_0} = -i\langle\Omega|\phi(x_1)...\phi(x_n)|\Omega\rangle_{\text{1PI}}. \tag{4.9}$$

4.2 One-loop approximation

Apart from very simple settings, it is not possible to calculate the effective action exactly. Often one resorts to the so called loop expansion which is equivalent to an expansion in powers of $\hbar$. The zero loop effects are captured at tree level and the one-loop effect are of $\mathcal{O}(\hbar)$. There are several ways of obtaining the one-loop approximation for the effective action. In the following, we sketch an approach based on functional methods. This was originally derived in Ref. [158].

The tree level effects are captured by the stationary-phase evaluation of the generating functional. Eq. (4.1) is dominated by the field configurations $\phi^{(0)}$ that fulfill the classical equations of motion in presence of the source, i.e.

$$\left.\frac{\delta S}{\delta\phi(x)}\right|_{\phi=\phi^{(0)}} = -J(x). \tag{4.10}$$

At leading order, the generating functional is then given by

$$Z[J] \approx \exp\left\{ iS[\phi^{(0)}] + i\int d^4x\, J(x)\phi^{(0)}(x) \right\}, \tag{4.11}$$

and Eq. (4.5) implies

$$\Gamma[\varphi_{\text{cl}}] \approx S[\varphi_{\text{cl}}]. \tag{4.12}$$

The tree level (or zero loop) approximation of the effective action is simply given by the classical action.

Now we include fluctuations around $\phi^{(0)}$ by expanding $\phi = \phi^{(0)} + \hat{\phi}$. The classical action is then expanded as

$$\begin{aligned} S[\phi^{(0)}+\hat{\phi}] =& S[\phi^{(0)}] + \int d^4x \left(\left.\frac{\delta S}{\delta\phi(x)}\right|_{\phi=\phi^{(0)}} \right) \hat{\phi}(x) \\ &+ \int d^4x\, d^4y\, \frac{1}{2}\hat{\phi}(x) \left(\left.\frac{\delta^2 S}{\delta\phi(x)\delta\phi(y)}\right|_{\phi=\phi^{(0)}} \right) \hat{\phi}(y) + \mathcal{O}(\hat{\phi}^3) \\ =& S[\phi^{(0)}] - \int d^4x\, J(x)\hat{\phi}(x) + \int d^4x\, d^4y\, \frac{1}{2}\hat{\phi}(x)\, i\hat{D}^{-1}(x,y)\hat{\phi}(y) + \mathcal{O}(\hat{\phi}^3), \end{aligned} \tag{4.13}$$

where we used Eq. (4.10) in the second equality and defined $\hat{D}^{-1}$ as the inverse propagator (at tree level) in the shifted theory. The truncation at quadratic order implicitly keeps terms up to $\mathcal{O}(\hbar)$ and therefore corresponds to the one-loop expansion [157]. This approximation reduces the path integral to a Gaussian integral which can be evaluated as

$$\begin{aligned}Z[J] &= \exp\left\{iS[\phi^{(0)}] + i\int d^4x\, J(x)\phi^{(0)}(x)\right\}\times \\ &\qquad\times\int \mathcal{D}\phi\, \exp\left\{i\int d^4x\, d^4y\, \frac{1}{2}\hat{\phi}(x)\, i\hat{D}^{-1}(x,y)\hat{\phi}(y)\right\} \\ &= \exp\left\{iS[\phi^{(0)}] + i\int d^4x\, J(x)\phi^{(0)}(x) - \frac{1}{2}\ln\det\left(i\hat{D}^{-1}(x,y)\right)\right\}.\end{aligned} \tag{4.14}$$

The logarithm of this expression gives us $W[J]$. In order to obtain the effective action, we need to perform the Legendre transform. We find

$$\begin{aligned}\Gamma[\varphi_{\rm cl}] &= W[J_\varphi] - \int d^4x\, J_\varphi(x)\varphi_{\rm cl}(x) \\ &= S[\phi^{(0)}] + \int d^4x\, J(x)\left(\phi^{(0)}(x) - \varphi_{\rm cl}(x)\right) + i\frac{1}{2}\ln\det\left(i\hat{D}^{-1}(x,y)\right) \\ &\overset{(4.10)}{=} S[\phi^{(0)}] + \int d^4x\, \left(\left.\frac{\delta S}{\delta\phi(x)}\right|_{\phi=\phi^{(0)}}\right)\left(\varphi_{\rm cl}(x) - \phi^{(0)}(x)\right) + i\frac{1}{2}\ln\det\left(i\hat{D}^{-1}(x,y)\right) \\ &= S[\varphi_{\rm cl}] + i\frac{1}{2}\ln\det\left(i\hat{D}^{-1}(x,y)\right),\end{aligned} \tag{4.15}$$

where in the last equality we used the Taylor expansion

$$S[\varphi_{\rm cl}] = S[\phi^{(0)}] + \int d^4x\, J(x)\left(\phi^{(0)}(x) - \varphi_{\rm cl}(x)\right) + \mathcal{O}(\hbar^2). \tag{4.16}$$

$\hat{D}^{-1}$ is defined as the second functional derivative of the action evaluated at $\phi = \phi^{(0)}$. We might as well evaluate it at $\varphi_{\rm cl}$ since difference in the effective action is of $\mathcal{O}(\hbar^2)$.

To summarize, the one-loop effective action is given by

$$\Gamma[\varphi_{\rm cl}] = S[\varphi_{\rm cl}] + i\frac{1}{2}\ln\det\left(\left.\frac{\delta^2 S}{\delta\phi(x)\delta\phi(y)}\right|_{\phi=\varphi_{\rm cl}}\right). \tag{4.17}$$

For general functions $\varphi_{\rm cl}(x)$, it is not possible to evaluate the functional determinant. If we employ the derivative expansion, we can obtain explicit results. This leads to the definition of the effective potential.

4.3 Effective potential

In this work, we are mainly concerned with the vacuum expectation values (VEVs) of scalar fields which can be obtained by using Eq. (4.7). We will now assume translation invariance for φ_{cl} (or equivalently keep the 0th order of the derivative expansion). From now on, we denote these constant background fields for scalar fields as ϕ_b. Then we define the effective potential as

$$\Gamma[\phi_b] =: -\int d^4x\, V_{\text{eff}}[\phi_b]. \tag{4.18}$$

The condition for the true vacuum value $\langle\phi\rangle$ of the background field ϕ_b follows from Eq. (4.7) and is given by

$$\left.\frac{\delta V_{\text{eff}}[\phi_b]}{\delta \phi_b}\right|_{\phi_b=\langle\phi\rangle} = 0. \tag{4.19}$$

With the assumption of constant background fields, we can now explicitly calculate the one-loop contributions to the effective potential.

Consider the case where ϕ is a real scalar field. Then the inverse propagator is given by

$$i\hat{D}^{-1} = -\Box - m_{\text{eff}}^2(\phi_b), \tag{4.20}$$

where $m_{\text{eff}}^2 = \frac{\delta^2 V_{\text{tree}}}{\delta\phi^2}\Big|_{\phi=\phi_b}$ for the tree level potential V_{tree}. In order to evaluate the functional determinant we write

$$\begin{aligned}
\ln\det\left(i\hat{D}^{-1}\right) =& \operatorname{Tr}\ln\left(i\hat{D}^{-1}\right) = \int d^4x \langle x|\ln\left(-\Box - m_{\text{eff}}^2(\phi_b)\right)|x\rangle \\
=& \int d^4x \int \frac{d^4k}{(2\pi)^4}\frac{d^4k'}{(2\pi)^4}\langle x|k\rangle\langle k|\ln\left(-\Box - m_{\text{eff}}^2(\phi_b)\right)|k'\rangle\langle k'|x\rangle \\
=& \int d^4x \int \frac{d^4k}{(2\pi)^4}\ln\left(k^2 - m_{\text{eff}}^2(\phi_b)\right) \\
=& \int d^4x \int \frac{d^4k}{(2\pi)^4}\ln\left(-k^2 + m_{\text{eff}}^2(\phi_b)\right) + i\text{ const.}
\end{aligned} \tag{4.21}$$

The constant, which originates from the minus sign in the logarithm, is field independent and can be dropped. Now the momentum integral can be evaluated, for example, in dimensional regularization. This is done using a trick, where we Wick rotate and then introduce a dummy variable α [159]. We find

$$\begin{aligned}
\mu^{4-d}\int\frac{d^dk}{(2\pi)^d}\ln\left(-k^2+m_{\text{eff}}^2(\phi_b)\right) &= i\mu^{4-d}\int\frac{d^dk_E}{(2\pi)^d}\ln\left(k_E^2+m_{\text{eff}}^2(\phi_b)\right)\\
&= -i\mu^{4-d}\frac{\partial}{\partial\alpha}\int\frac{d^dk_E}{(2\pi)^d}\frac{1}{\left(k_E^2+m_{\text{eff}}^2(\phi_b)\right)^\alpha}\Bigg|_{\alpha=0}\\
&= -i\mu^{4-d}\frac{\partial}{\partial\alpha}\left(\frac{1}{(4\pi)^{d/2}}\frac{\Gamma\left(\alpha-\frac{d}{2}\right)}{\Gamma(\alpha)}\frac{1}{\left(m_{\text{eff}}^2(\phi_b)\right)^{\alpha-d/2}}\right)\Bigg|_{\alpha=0}\\
&= -i\mu^{4-d}\frac{\Gamma\left(-\frac{d}{2}\right)}{(4\pi)^{d/2}}\left(m_{\text{eff}}^2(\phi_b)\right)^{d/2},
\end{aligned} \tag{4.22}$$

where μ is the usual RG scale. In the last equality we used that $\Gamma(\alpha)\to 1/\alpha$ as $\alpha\to 0$ following Ref. [159]. Expanding around the standard 4-dimensional space-time $d=4-\epsilon$ gives

$$-i\mu^{4-d}\frac{\Gamma\left(-\frac{d}{2}\right)}{(4\pi)^{d/2}}\left(m_{\text{eff}}^2(\phi_b)\right)^{d/2} = -i\frac{m_{\text{eff}}^4(\phi_b)}{32\pi^2}\left[\frac{2}{\epsilon}+\ln\left(\frac{4\pi e^{-\gamma_E}\mu^2}{m_{\text{eff}}^2(\phi_b)}\right)+\frac{3}{2}\right]. \tag{4.23}$$

Combining this result with Eqs. (4.15) and (4.18) and absorbing the appropriate $\overline{\text{MS}}$ counterterms gives

$$V_{\text{eff}}[\phi_b] = V_{\text{tree}}[\phi_b]+\frac{m_{\text{eff}}^4(\phi_b)}{64\pi^2}\left[\ln\left(\frac{m_{\text{eff}}^2(\phi_b)}{\mu^2}\right)-\frac{3}{2}\right]. \tag{4.24}$$

The first term is the tree level potential V_{tree} which comes from the classical action and the second term is the one-loop contribution to the effective potential.

Next we consider how fermion loops contribute to the effective potential. We assume that only scalar fields obtain a non zero expectation value. In the expansion of the action as in Eq. (4.14) there will be an additional term given by

$$\int d^4x\, d^4y\, \bar\psi(x)\left(\frac{\delta^2 S}{\delta\bar\psi(x)\psi(y)}\Bigg|_{\phi=\phi_b,\psi=0}\right)\psi(y) =: \int d^4x\, d^4y\, \bar\psi(x)\left(i\hat{D}^{-1}\right)\psi(y). \tag{4.25}$$

For fermions the Gaussian path integral is evaluated (analogously to Eq. (4.14)) as

$$\int\mathcal{D}\bar\psi\mathcal{D}\psi\,\exp\left\{i\int d^4x\, d^4y\,\bar\psi(x)\, i\hat{D}^{-1}(x,y)\psi(y)\right\} = \exp\left\{\ln\det\left(i\hat{D}^{-1}(x,y)\right)\right\}. \tag{4.26}$$

Note the relative minus sign compared to the contribution from scalar fields. For Dirac fermions the inverse propagator can be written as

$$i\hat{D}^{-1} = -(i\partial\!\!\!/ - m_{\text{eff}}), \tag{4.27}$$

and, assuming real effective masses, the contribution to Eq. (4.15) is given

$$\begin{aligned} i \ln\det\left[-(i\partial\!\!\!/ - m_{\text{eff}})\right] =& i\ln\sqrt{\det\left[-\left(i\partial\!\!\!/ - m_{\text{eff}}\right)\left(i\partial\!\!\!/ - m_{\text{eff}}\right)\right]} \\ =& i\ln\sqrt{\det\left[-\left(-i\partial\!\!\!/ - m_{\text{eff}}\right)\left(i\partial\!\!\!/ - m_{\text{eff}}\right)\right]} \\ =& i\frac{1}{2}\ln\det\left[-\Box - m_{\text{eff}}^2\right], \end{aligned} \tag{4.28}$$

where we used that $i\partial\!\!\!/ - m_{\text{eff}}$ has the same eigenvalues as $-i\partial\!\!\!/ - m_{\text{eff}}$ in the second equality. The determinant can then be evaluated similarly to the scalar field case. The only difference is that there are still spinor indices and the trace will give an additional total factor of 4. For Weyl fermions this factor would be 2. The contribution to the effective potential is then given by

$$V_{\text{eff}}[\phi_b]\Big|_{\text{Dirac fermion}} = -4\frac{m_{\text{eff}}^4(\phi_b)}{64\pi^2}\left[\ln\left(\frac{m_{\text{eff}}^2(\phi_b)}{\mu^2}\right) - \frac{3}{2}\right]. \tag{4.29}$$

Gauge boson contributions are simplest calculated in Landau gauge. After applying the condition $\partial_\mu A^\mu = 0$, the additional term in Eq. (4.14) is given by

$$\begin{aligned} &\int d^4x\, d^4y\, A^\mu(x)\left(\frac{\delta^2 S}{\delta A^\mu(x) A^\nu(y)}\Big|_{\phi=\phi_b, A^\mu=0}\right) A^\mu(y) \\ &\qquad =: \int d^4x\, d^4y\, A^\nu(x)\left(i\hat{D}^{-1}_{\mu\nu}\right) A^\mu\psi(y). \end{aligned} \tag{4.30}$$

The inverse propagator is given by

$$\left(i\hat{D}^{-1}\right)^{\mu\nu} = g^{\mu\nu}(\Box + m_{\text{eff}}^2) - \partial^\mu\partial^\nu. \tag{4.31}$$

Using the Weinstein–Aronszajn identity (Sylvester's determinant theorem)

$$\det\left(\lambda I_n + AB\right) = \lambda^{n-1}\left(\lambda + BA\right), \tag{4.32}$$

where λ is a number, A and B are $n \times 1$ and $1 \times n$ matrices respectively and I_n is the $n \times n$ identity matrix, we evaluate the determinant over the Lorentz indices $\det_{\mu\nu}$ and obtain in d dimensions

$$\det_{\mu\nu}\left(i\hat{D}^{-1}\right)^{\mu\nu} = \det_{\mu\nu}\left(g^{\mu\nu}(\Box + m_{\text{eff}}^2) - \partial^\mu\partial^\nu\right) = -m_{\text{eff}}^2\left(\Box + m_{\text{eff}}^2\right)^{d-1}. \tag{4.33}$$

The contribution to Eq. (4.14) is then

$$i \ln \det \left(-m_{\text{eff}}^2 \left(\Box + m_{\text{eff}}^2 \right)^{d-1} \right) = i \operatorname{Tr} \ln \left(-m_{\text{eff}}^2 \left(\Box + m_{\text{eff}}^2 \right)^{d-1} \right), \tag{4.34}$$

where the determinant and trace do not run over the Lorentz indices. Using the same steps as in Eq. (4.21)

$$i \operatorname{Tr} \ln \left(-m_{\text{eff}}^2 \left(\Box + m_{\text{eff}}^2 \right)^{d-1} \right) = \int d^4x \int \frac{d^4k}{(2\pi)^4} \ln \left(m_{\text{eff}}^2 (-k^2 + m_{\text{eff}}^2)^{d-1} \right) + i \text{ const.} \tag{4.35}$$

and the momentum integral is evaluated similarly to Eq. (4.22) as

$$\begin{aligned}
\mu^{4-d} \int \frac{d^dk}{(2\pi)^d} \ln \left(m_{\text{eff}}^2 (-k^2 + m_{\text{eff}}^2)^{d-1} \right) &= i\mu^{4-d} \int \frac{d^dk_E}{(2\pi)^d} \ln \left(m_{\text{eff}}^2 (k_E^2 + m_{\text{eff}}^2)^{d-1} \right) \\
&= -\, i\mu^{4-d} \frac{\partial}{\partial \alpha} \int \frac{d^dk_E}{(2\pi)^d} \frac{1}{(m_{\text{eff}}^2 (k_E^2 + m_{\text{eff}}^2)^{d-1})^{\alpha}} \Bigg|_{\alpha=0} \\
&= -\, i\mu^{4-d} \frac{\partial}{\partial \alpha} \left(\frac{1}{(4\pi)^{d/2}} \frac{\Gamma\left((d-1)\alpha - \frac{d}{2} \right)}{\Gamma((d-1)\alpha)} \frac{1}{(m_{\text{eff}}^2)^{(d-1)\alpha - d/2 + \alpha}} \right) \Bigg|_{\alpha=0} \\
&= -\, i\mu^{4-d} (d-1) \frac{\Gamma\left(-\frac{d}{2} \right)}{(4\pi)^{d/2}} \left(m_{\text{eff}}^2 \right)^{d/2}.
\end{aligned} \tag{4.36}$$

Expanding for $d = 4 - \epsilon$ gives

$$-i\mu^{4-d} (d-1) \frac{\Gamma\left(-\frac{d}{2} \right)}{(4\pi)^{d/2}} \left(m_{\text{eff}}^2 \right)^{d/2} = -i\, 3 \frac{m_{\text{eff}}^4}{32\pi^2} \left[\frac{2}{\epsilon} + \ln \left(\frac{4\pi e^{-\gamma_E} \mu^2}{m_{\text{eff}}^2} \right) + \frac{5}{6} \right]. \tag{4.37}$$

Again combining this result with Eqs. (4.15) and (4.18) and absorbing the appropriate $\overline{\text{MS}}$ terms gives the gauge boson contribution to the effective potential

$$V_{\text{eff}}[\phi_b] \Big|_{\text{gauge}} = 3 \frac{m_{\text{eff}}^4(\phi_b)}{64\pi^2} \left[\ln \left(\frac{m_{\text{eff}}^2(\phi_b)}{\mu^2} \right) - \frac{5}{6} \right]. \tag{4.38}$$

The contributions to the one-loop effective potential and generalized to multiple fields scalar background fields, described as a vector $\vec{\phi}_b$, can be summarized as

$$V_{\text{eff}} \left[\vec{\phi}_b \right] = V_{\text{tree}} \left[\vec{\phi}_b \right] + \sum_i \frac{n_i (-1)^{2s_i}}{64\pi^2} m_{\text{eff}}^4 \left(\vec{\phi}_b \right) \left[\ln \left(\frac{m_{\text{eff}}^2 \left(\vec{\phi}_b \right)}{\mu^2} \right) - C_i \right] \tag{4.39}$$

where the sum runs over all effective masses. $C_i = \frac{5}{6} (\frac{3}{2})$ for vector bosons (scalars and fermions), $(-1)^{2s_i} = {}_{(-)}^{+}1$ for bosons (fermions) and n_i is the number of degrees of freedom. The number of degrees of freedom are found by multiplying the internal degrees of freedom with the space-time degrees of freedom which are given by

$$n_i\Big|_{\text{space-time}} = \begin{cases} 1 & \text{real scalar fields} \\ 2 & \text{complex scalar fields} \\ 2 & \text{Weyl fermions} \\ 4 & \text{Dirac fermions} \\ 3 & \text{gauge bosons} \end{cases} . \tag{4.40}$$

The effective masses are given by

$$\left(m^2_{\text{eff}}\right)_{ab} = \frac{\delta^2 S}{\delta\phi_a \delta\phi_b}\bigg|_{\vec{\phi}=\vec{\phi}_b, A^\mu=0, \psi=0} \qquad \text{for real scalar fields,} \tag{4.41}$$

$$\left(m^2_{\text{eff}}\right)_{ab} = \frac{\delta^2 S}{\delta A^\mu_a \delta A_{b,\mu}}\bigg|_{\vec{\phi}=\vec{\phi}_b, A^\mu=0, \psi=0} \qquad \text{for vector bosons,} \tag{4.42}$$

$$\left(m_{\text{eff}}\right)_{ab} = \frac{\delta^2 S}{\delta\bar{\psi}_a \delta\psi_b}\bigg|_{\vec{\phi}=\vec{\phi}_b, A^\mu=0, \psi=0} \qquad \text{for fermions.} \tag{4.43}$$

The effective masses are, in general, matrices and in Eq. (4.39) the eigenvalues should be used. Alternatively one can use the full matrices, in which case the logarithm should be interpreted as the matrix logarithm (i.e. the inverse function of the matrix exponential).

It turns out that the effective potential depends on the choice of gauge [158]. In our previous calculation, we worked in Landau gauge and a different gauge would lead to a different effective potential. This gauge dependence is in principle unproblematic as the effective potential itself is not directly observable. Crucially the minimum of the effective potential is gauge independent. In this thesis we will always use Landau gauge and for a discussion of the subtleties of the gauge dependence of the effective potential, we refer to Ref. [160].

The effective potential is defined by a Legendre transform of the generating functional. Therefore we expect the effective potential to be convex. However, in many examples calculated from Eq. (4.39) it is not [161–163]. The issue of non-convex potential is related to the issue of imaginary parts in the effective potential. For example, if we have an effective mass given by $m^2_{\text{eff}} = -m^2 + 3\lambda\phi_b^2$, for $\phi_b^2 \ll m^2$ the argument of the logarithm is negative and the effective potential is complex. A discussion of this issue is beyond the scope of this thesis and we refer to Refs. [13, 164]. For the practical purpose of determining the VEVs, one should use the absolute value of the effective potential.

4.4 Massless scalar electrodynamics

In their original work [22], Coleman and Weinberg discuss the massless ϕ^4 model, and also massless scalar electrodynamics. For the first model, the potential simply has a minimum at $\phi_b = 0$ and no spontaneous symmetry breaking occurs. Massless scalar electrodynamics turns out to be more interesting.

Consider a single scalar field ϕ and a gauged U(1) symmetry under which the scalar field has charge $Q_\phi = 1$. The potential can be written as[1]

$$V_{\text{tree}} = \lambda|\phi|^4. \tag{4.44}$$

At one-loop, the beta function for λ is given by

$$\beta_\lambda = \frac{1}{16\pi^2}\left(6g^4 + 20\lambda^2 - 12g^2\lambda\right), \tag{4.45}$$

where g is the U(1) gauge coupling. For $g \neq 0$, this beta function is strictly positive. Therefore λ will turn negative along the RG flow towards the IR for any positive (perturbative) initial value for λ. Negative values for λ are problematic as the tree level potential becomes unbounded. Coleman and Weinberg showed that massless scalar electrodynamics is not ill-defined and this apparent instability is naturally evaded. This can be easily seen by considering the effective potential. We choose the RG scale μ close to the scale where the tree level potential turns unstable and therefore $\lambda \ll 1$. We can use global U(1) transformations to ensure that the background field ϕ_b is real. The effective potential, where we only include gauge boson loops[2], follows from Eq. (4.39) and is given by

$$V_{\text{eff}} = \lambda\phi_b^4 + \frac{3}{64\pi^2}(2g^2\phi_b^2)^2\left[\ln\left(\frac{2g^2\phi_b^2}{\mu^2}\right) - \frac{5}{6}\right], \tag{4.46}$$

which has a minimum at $\phi_b = \langle\phi\rangle$ with

$$\ln\left(\frac{\langle\phi\rangle^2}{\mu^2}\right) = -\frac{16\pi^2\lambda}{3g^4} - \ln\left(2g^2\right) + \frac{1}{3}. \tag{4.47}$$

Massless scalar electrodynamics does not have a vacuum instability. The true minimum of the scalar potential is not at the origin and electrodynamics is spontaneously broken. Expanding around the minimum yields the mass for the vector boson

$$m_V^2 = 2g^2\langle\phi\rangle^2. \tag{4.48}$$

[1] We use a different normalization of fields and couplings compared to Ref. [22].

[2] Scalar loops come with λ^2 and can be neglected.

The field corresponding to the radial excitation of the scalar field is often called dilaton and its mass is given by

$$m_S^2 = \frac{3g^4\langle\phi\rangle^2}{4\pi^2} \approx \frac{\beta_\lambda}{2}\langle\phi\rangle^2. \tag{4.49}$$

The dilaton mass is suppressed with respect to the symmetry breaking VEV $\langle\phi\rangle$ by the beta function β_λ. This can be understood by the observation that scale symmetry is spontaneously broken and the dilaton is the Goldstone boson associated with this breaking. Since scale symmetry is also explicitly broken by the anomaly i.e. the beta functions, the dilaton mass is proportional to this explicit breaking.

The Coleman-Weinberg mechanism is an example of dimensional transmutation in the weak coupling regime. Initially the Lagrangian has no explicit scale and due to the running of couplings, λ reaches a critical value and ϕ obtains a VEV, generating a scale. This happens for small values of the couplings and which allows us to use perturbation theory methods.

4.5 Gildener Weinberg approximation

In the previous section we discussed scalar electrodynamics, where we could solve the minimum equation of the single scalar field analytically. In case of multiple scalar fields this is in general not possible. Gildener and Weinberg proposed a widely used approximation scheme for the multi scalar case [24, 165]. This approximation estimates the alignment of the VEV from the tree level potential. We present the general procedure following Ref. [24] and then give an example calculation in a case with two scalar fields.

Any scale invariant tree level potential can be written as

$$V_{\text{tree}} = \sum_{ijkl} \frac{f_{ijkl}}{24}\Phi_i\Phi_j\Phi_k\Phi_l, \tag{4.50}$$

where Φ_i denotes the components of the scalar fields written in terms of real fields. The indices i, j, k, l run over all real scalar degrees of freedom. The scalar couplings are defined as

$$f_{ijkl} = \frac{\partial^4}{\partial\Phi_i\partial\Phi_j\partial\Phi_k\partial\Phi_l}V_{\text{tree}}, \tag{4.51}$$

which guarantees that f_{ijkl} is symmetric under exchange of two indices. Assuming $1 \gg f_{ijkl} \gg g^4$, where g denotes other couplings in the model, the potential is dominated by the tree level contributions. This also requires all scalar couplings to be positive which guarantees that the minimum of the tree level potential is at the origin. Now we assume that along the RG flow, the tree level potential develops a flat direction. We denote the scale where this happens as $\mu_{\rm GW}$. This condition can be written as

$$\min_{N_i N_i=1}\left(f_{ijkl}N_iN_jN_kN_l\right)=0 \qquad \text{at } \mu=\mu_{\rm GW}, \tag{4.52}$$

where N_i is a unit vector. Calling the solution to this equation $N_i = n_i$, then the flat direction is along the ray $\Phi_i = n_i\phi$, where ϕ is the distance from the origin. In order to find n_i, we need to solve

$$f_{ijkl}n_in_jn_kn_l=0, \qquad f_{ijkl}n_jn_kn_l=0, \qquad f_{ijkl}u_iu_jn_kn_l\geq 0, \tag{4.53}$$

for any vector u_i. This procedure gives a tree level estimate for the direction of the VEV. In order to determine the distance from the origin ϕ, one needs to find the minimum of the effective potential along the ray $\Phi_i = n_i\phi$, i.e. solve

$$\frac{\partial}{\partial\phi}V_{\rm eff}\left(n_i\phi\right)=0. \tag{4.54}$$

As an example, consider a model with two scalar fields H and Φ[3] and a tree level potential given by

$$V_{\rm tree}=\lambda_H|H|^4+2\lambda_p|H|^2|\Phi|^2+\lambda_\Phi|\Phi|^4. \tag{4.55}$$

Solving Eq. (4.53), we find the following solutions

$$\Phi=\phi, \qquad H=0, \qquad \lambda_\Phi=0, \qquad \lambda_p\geq 0, \tag{4.56}$$

$$\Phi=0, \qquad H=\phi, \qquad \lambda_H=0, \qquad \lambda_p\geq 0, \tag{4.57}$$

$$\Phi=\sqrt{\frac{\lambda_H}{\lambda_H-\lambda_p}}\phi, \qquad H=\sqrt{\frac{-\lambda_p}{\lambda_H-\lambda_p}}\phi, \qquad \lambda_\Phi=\frac{\lambda_p^2}{\lambda_H}, \qquad \lambda_p\leq 0. \tag{4.58}$$

The conditions on the couplings, i.e. $\lambda_\Phi = 0$, $\lambda_H = 0$ or $\lambda_\Phi = \lambda_p^2/\lambda_H$ are not fine tuning. There exists a RG scale where one of these conditions is true [13]. Along the flat direction, loop corrections generate a non-trivial minimum.

[3] Φ should not be confused with Φ_i.

4.6 Renormalization group equation for the effective potential

The effective action is independent of the choice of the artificial RG scale μ. This can be expressed as [22]

$$\mu\frac{d}{d\mu}\Gamma[\varphi_{\rm cl}] = \left[\mu\frac{\partial}{\partial\mu} + \sum_i \beta_{\lambda_i}\frac{\partial}{\partial\lambda_i} + \sum_a \gamma_a \int d^4x\, \varphi^a_{\rm cl}(x)\frac{\delta}{\delta\varphi^a_{\rm cl}(x)}\right]\Gamma[\varphi_{\rm cl}] = 0, \tag{4.59}$$

where β_{λ_i} is the beta function for the generic coupling λ_i defined as

$$\beta_{\lambda_i} = \mu\frac{\partial\lambda_i}{\partial\mu}, \tag{4.60}$$

and γ_a is the anomalous dimension for the field $\varphi^a_{\rm cl}$ given by

$$\gamma_a\varphi^a_{\rm cl} = \mu\frac{\partial\varphi^a_{\rm cl}}{\partial\mu}. \tag{4.61}$$

With the definition of the effective potential Eq. (4.18), we find

$$\mu\frac{d}{d\mu}V_{\rm eff}[\phi_b] = \left[\mu\frac{\partial}{\partial\mu} + \sum_i \beta_{\lambda_i}\frac{\partial}{\partial\lambda_i} + \sum_a \gamma_a\phi^a_b\frac{\partial}{\partial\phi^a_b}\right]V_{\rm eff}[\varphi_{\rm cl}] = 0. \tag{4.62}$$

A solution to Eq. (4.62) is called the RG improved effective potential. However finding such a solution is difficult and not always possible. For practical application one typically chooses the RG scale μ close to the physical scales and then one can safely use the effective potential in the fixed order loop expansion. If there are two or more physical scales, the situation is more involved. A number of approaches have been suggested, for example in Refs. [166–174].

Chapter 5

Effective potential and RGEs

The effective potential obeys the Callan-Symanzik equation Eq. (4.62). In very simple cases this equation can be integrated and the effective potential can be written in term of the beta functions. In this Chapter, we review how this can be done in the case of a single massless scalar field. We then discuss how the effective potential of two massless scalar fields is connected to the beta functions and investigate how the mass of a pNGB is generated in such a setting. We restrict ourselves to the one-loop effective potential.

We start by expanding the effective potential formally in terms of $\hbar$ which is equivalent to the loop expansion. Up to $\mathcal{O}(\hbar)$ we write[1]

$$V_{\text{eff}}[\phi_b] = V_{\text{tree}}[\phi_b] + V_1[\phi_b], \tag{5.1}$$

with the tree level potential V_{tree} and the one-loop contribution (see Eq. (4.39))

$$V_1 = \sum_i \frac{(-1)^{2s_i} n_i}{64\pi^2} m^4_{\text{eff},i} \left(\ln\left(\frac{m^2_{\text{eff},i}}{\mu^2}\right) - C_i \right). \tag{5.2}$$

Now we apply the renormalization group equation of the effective potential Eq. (4.62). Equating terms of $\mathcal{O}(\hbar)$ yields [13]

$$\left(\sum_i \beta_{\lambda_i} \frac{\partial}{\partial \lambda_i} + \sum_a \gamma_a \phi^a_b \frac{\partial}{\partial \phi^a_b} \right) V_{\text{tree}}[\phi_b] = -\mu \frac{\partial}{\partial \mu} V_1[\phi_b]. \tag{5.3}$$

One immediate use of this equation is that it gives a way to calculate the one-loop beta functions. Combining Eqs. (5.2) and (5.3) yields

$$\left(\sum_i \beta_{\lambda_i} \frac{\partial}{\partial \lambda_i} + \sum_a \gamma_a \phi^a_b \frac{\partial}{\partial \phi^a_b} \right) V_{\text{tree}}[\phi_b] = 2 \sum_i \frac{(-1)^{2s_i} n_i}{64\pi^2} m^4_{\text{eff},i}, \tag{5.4}$$

[1] This approach is found in Ref. [13]

and the beta functions are found by comparing coefficients (assuming the anomalous dimensions are known). In some cases, Eq. (5.3) can be used to write the effective potential in terms of beta functions (and anomalous dimensions). In the next section we will show how this can be done in the single scalar model.

5.1 Single scalar field potential

Consider the tree level potential of a single massless real scalar field ϕ, given by

$$V_{\text{tree}} = \frac{\lambda}{4!}\phi^4. \tag{5.5}$$

Then Eq. (5.3) reads

$$-\mu\frac{\partial}{\partial\mu}V_1 = (\beta_\lambda + 4\gamma)\,\frac{\phi_b^4}{4!}. \tag{5.6}$$

Before integrating this equation, we need to clarify some points. The beta function and anomalous dimensions are of $\mathcal{O}(\hbar)$ and since we are working at $\mathcal{O}(\hbar)$, they can be considered to be constant. Next we need to specify the initial condition. At $\mu = \phi_b$ there is only one dimensionful quantity present and $V_1/\phi_b^4 =: D/4!$ is dimensionless and therefore field independent.[2] With this in mind, we integrate

$$V_1 = \left(D - \int_{\phi_b}^{\mu}\frac{d\mu'}{\mu'}\,(\beta_\lambda + 4\gamma)\right)\frac{\phi_b^4}{4!} = \left(D + \frac{(\beta_\lambda + 4\gamma)}{2}\ln\left(\frac{\phi_b^2}{\mu^2}\right)\right)\frac{\phi_b^4}{4!}. \tag{5.7}$$

The one-loop effective potential is then given by

$$V_{\text{eff}} = \frac{\lambda + D}{4!}\phi_b^4 + \frac{\beta_\lambda + 4\gamma}{2\cdot 4!}\phi_b^4\ln\left(\frac{\phi_b^2}{\mu^2}\right). \tag{5.8}$$

A similar result has been obtained in Ref. [13]. We stress that this procedure crucially depends on the fact that there is only one physical scale present in this model.

5.2 Two scalar fields potential

In case of several scalar fields, we cannot simply integrate Eq. (5.3). In the single scalar case, the argument of the logarithm is fixed by the fact that there is only one physical scale present. This does not work in the two scalar case. If there are two

[2] Note that this only holds in the case of a single scalar field.

scalar fields whose VEVs are similar in size, there is no way around analyzing the full one-loop effective potential. In many physical settings one is interested in the case with a hierarchy between the VEVs of the scalar fields. In the following, we show how the effective potential is related to the beta functions in the hierarchical setting.

We focus on a scale invariant potential with two scalar fields Φ and H, and assume that the symmetries of our model lead to a scalar potential which can be written as

$$V_{\text{tree}} = \lambda_\Phi |\Phi|^4 + \lambda_H |H|^4 + 2\lambda_p |\Phi|^2 |H|^2. \tag{5.9}$$

Further we assume that, at some scale μ, both λ_Φ and λ_p turn small simultaneously and the potential develops a flat direction. (The Gildener Weinberg approximation for this potential is discussed in Chap. 4.) The field Φ obtains a VEV given by $\langle\Phi\rangle$ and the portal coupling generates a small (positive or negative) mass term for H. We will study the effective potential in the region where $H_b \ll \Phi_b \approx \langle\Phi\rangle$. We also assume that for each field only one real component will obtain a non-zero expectation value. In Chap. 6 we will have such a setup, where H is the SM Higgs doublet and Φ is a complex scalar singlet charged under an U(1) symmetry. By assumption, λ_Φ and λ_p are small and we will not include them in the calculation of the effective masses. In Chap. 6 we will include λ_p however the numerical difference is small.

The symmetry that enforces the shape of the potential in Eq. (5.9) also ensures that the effective masses only depend on the scalar fields squared, i.e. $m^2_{\text{eff}}(\Phi_b^2, H_b^2)$. Expanding Eq. (5.2) for $H_b \ll \Phi_b$ yields

$$\begin{aligned} V_1 =& D_\Phi \Phi_b^4 + D_H H_b^4 + 2D_p \Phi_b^2 H_b^2 \\ &+ \frac{C_{\lambda_\Phi}}{2}\Phi_b^4 \ln\left(\frac{\Phi_b^2}{\mu^2}\right) + \frac{C_{\lambda_H}}{2} H_b^4 \ln\left(\frac{H_b^2}{\mu^2}\right) + \frac{\tilde{C}_{\lambda_H}}{2} H_b^4 \ln\left(\frac{\Phi_b^2}{\mu^2}\right) + C_{\lambda_p}\Phi_b^2 H_b^2 \ln\left(\frac{\Phi_b^2}{\mu^2}\right) \\ &+ \lambda_6 \frac{H_b^6}{\Phi_b^2} + C_{\lambda_6}\frac{H_b^6}{\Phi_b^2}\ln\left(\frac{H_b^2}{\mu^2}\right) + \tilde{C}_{\lambda_6}\frac{H_b^6}{\Phi_b^2}\ln\left(\frac{\Phi_b^2}{\mu^2}\right) + \dots , \end{aligned} \tag{5.10}$$

for some model dependent coefficients D_i, C_i and $\tilde{C}_i$. If we plug this into Eq. (5.3) and compare the coefficients of powers of Φ_b and H_b, we find

$$C_{\lambda_\Phi} = \beta_{\lambda_\Phi} - 4\lambda_\Phi \gamma_\Phi, \qquad \tilde{C}_{\lambda_H} + C_{\lambda_H} = \beta_{\lambda_H} - 4\lambda_H\gamma_H, \tag{5.11}$$

$$C_{\lambda_p} = \beta_{\lambda_p} - 2\lambda_p(\gamma_\Phi + \gamma_H), \qquad \tilde{C}_{\lambda_6} = -C_{\lambda_6}. \tag{5.12}$$

The beta function will always occur together with the anomalous dimensions, so we define

$$\tilde{\beta}_{\lambda_\Phi} := \beta_{\lambda_\Phi} - 4\lambda_\Phi \gamma_\Phi, \qquad \tilde{\beta}_{\lambda_H} := \beta_{\lambda_H} - 4\lambda_H \gamma_H, \qquad \tilde{\beta}_{\lambda_p} := \beta_{\lambda_p} - 2\lambda_p(\gamma_\Phi + \gamma_H). \tag{5.13}$$

Further, $\tilde{\beta}_{\lambda_H}$ is split up into $\tilde{\beta}_{\lambda_H} = \tilde{\beta}^h_{\lambda_H} + \tilde{\beta}^l_{\lambda_H}$ by defining

$$\tilde{\beta}^h_{\lambda_H} := \tilde{C}_{\lambda_H}, \qquad \tilde{\beta}^l_{\lambda_H} := C_{\lambda_H}. \tag{5.14}$$

With the final definition

$$\tilde{\lambda}_\Phi = \lambda_\Phi + D_\Phi, \qquad \tilde{\lambda}_H = \lambda_H + D_H, \qquad \tilde{\lambda}_p = \lambda_p + D_p, \tag{5.15}$$

the expanded one-loop effective potential can be written as

$$\begin{aligned} V_{\text{eff}} =& \tilde{\lambda}_\Phi \Phi_b^4 + \tilde{\lambda}_H H_b^4 + 2\tilde{\lambda}_p \Phi_b^2 H_b^2 \\ &+ \frac{\tilde{\beta}_{\lambda_\Phi}}{2}\Phi_b^4 \ln\left(\frac{\Phi_b^2}{\mu^2}\right) + \frac{\tilde{\beta}^l_{\lambda_H}}{2} H_b^4 \ln\left(\frac{H_b^2}{\mu^2}\right) + \frac{\tilde{\beta}^h_{\lambda_H}}{2} H_b^4 \ln\left(\frac{\Phi_b^2}{\mu^2}\right) + \tilde{\beta}_{\lambda_p}\Phi_b^2 H_b^2 \ln\left(\frac{\Phi_b^2}{\mu^2}\right) \\ &+ \lambda_6 \frac{H_b^6}{\Phi_b^2} + C_{\lambda_6}\frac{H_b^6}{\Phi_b^2}\ln\left(\frac{H_b^2}{\Phi_b^2}\right) + \dots\,. \end{aligned} \tag{5.16}$$

This equation shows how the effective potential is related to the beta function in case of two scalar fields. When studying the effective potential, one is typically interested in the VEVs of the scalar fields. For this purpose, the above equation is not particularly helpful. We discuss an approach to understand the VEVs of the two scalar system in the following section.

5.2.1 Minimum of the two scalar effective potential

The minimum of the effective potential is found by solving

$$\left.\frac{\partial V_{\text{eff}}}{\partial \Phi_b}\right|_{\Phi_b=\langle\Phi\rangle, H_b=\langle H\rangle} = 0, \qquad \left.\frac{\partial V_{\text{eff}}}{\partial \phi_b}\right|_{\Phi_b=\langle\Phi\rangle, H_b=\langle H\rangle} = 0. \tag{5.17}$$

These equations can usually only be solved numerically which is not very insightful. In the following we propose an analytic way of studying the minimum structure of the effective potential. Our procedure resembles the functional approach to Effective Field Theories (EFTs) (see e.g. Ref. [175]). However, we are working with effective potentials which are functions of the background fields and our procedure can be understood purely as expanding the effective potential in the region of interest.

We start by solving the minimum condition for Φ_b while allowing for general values of H_b. This defines $\tilde{\Phi}(H_b)$ via

$$\left.\frac{\partial V_{\text{eff}}}{\partial \Phi_b}\right|_{\Phi_b=\tilde{\Phi}(H_b)} = 0. \tag{5.18}$$

Note that $\tilde{\Phi}(H_b = \langle H \rangle) = \langle \Phi \rangle$. Now we define a new potential for H_b as

$$V_{\text{EFT}}(H_b) := V_{\text{eff}}(H_b, \tilde{\Phi}(H_b)). \tag{5.19}$$

One can easily check that this new potential has a minimum at $H_b = \langle H \rangle$ since the first derivative vanishes, i.e.

$$\left.\frac{\partial V_{\text{EFT}}}{\partial H_b}\right|_{H_b=\langle H \rangle} = \left.\frac{\partial V_{\text{eff}}}{\partial H_b} + \frac{\partial V_{\text{eff}}}{\partial \Phi_b}\frac{\partial \tilde{\Phi}}{\partial H_b}\right|_{H_b=\langle H \rangle, \Phi_b=\langle \Phi \rangle} = 0, \tag{5.20}$$

which simply follows from the definition Eq. (5.19) and the fact that $\langle \Phi \rangle$ and $\langle H \rangle$ fulfill the minimum conditions Eq. (5.17).

Before approximating V_{eff}, we first want to know about the values of Φ_b near the minimum. We expand

$$\tilde{\Phi}(H_b) = \Phi_0 \left(1 + \delta\Phi_2 \frac{H_b^2}{\mu^2} + \delta\Phi_4 \frac{H_b^4}{\mu^4} + ...\right), \tag{5.21}$$

and solve Eq. (5.18) order by order in H_b. We find at leading order

$$\Phi_0 = e^{-\frac{1}{4} - \frac{\tilde{\lambda}_\Phi}{\tilde{\beta}_{\lambda_\Phi}}} \mu, \tag{5.22}$$

which agrees with the usual result of dimensional transmutation. To $\mathcal{O}\left(H_b^2\right)$ we find

$$\tilde{\Phi}(H_b) = \Phi_0 \left(1 - \frac{\tilde{\lambda}_p + \tilde{\beta}_{\lambda_p}\left(\frac{1}{4} - \frac{\tilde{\lambda}_\Phi}{\tilde{\beta}_{\lambda_\Phi}}\right)}{\tilde{\beta}_{\lambda_\Phi}} \frac{H_b^2}{\Phi_0^2} + ...\right), \tag{5.23}$$

indicating that the VEV of Φ is well approximated by $\langle\Phi\rangle \approx \Phi_0$, if $\tilde{\lambda}_p$ is small. We now expand Eq. (5.19) in powers of H_b/Φ_0 and we find up to $\mathcal{O}(H_b^4)$[3]

$$\begin{aligned} V_{\rm EFT} =& -\frac{\tilde{\beta}_{\lambda_\Phi}}{4}\Phi_0^4 + 2\left[\tilde{\lambda}_p - \tilde{\beta}_{\lambda_p}\left(\frac{1}{4}+\frac{\tilde{\lambda}_\Phi}{\tilde{\beta}_{\lambda_\Phi}}\right)\right]\Phi_0^2 H_b^2 \\ &+ \left[\tilde{\lambda}_H - \left(\frac{1}{4}+\frac{\tilde{\lambda}_\Phi}{\tilde{\beta}_{\lambda_\Phi}}\right)\tilde{\beta}^h_{\lambda_H} - 2\frac{\left(\tilde{\beta}_{\lambda_p}\left(\frac{1}{4}-\frac{\tilde{\lambda}_\Phi}{\tilde{\beta}_{\lambda_\Phi}}\right)+\tilde{\lambda}_p\right)^2}{\tilde{\beta}_{\lambda_\Phi}}\right] H_b^4 \\ &+ \frac{\tilde{\beta}^l_{\lambda_H}}{2} H_b^4 \ln\left(\frac{H_b^2}{\mu^2}\right). \end{aligned} \tag{5.24}$$

The shape of this expression is quite similar to the expression found for the effective potential of a single scalar field (see Eq. (5.8)). In fact the effective potential for a singe massive scalar field H can be written as

$$V_{\rm eff} = m^2 H_b^2 + \tilde{\lambda} H_b^4 + \frac{\beta_{\lambda_H}\big|_{\text{no scalar}}}{2} H_b^4 \ln\left(\frac{H_b^2}{\mu^2}\right) + \text{contributions from scalar loops,} \tag{5.25}$$

where $\tilde{\lambda} \sim \lambda + \frac{1}{64\pi^2}(g^4 \ln g^2 + \ldots)$ and g stands for the gauge and Yukawa couplings. Scalar loops play a special role, since the scalar effective masses contain a sum of m^2 and λH_b^2 and therefore the logarithm cannot be written as $\ln(H_b^2/\mu^2)$. In the case with two scalar fields we ignored the portal coupling λ_p for the calculation of the effective masses $m^2_{\rm eff}$ and therefore no such terms occur in Eq. (5.24). In Chap. 6 we will treat the portal coupling consistently while in this chapter we ignore scalar loops.

We also provide the expression for $V_{\rm eff}$ up to $\mathcal{O}(H_b^6)$. In order to simplify the expression, we give the result for $\mu = \Phi_0$. Then we have

$$\begin{aligned} V_{\rm EFT} =& -\frac{\tilde{\beta}_{\lambda_\Phi}}{4}\Phi_0^4 + 2\tilde{\lambda}_p \Phi_0^2 H^2 + \left[\tilde{\lambda}_H - \frac{\left(2\tilde{\lambda}_p + \tilde{\beta}_{\lambda_p}\right)^2}{2\tilde{\beta}_{\lambda_\Phi}}\right] H^4 + \frac{\tilde{\beta}^l_{\lambda_H}}{2} H^4 \ln\left(\frac{H^2}{\Phi_0^2}\right) \\ &+ \left[\lambda_6 + \frac{\left(2\tilde{\lambda}_p + \tilde{\beta}_{\lambda_p}\right)\left(2\left(\tilde{\beta}^2_{\lambda_p} + \tilde{\lambda}_p\tilde{\beta}_{\lambda_p} - 2\tilde{\lambda}_p^2\right) - 3\tilde{\beta}_{\lambda_\Phi}\tilde{\beta}^h{}_{\lambda_H}\right)}{6\tilde{\beta}^2_{\lambda_\Phi}}\right]\frac{H^6}{\Phi_0^2} \\ &+ C_{\lambda_6}\frac{H^6}{\Phi^2}\ln\left(\frac{H^2}{\Phi_0^2}\right). \end{aligned} \tag{5.26}$$

[3] μ and Φ_0 are not independent, but connected by Eq. (5.22).

The form of Eq. (5.24) suggests that $\tilde{\beta}^l_{\lambda_H}$ is related to the beta function of λ_H in the effective field theory, i.e. the model obtained by integrating out the fields that obtain a mass of $\mathcal{O}(\langle\Phi\rangle)$. We show in the following example that $\tilde{\beta}^l_{\lambda_H}$ actually is the beta function calculated only using degrees of freedom that do not obtain a mass from VEV of Φ.

5.2.2 Example

Consider a toy model with two scalar fields Φ and H and a gauge group given by $\mathrm{U}(1)_A \times \mathrm{U}(1)_B$. The charges of the scalar fields are given by $H \sim (\frac{1}{2}, 0)$ and $\Phi \sim (\frac{1}{2}, \frac{1}{2})$. The effective mass matrix for the gauge boson is given by

$$m_V = \begin{pmatrix} \frac{g_A^2}{2}\Phi_b^2 & \frac{g_A g_B}{2}\Phi_b^2 \\ \frac{g_A g_B}{2}\Phi_b^2 & \frac{g_B^2}{2}\left(H_b^2 + \Phi_b^2\right) \end{pmatrix}, \tag{5.27}$$

where g_A and g_B are the $\mathrm{U}(1)_A$ and $\mathrm{U}(1)_B$ gauge couplings respectively. The effective potential is obtained from Eq. (4.39). For simplicity, we do not include scalar loops. We now expand the potential similarly to Eq. (5.16) and obtain

$$\begin{aligned} V_{\text{eff}} = &\left\{\lambda_\Phi + \frac{3(g_A^2+g_B^2)^2}{256\pi^2}\left[\ln\left(\frac{g_A^2+g_B^2}{2}\right) - \frac{5}{6}\right]\right\}\Phi_b^4 + \frac{3(g_A^2+g_B^2)^2}{256\pi^2}\Phi_b^4 \ln\left(\frac{\Phi_b^2}{\mu^2}\right) \\ &+ \left\{2\lambda_p - \frac{3g_B^4}{128\pi^2}\left[\ln\left(\frac{g_A^2+g_B^2}{2}\right) - \frac{1}{3}\right]\right\}\Phi_b^2 H_b^2 + \frac{3g_B^4}{128\pi^2} H_b^2 \Phi_b^2 \ln\left(\frac{\Phi_b^2}{\mu^2}\right) \\ &+ \left\{\lambda_H + \frac{3g_B^4}{256\pi^2}\left[\ln\left(\frac{g_A^2+g_B^2}{2}\right) - \frac{5}{6} + \frac{3g_B^4 + 2g_A^2 g_B^2 + 4g_A^4 \ln\left(\frac{g_A g_B}{g_A^2+g_B^2}\right)}{2\left(g_A^2+g_B^2\right)^2}\right]\right\} H_b^4 \\ &+ \frac{3g_B^4}{256\pi^2\left(g_A^2+g_B^2\right)^2}\left(2g_A^2 g_B^2 + g_B^4\right) H_b^4 \ln\left(\frac{\Phi_b^2}{\mu^2}\right) \\ &+ \frac{3g_B^4 g_A^2}{256\pi^2\left(g_A^2+g_B^2\right)^2} H_b^4 \ln\left(\frac{H_b^2}{\mu^2}\right). \end{aligned} \tag{5.28}$$

By comparing coefficients with Eq. (5.16), we can now read of $\tilde{\lambda}_i$ and $\tilde{\beta}_{\lambda_i}$. Eq. (5.24) at $\mu = \Phi_0$ reads explicitly

$$
\begin{aligned}
V_{\text{EFT}} = &-\frac{3(g_A^2+g_B^2)^2}{512\pi^2}\Phi_0^2 + \left\{2\lambda_p + \frac{3g_B^4}{128\pi^2}\left[\ln\left(\frac{g_A^2+g_B^2}{2}\right) - \frac{1}{3}\right]\right\}\Phi_0^2 H_b^2 \\
&+ \left\{\lambda_H + \frac{3g_B^4}{256\pi^2}\left[\ln\left(\frac{g_A^2+g_B^2}{2}\right) - \frac{5}{6} + \frac{3g_B^4 + 2g_A^2 g_B^2 + 4g_A^4 \ln\left(\frac{g_A g_B}{g_A^2+g_B^2}\right)}{2\left(g_A^2+g_B^2\right)^2}\right]\right. \\
&\qquad \left. - \frac{\left(2\lambda_p + \frac{3g_B^4}{128\pi^2}\left[\ln\left(\frac{g_A^2+g_B^2}{2}\right) + \frac{2}{3}\right]\right)^2}{2\frac{3\left(g_A^2+g_B^2\right)^2}{128\pi^2}}\right\} H_b^4 \\
&+ \frac{3g_B^4 g_A^2}{256\pi^2\left(g_A^2+g_B^2\right)^2} H_b^4 \ln\left(\frac{H_b^2}{\mu^2}\right).
\end{aligned}
\tag{5.29}
$$

The VEV of Φ breaks the gauge group as $\mathrm{U}(1)_A \times \mathrm{U}(1)_B \to \mathrm{U}(1)$ where the unbroken U(1) has a gauge coupling g related to the original gauge couplings by

$$
\frac{1}{g^2} = \frac{1}{g_A^2} + \frac{1}{g_B^2}. \tag{5.30}
$$

With this definition, we find for $\tilde{\beta}^l_{\lambda_H}$

$$
\tilde{\beta}^l_{\lambda_H} = \frac{3g_B^4 g_A^2}{128\pi^2\left(g_A^2+g_B^2\right)^2} = \frac{3g^4}{128\pi^2}, \tag{5.31}
$$

which demonstrates that $\tilde{\beta}^l_{\lambda_H}$ is (at least in this example) the beta function for λ_H in the phase where the heavy fields with masses proportional to $\langle\Phi\rangle$ are integrated out.

We show the running of couplings for a benchmark point in Fig. 5.1 (left). The VEV of Φ is roughly given by the scale where $\lambda_\Phi \approx \beta_{\lambda_\Phi}$ and therefore also close to the scale where λ_Φ crosses zero. At the scale of symmetry breaking, λ_p needs to be small in order to insure a hierarchy between $\langle\Phi\rangle$ and the mass term for H.

5.3 Goldstone boson calculation

From Eq. (5.26), we can tell that there is a hierarchy between Φ_0 and H only if $\tilde{\lambda}_p$ is small at $\mu = \Phi_0$. An often used mechanism to explain hierarchies in scalar

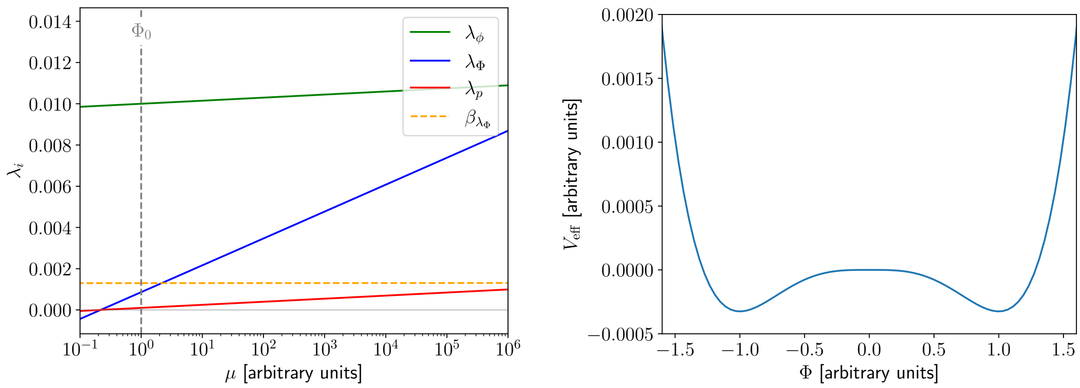

Figure 5.1: The running of the scalar quartic couplings in the toy model (left) and the effective potential in the direction of Φ_b (with $H_b = 0$). The couplings at $\mu = 1$ are chosen as $g_A = 0.7$, $g_B = 0.5$, $\lambda_H = 0.01$ and $\lambda_p = 10^{-4}$. λ_Φ is chosen in such a way that $\mu = \Phi_0$ and is numerically given by $\lambda_\Phi = 8.6 \cdot 10^{-4}$.

masses, is to have the light scalar field as a Goldstone boson of a spontaneously broken global symmetry. In this section we show that our calculation is explicitly consistent with Goldstones theorem [68–70]. If the global symmetry is explicitly broken, we expect the mass of the pNGB to have a mass proportional to the scale of symmetry breaking multiplied by the amount of explicit symmetry breaking. We also demonstrate that this intuition is not quite correct as the explicit symmetry breaking might only contribute to the mass of the pNGB at subleading level.

5.3.1 Exact symmetry

Consider the case where we have an exact global symmetry of rotations between Φ and H. In this case, the one-loop potential is given by

$$V_{\text{eff}} = \tilde{\lambda} \left(\Phi_b^2 + H_b^2\right)^2 + \frac{\tilde{\beta}_\lambda}{2} \left(\Phi_b^2 + H_b^2\right)^2 \ln\left(\frac{\Phi_b^2 + H_b^2}{\mu^2}\right). \tag{5.32}$$

V_{EFT}, i.e. Eq. (5.24) is then given by

$$V_{\text{EFT}} = -\frac{\tilde{\beta}_\lambda}{4}\Phi_0^4. \tag{5.33}$$

This results agrees with the expectation that Goldstone bosons have only derivative interactions and the potential is flat. We have checked that this result also holds for higher order terms. The derivative interactions of a Goldstone boson do not show up in our calculations, as we calculate the effective potential for constant background fields.

5.3.2 Approximate symmetry

Now consider the case where the global symmetry is explicitly broken, however the interactions that violate the symmetry only involve H and do not involve Φ. In this case the effective potential is approximated by

$$
\begin{aligned}
V_{\text{eff}} \approx \lambda \left(\Phi_b^2 + H_b^2\right)^2 + \frac{\tilde{\beta}_\lambda}{2} \left(\Phi_b^2 + H_b^2\right)^2 \ln\left(\frac{\Phi_b^2 + H_b^2}{\mu^2}\right) \\
+ (\lambda_H - \lambda) H_b^4 + \frac{\tilde{\beta}^h_{\Delta\lambda_H}}{2} H_b^4 \ln\left(\frac{\Phi_b^2}{\mu^2}\right) + \frac{\tilde{\beta}^l_{\Delta\lambda_H}}{2} H_b^4 \ln\left(\frac{H_b^2}{\mu^2}\right),
\end{aligned}
\tag{5.34}
$$

where $(\lambda_H - \lambda), \tilde{\beta}^h_{\Delta\lambda_H}$ and $\tilde{\beta}^l_{\Delta\lambda_H}$ explicitly violate the global symmetry. The potential V_{EFT} is then given by

$$
V_{\text{EFT}} \approx -\frac{\tilde{\beta}_\lambda}{4}\Phi_0^4 + \left((\lambda_H - \lambda) - \frac{\tilde{\beta}^h_{\Delta\lambda_H}}{4}\frac{\tilde{\beta}_\lambda + 4\lambda}{\tilde{\beta}_\lambda}\right) H_b^4 + \frac{\tilde{\beta}^l_{\Delta\lambda_h}}{2} H_b^4 \ln\left(\frac{H_b^2}{\mu^2}\right), \tag{5.35}
$$

and H is massless. In realistic models, higher order corrections will generate a mass term for H which is however loop suppressed compared to the naive expectation for a mass term of a pNGB.

5.3.3 Non-conformal case

Qualitatively similar results are found in the case where tree level mass terms are present. We first consider a potential with global symmetry of rotations between Φ and H given by

$$
V = -m^2\left(|H|^2 + |\Phi|^2\right) + \lambda\left(|H|^2 + |\Phi|^2\right)^2. \tag{5.36}
$$

For $m^2 > 0$, the potential has a minimum at $|\Phi|^2 + |H|^2 = m^2/(2\lambda)$. Integrating out the massive radial excitation at tree level gives a flat potential

$$
V_{\text{EFT}} = -\frac{m^4}{2\lambda}, \tag{5.37}
$$

as one expects from Goldstones theorem.

If we now consider a slight variation of the potential given by

$$V = -m^2\left(|H|^2 + |\Phi|^2\right) + \lambda\left(|H|^2 + |\Phi|^2\right)^2 + (\lambda_H - \lambda)|H|^4. \tag{5.38}$$

For $\lambda_H > \lambda$, the minimum is given by $\langle H\rangle = 0$ and $\langle\Phi\rangle = \sqrt{m^2/(2\lambda)}$. Integrating out the heavy radial excitation at tree level yields

$$V_{\mathrm{EFT}} = -\frac{m^4}{2\lambda} + (\lambda_H - \lambda)\,|H|^4. \tag{5.39}$$

The difference $(\lambda_H - \lambda)$ explicitly breaks the global symmetry of rotations. At leading order this breaking does not contribute to the mass term of the pNGB. However a quartic interaction for the pNGB H is generated. Higher order corrections will introduce a mass term which is suppressed by loop factors.

Generally, if we have an explicitly broken global continuous symmetry, where the symmetry violating interactions only involve the pNGB, then the mass term for the pNGB is only generated at subleading order.

Chapter 6

Custodial Naturalness

In this chapter, we propose a mechanism called Custodial Naturalness which explains the separation of the EW scale and potential UV completions of the SM.

Custodial Naturalness is based on a combination of classical scale invariance and enlarged custodial symmetry. Both symmetries are explicitly broken by quantum effects and spontaneously broken by the Coleman-Weinberg mechanism. We realize Custodial Naturalness in models where the scalar sector consists of the SM Higgs doublet H and a complex scalar field Φ which is a singlet under the SM gauge group. Both scalar fields have the identical charge under a new gauged U(1) group. After spontaneous symmetry breaking, the pNGB associated with the breaking of the enlarged custodial symmetry is given by the SM Higgs boson.

The results presented in this chapter are published in Refs. [1,2] in collaboration with *Manfred Lindner* and *Andreas Trautner*.

6.1 General Idea

Consider a potential which is symmetric under a SO(6) custodial symmetry[1]

$$V = \lambda \left(|H|^2 + |\Phi|^2\right)^2 . \tag{6.1}$$

A VEV in the $H - \Phi$ system breaks the enlarged custodial symmetry as $\mathrm{SO}(6) \to \mathrm{SO}(5)$ giving rise to five Goldstone bosons and the radial mode, which is the dilaton. Such a VEV also breaks the gauge group $\mathrm{SU}(2)_\mathrm{L} \times \mathrm{U}(1)_\mathrm{Y} \times \mathrm{U}(1)_\mathrm{X}$ to

[1]This symmetry is a symmetry of the scalar potential, explicitly broken by gauge and Yukawa interactions and we call this symmetry "custodial symmetry". The SM SO(4) custodial symmetry is a subgroup of this SO(6) group.

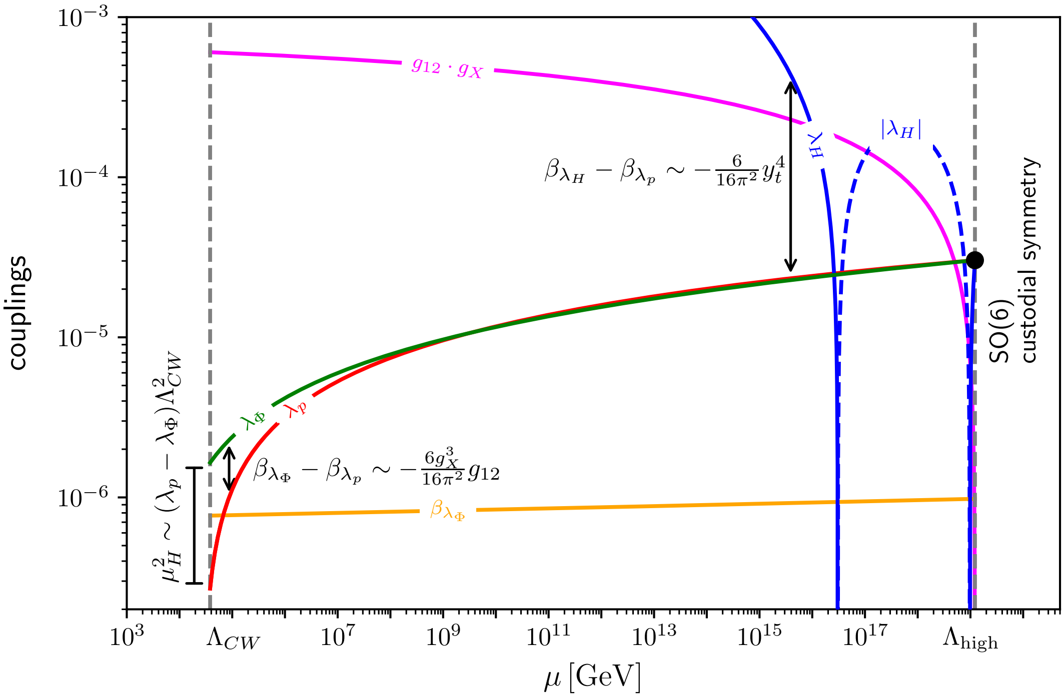

Figure 6.1: The running of the scalar quartic couplings for a typical parameter point. At the high scale $\Lambda_{\rm high} = M_{\rm Pl}$, we have $\lambda_\Phi = \lambda_p = \lambda_H$ and SO(6) custodial symmetry is realized. λ_H crosses zero and $|\lambda_H|$ is shown by the dashed line. λ_p and λ_Φ remain close to each other due to custodial symmetry. This figure is published in Ref. [1].

electromagnetism $\mathrm{U}(1)_{\rm em}$ and four of the Goldstone modes are absorbed into the longitudinal degrees of freedom of the massive gauge bosons. The final Goldstone boson takes the role of the SM Higgs boson. The dilaton is the also a pNGB namely the pNGB associated spontaneous breaking of scale symmetry.

SO(6) custodial symmetry is not an exact symmetry. It is broken by gauge and Yukawa interactions. We need to specify the scale where we impose custodial symmetry. In this work we always take this scale to be the Planck scale $M_{\rm Pl}$. To be precise, Eq. (6.1) is now understood as

$$V_{\rm tree} = \lambda \left(|H|^2 + |\Phi|^2\right)^2 \qquad \text{at } \mu = M_{\rm Pl}. \tag{6.2}$$

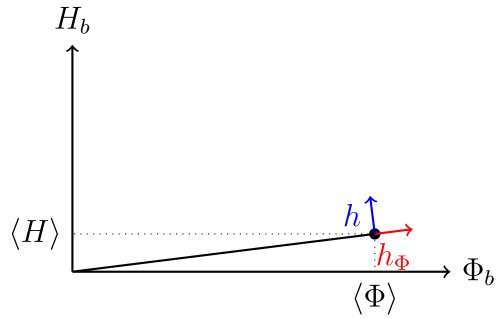

Figure 6.2: An illustration for the alignment of the VEV in the $\Phi - H$ plane. The dilaton h_Φ is given by the radial excitation and the orthogonal excitation corresponds to the Higgs boson h. This figure is published in Ref. [2].

The RG flow radiatively breaks SO(6) custodial symmetry and the scalar potential takes the more general form

$$V_{\text{tree}} = \lambda_H |H|^4 + 2\lambda_p |H|^2 |\Phi|^2 + \lambda_\Phi |\Phi|^4. \tag{6.3}$$

Fig. 6.1 shows the running of the couplings for a typical parameter point illustrating how λ_H runs to large positive values while λ_p and λ_Φ stay close to each other. Custodial symmetry protects the difference $\lambda_p - \lambda_\Phi$. At some intermediate scale λ_Φ becomes small and λ_p turns negative, and the tree level potential develops a flat direction. This happens typically around $\sim 10^5\,\text{GeV}$. In order to understand the orientation of the VEV, one can use the Gildener Weinberg approximation. We discuss this approximation for the same potential as Eq. (6.3) in Sec. 4.5. At the scale μ_{GW}, where the potential develops the flat direction, we have $\lambda_p < 0$ and the Gildener Weinberg approximation yields

$$\frac{H^2}{\Phi^2} = \frac{-\lambda_p}{\lambda_H}, \qquad \lambda_\Phi = \frac{\lambda_p^2}{\lambda_H} \qquad \text{at } \mu = \mu_{\text{GW}}. \tag{6.4}$$

The orientation of the VEV in the $H - \Phi$ plane is visualized in Fig. 6.2. The VEV is close to the boundary between the phase of unbroken and broken EW symmetry realizing the multi-phase criticality scenario [176–178].

6.1.1 Particle content and charge assignment

Custodial Naturalness can be realized in minimal extensions of the SM. We restrict ourselves to family-universal charges under the gauge group. The particle content includes the SM (with 3 right-handed neutrinos), the complex scalar singlet Φ and a new gauge group $\mathrm{U}(1)_X$. We also consider models with additional vector-like fermions. Gauge anomaly cancellation requires that the $\mathrm{U}(1)_X$ charges are a linear combination of hypercharge and $B-L$. We give the charges of all fields in Tab. 6.1. One can freely choose the basis of the two U(1) gauge groups. For our purposes, it is most convenient to choose the basis in such a way that the Higgs boson and Φ both have $\mathrm{U}(1)_X$ charge of 1. This relates the $\mathrm{U}(1)_X$ charge of a general field $Q^{(\mathrm{X})}$ to its hypercharge $Q^{(\mathrm{Y})}$ and its $B-L$ charge $Q^{(\mathrm{B-L})}$ by

$$Q^{(\mathrm{X})} = 2Q^{(\mathrm{Y})} + \frac{1}{q_\Phi} Q^{(\mathrm{B-L})}, \tag{6.5}$$

where q_Φ is the $B-L$ charge of Φ.

Adding a single set of new vector-like fermions can couple the new sector via the neutrino portal. With the charges given in Tab. 6.1 (middle), we have the following Yukawa interaction

$$\mathcal{L}_{\mathrm{Yuk}} \supset y_\psi^\alpha \bar{\psi}_L \Phi^\dagger \nu_R^\alpha + \mathrm{h.c.}, \tag{6.6}$$

which is the minimal possibility to introduce a Yukawa interaction involving Φ. We refer to this model as the neutrino portal model. We also discuss a model with two additional fermions (Tab 6.1 (bottom)). In principle, α is a free parameter and for any choice that prohibits Yukawa interactions to the right-handed neutrinos, the new fermions are stable and therefore DM candidates. In this case the new Yukawa interactions are given by

$$\mathcal{L}_{\mathrm{Yuk}} \supset y_\psi \bar{\psi}_L \Phi^\dagger \psi_R + y_{\psi'} \bar{\psi}'_L \Phi \psi'_R + \mathrm{h.c.} \tag{6.7}$$

6.1.2 Custodial symmetry violation

Gauge and Yukawa interactions explicitly break SO(6) custodial symmetry. In Fig. 6.1, λ_p and λ_Φ remain close to each other while λ_H runs to large positive values driven by the top Yukawa coupling. This is an important feature of our model. We show in Sec. 6.1.3 that the hierarchy between the intermediate scale and the EW scale is, to leading order, given by the splitting $\lambda_p - \lambda_\Phi$. This dependence might also be guessed from Eq. (6.4). This section is devoted to a discussion of the different contributions to $\beta_{\lambda_p} - \beta_{\lambda_\Phi}$.

Table 6.1: The particle content and charge assignments for the models realizing Custodial Naturalness. The "minimal particle content", i.e. the SM fields and Φ, is present in every model. Also shown are the additional fermions which populate the neutrino portal or might make up DM. The $\mathrm{U}(1)_X$ charges are a linear combination of hypercharge and $B - L$.

Name	Generations	$\mathrm{SU(3)_c \times SU(2)_L \times U(1)_Y}$	$\times\ \mathrm{U(1)_X}$	$\mathrm{U(1)_{B-L}}$
Minimal particle content				
Q	3	$\left(\mathbf{3}, \mathbf{2}, +\frac{1}{6}\right)$	$+\frac{1}{3} + \frac{1}{3q_\Phi}$	$+\frac{1}{3}$
L	3	$\left(\mathbf{1}, \mathbf{2}, -\frac{1}{2}\right)$	$-1 - \frac{1}{q_\Phi}$	-1
u_R	3	$\left(\mathbf{3}, \mathbf{1}, +\frac{2}{3}\right)$	$+\frac{4}{3} + \frac{1}{3q_\Phi}$	$+\frac{1}{3}$
d_R	3	$\left(\mathbf{3}, \mathbf{1}, -\frac{1}{3}\right)$	$-\frac{2}{3} + \frac{1}{3q_\Phi}$	$+\frac{1}{3}$
e_R	3	$(\mathbf{1}, \mathbf{1}, -1)$	$-2 - \frac{1}{q_\Phi}$	-1
ν_R	3	$(\mathbf{1}, \mathbf{1}, \ \ 0)$	$-\frac{1}{q_\Phi}$	-1
H	1	$\left(\mathbf{1}, \mathbf{2}, +\frac{1}{2}\right)$	$+1$	0
Φ	1	$(\mathbf{1}, \mathbf{1}, \ \ 0)$	$+1$	q_Φ
Minimal set of additional fermions				
ψ_L	1	$(\mathbf{1}, \mathbf{1}, 0)$	$-\left(\frac{1}{q_\Phi} + 1\right)$	$-(1 + q_\Phi)$
ψ_R	1	$(\mathbf{1}, \mathbf{1}, 0)$	$-\left(\frac{1}{q_\Phi} + 1\right)$	$-(1 + q_\Phi)$
Additional fermions that allow for DM				
ψ_L	1	$(\mathbf{1}, \mathbf{1}, 0)$	$\frac{\alpha}{q_\Phi}$	α
ψ_R	1	$(\mathbf{1}, \mathbf{1}, 0)$	$\frac{\alpha}{q_\Phi} + 1$	$\alpha + q_\Phi$
ψ'_L	1	$(\mathbf{1}, \mathbf{1}, 0)$	$\frac{\alpha}{q_\Phi} + 1$	$\alpha + q_\Phi$
ψ'_R	1	$(\mathbf{1}, \mathbf{1}, 0)$	$\frac{\alpha}{q_\Phi}$	α

SM contributions

The SM gauge and Yukawa interactions, especially the $\mathcal{O}(1)$ top Yukawa coupling, break SO(6) custodial symmetry. All of these interactions only couple to H and not to Φ. Therefore, they drive λ_H away from the symmetric point while the effect on $\lambda_p - \lambda_\Phi$ is much smaller. The difference in beta functions induced by the SM interactions is given by

$$\beta_{\lambda_p} - \beta_{\lambda_\Phi}\Big|_{\rm SM} \simeq \frac{1}{16\pi^2}\lambda_p\left[-\frac{9}{2}g_L^2 - \frac{3}{2}g_Y^2 + 12\lambda_H + 6y_t^2\right], \tag{6.8}$$

where g_L and g_Y are the $\mathrm{SU}(2)_L$ and hypercharge gauge couplings respectively and y_t is the top Yukawa coupling. Since λ_Φ reaches critical values around $\mu_{\rm GW}$, typical values for the custodially symmetric coupling λ are given by $\lambda \approx \frac{6g_X^4}{16\pi^2}\ln\left(\frac{M_{\rm Pl}}{\mu_{\rm GW}}\right)$. For $g_X = 0.1$ we find $\lambda \approx 10^{-4}$ and therefore $\lambda_p \lesssim 10^{-4}$. The contribution from Eq. (6.8) is negative for $10^{11}\,\mathrm{GeV} \lesssim \mu < M_{\rm Pl}$ and positive for $\mu \lesssim 10^{11}\,\mathrm{GeV}$. The integrated effect gives $\lambda_p - \lambda_\Phi > 0$. Therefore, if there were no additional sources of custodial symmetry violation, the Higgs doublet would not obtain a VEV (see Eq. (6.4)). Additional custodial symmetry violation needs to contribute with opposite sign. Alternatively, we could to lower the scale at which we impose custodial symmetry to $\Lambda_{\rm high} \approx 10^{11}$GeV.

Contributions from the new gauge sector

The new U(1) gauge group also contributes to custodial symmetry violation, however the explicit form depends on the basis of U(1) charges. If Φ and H have different U(1) charges, then this charge difference contributes to $\beta_{\lambda_p} - \beta_{\lambda_\Phi}$. The $\mathrm{U}(1)_X$ basis is defined in a way that there is no charge difference. Since we have two U(1) gauge groups, we also need to consider gauge kinetic mixing,[2] which also violates custodial symmetry. When rotating to the (symmetric) $\mathrm{U}(1)_X$ basis, the contribution of the charge difference to $\beta_{\lambda_p} - \beta_{\lambda_\Phi}$ is shifted into the gauge kinetic mixing parameter. The covariant derivative in the $B-L$ basis is given by

$$\left[\partial_\mu + i\left(Q^{(\rm Y)}, Q^{(\rm B-L)}\right)\begin{pmatrix} g_Y & \tilde{g} \\ 0 & g_{\rm B-L}\end{pmatrix}\begin{pmatrix} A_\mu^{(\rm Y)} \\ A_\mu^{(\rm X)}\end{pmatrix}\right]\phi, \tag{6.9}$$

[2] Terms such as $\epsilon F^{\mu\nu}F'_{\mu\nu}$ and off-diagonal gauge couplings do not violate gauge invariance and need to be included [179, 180]. All these terms can be absorbed into a single off-diagonal entry in the gauge coupling matrix [181].

where $\tilde{g}$ is the gauge kinetic mixing parameter, $g_{\rm B-L}$ is the $B-L$ gauge coupling, and $A_\mu^{(\rm Y)}$ and $A_\mu^{(\rm X)}$ are the U(1) gauge fields. ϕ denotes a generic field. With the definition of the charges in the $\mathrm{U}(1)_X$ basis in Eq. (6.5), we can rewrite the covariant derivative as

$$\begin{aligned}\left[\partial_\mu + i\left(Q^{(\rm Y)}, Q^{(\rm X)}\right)\begin{pmatrix} g_Y & \tilde{g} - 2q_\Phi g_{\rm B-L} \\ 0 & q_\Phi g_{\rm B-L}\end{pmatrix}\begin{pmatrix} A_\mu^{(\rm Y)} \\ A_\mu^{(\rm X)}\end{pmatrix}\right]\phi \\ =: \left[\partial_\mu + i\left(Q^{(\rm Y)}, Q^{(\rm X)}\right)\begin{pmatrix} g_Y & g_{12} \\ 0 & g_X\end{pmatrix}\begin{pmatrix} A_\mu^{(\rm Y)} \\ A_\mu^{(\rm X)}\end{pmatrix}\right]\phi,\end{aligned} \tag{6.10}$$

where we defined g_{12} as the gauge kinetic mixing parameter in the $\mathrm{U}(1)_X$ basis and g_X as the corresponding gauge coupling. In the $\mathrm{U}(1)_X$ basis the charges of H and Φ are identical and therefore only gauge kinetic mixing contributes to the differential running of λ_p and λ_Φ. The contribution is given by

$$\beta_{\lambda_p} - \beta_{\lambda_\Phi}\Big|_{g_{12}} \simeq \frac{1}{16\pi^2}\left[6 g_{12} g_X^3 + \frac{3}{2} g_{12}^2 g_X^2\right]. \tag{6.11}$$

In order for the difference $\lambda_p - \lambda_\Phi$ to remain small, g_{12} needs to be small.[3] We cannot simply set g_{12} to zero since it will be generated at loop level. We need to construct our models in such a way, that g_{12} can be small for all scales. For the value $q_\Phi = -\frac{16}{41}$, gauge kinetic mixing will not be generated at one-loop if set to zero at some scale. This value was independently found in Refs. [182–184] and aligns with the "charge orthogonality condition" [185]. We estimate that values of $|q_\Phi| \in \left[\frac{1}{3}, \frac{5}{11}\right]$ allow for small gauge kinetic mixing g_{12} and in this work we explicitly consider $q_\Phi = -\frac{1}{3}$ and $q_\Phi = -\frac{3}{8}$. The flow of g_{12} for these two values of q_Φ is shown in Fig. 6.3. At one-loop, g_{12} flows towards the line given by $g_{12} = \frac{14}{41} g_X$ for $q_\Phi = -\frac{1}{3}$ and towards the line given by $g_{12} = \frac{10}{123} g_X$ for $q_\Phi = -\frac{3}{8}$. In the minimal model we will often impose the boundary condition of $g_{12}\big|_{M_{\rm Pl}} = 0$. Such a trajectory is highlighted in Fig. 6.3 (left).

Without loss of generality, we can assume $g_X > 0$. Typically $|g_{12}| \ll g_X$ and the first term in Eq. (6.11) dominates. If g_{12} is positive, the contributions from gauge kinetic mixing counteract the SM contributions to $\beta_{\lambda_p} - \beta_{\lambda_\Phi}$ which can lead to $\lambda_p < \lambda_\Phi$ and therefore the Higgs field will obtain a VEV. It is also possible that g_{12} flips the sign along the RG flow and the integrated effect should be considered.

[3] In principle we could also require g_X to be small which would lead to a new sector which has only small couplings to the SM.

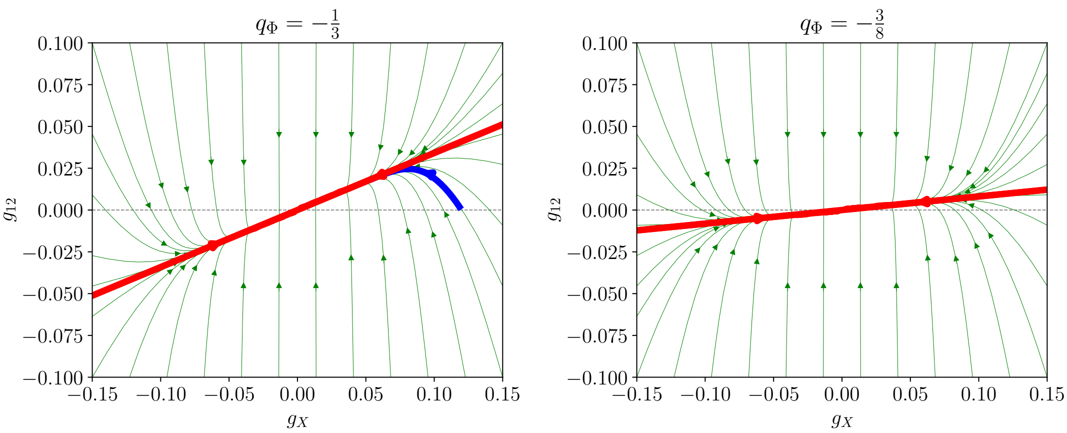

Figure 6.3: The one-loop RG flow from the UV to the IR in the $g_X - g_{12}$ plane. The lines with $g_{12} = \frac{14}{41} g_X$ for $q_\Phi = -\frac{1}{3}$ and $g_{12} = \frac{10}{123} g_X$ for $q_\Phi = -\frac{3}{8}$ are highlighted in red and a typical trajectory for the minimal model is marked in blue. The hypercharge gauge coupling is set to $g_Y = 0.48$. This figure is published in Ref. [2].

Contributions from the new Yukawa sector

New fermions introduce Yukawa interactions involving Φ (see Eqs. (6.6) and (6.7)). Since these interactions only involve Φ, they drive λ_Φ and λ_p away from each other. Assuming real Yukawa couplings, the contribution is given by

$$\beta_{\lambda_p} - \beta_{\lambda_\Phi}\bigg|_{y_\psi} \simeq \frac{\sum_k 2 y_{\psi_k}^4}{16\pi^2}. \tag{6.12}$$

Here, and in this entire chapter, the sum over k should be understood as follows: In the neutrino portal model, the sum runs over the single value $\bar{y}_\psi := \sqrt{y_\psi^\alpha y_\psi^\alpha}$ and in the DM model, the sum runs over y_ψ and y'_ψ. The contributions of the new Yukawa interactions lead to $\lambda_p < \lambda_\Phi$ therefore leading to EWSB.

6.1.3 Effective potential

We derive the one-loop effective potential in Chap. 4. In our model, the effective potential is a function of the background fields Φ_b and H_b and the minimum is given by $\Phi_b = \langle \Phi \rangle$ and $H_b = \langle H \rangle$. The formula for the effective potential is given by

$$V_{\text{eff}} = V_{\text{tree}} + \sum_i \frac{n_i (-1)^{2s_i}}{64\pi^2} m_{i,\text{eff}}^4 \left[\ln\left(\frac{m_{i,\text{eff}}^2}{\mu^2} \right) - C_i \right], \tag{6.13}$$

where the sum runs over the effective masses of all fields. n_i is the number of degrees of freedom, $(-1)^{1s_i}$ is $\genfrac{}{}{0pt}{}{+}{(-)}1$ for bosons (fermions). In $\overline{\text{MS}}$, $C_i = \frac{3}{2}$ for scalar fields and fermions and $C_i = \frac{5}{6}$ for vector bosons. For the neutral gauge bosons the effective masses are given by the eigenvalues of

$$M_V = \begin{pmatrix} \frac{g_Y^2}{2} H_b^2 & -\frac{g_Y g_L}{2} H_b^2 & \frac{(2g_X+g_{12})g_Y}{2} H_b^2 \\ -\frac{g_Y g_L}{2} H_b^2 & \frac{g_L^2}{2} H_b^2 & -\frac{(2g_X+g_{12})g_L}{2} H_b^2 \\ \frac{(2g_X+g_{12})g_Y}{2} H_b^2 & -\frac{(2g_X+g_{12})g_L}{2} H_b^2 & 2\left(\frac{2g_X+g_{12}}{2}\right)^2 H_b^2 + 2g_X^2 \Phi_b^2 \end{pmatrix}, \tag{6.14}$$

and for the charged gauge bosons we have $m_{W^\pm}^2 = g_L^2/2H_b^2$. g_Y is the hypercharge gauge coupling and g_L is the $\text{SU}(2)_L$ gauge coupling. For the top quark with Yukawa coupling y_t, we have an effective mass of $m_t = y_t H_b$ and we ignore all other SM Yukawa interactions. From the tree level potential, we find the effective mass matrix for the neutral CP even scalar fields to be

$$\begin{pmatrix} 2\lambda_p H_b^2 + 6\lambda_\Phi \Phi_b^2 & 4\lambda_p H_b \Phi_b \\ 4\lambda_p H_b \Phi_b & 2\lambda_p \Phi_b^2 + 6\lambda_H H_b^2 \end{pmatrix}. \tag{6.15}$$

The other scalar degrees of freedom contribute with effective masses given by $(2\lambda_p\Phi_b^2 + 2\lambda_H H_b^2, 2\lambda_p\Phi_b^2 + 2\lambda_H H_b^2, 2\lambda_p\Phi_b^2 + 2\lambda_H H_b^2, 2\lambda_p H_b^2 + 2\lambda_\Phi \Phi_b^2)$. In the neutrino portal model we also include the effective mass $m_\psi^2 = y_\psi^\alpha y_\psi^\alpha \Phi_b^2 = \bar{y}_\psi^2 \Phi_b^2$ and in the DM model we have two additional effective masses given by $m_\psi = y_\psi \Phi_b$ and $m_{\psi'} = y_{\psi'} \Phi_b$.

In order to analyze the effective potential, we use techniques very similar to those developed in Chap. 5. We define $\tilde{\Phi}(H_b)$ via

$$\left.\frac{\partial V_{\text{eff}}}{\partial \Phi_b}\right|_{\Phi_b = \tilde{\Phi}(H_b)} = 0, \tag{6.16}$$

for general values of H_b and use the solution to define

$$V_{\text{EFT}}(H_b) := V_{\text{eff}}(H_b, \tilde{\Phi}(H_b)). \tag{6.17}$$

As shown in Chap. 5,

$$\left.\frac{\partial V_{\text{EFT}}}{\partial H_b}\right|_{H_b=\langle H\rangle} = \left.\frac{\partial V_{\text{eff}}}{\partial H_b} + \frac{\partial V_{\text{eff}}}{\partial \Phi_b}\frac{\partial \tilde{\Phi}}{\partial H_b}\right|_{H_b=\langle H\rangle, \Phi_b=\langle \Phi\rangle} = 0, \tag{6.18}$$

which follows from the fact that $\langle H\rangle$ and $\langle\Phi\rangle$ fulfill the minimum conditions of $V_{\rm eff}$. From the Gildener Weinberg approximation (Eq. (6.4)), we expect that $\langle H\rangle \ll \langle\Phi\rangle$. We can approximate $\langle\Phi\rangle = \tilde{\Phi}(\langle H\rangle) \approx \tilde{\Phi}(0) =: \Phi_0$. Analytically we obtain

$$\ln\left(\frac{\Phi_0^2}{\mu^2}\right) = -\frac{16\pi^2\lambda_\Phi}{\left(3g_X^4+4\lambda_p^2-\sum_k y_{\psi_k}^4\right)} \\ -\frac{\left\{g_X^4\left[3\ln\left(2g_X^2\right)-1\right]+4\lambda_p^2\left[\ln\left(2\lambda_p\right)-1\right]-\sum_k\left[y_{\psi_k}^4\left(\ln y_{\psi_k}^2-1\right)\right]\right\}}{\left(3g_X^4+4\lambda_p^2-\sum_k y_{\psi_k}^4\right)}, \tag{6.19}$$

which is the usual Coleman-Weinberg result of dimensional transmutation. We now expand $V_{\rm EFT}$ for $H_b \ll \Phi_0$. At quadratic order we find

$$V_{\rm EFT} \supset 2\left[\lambda_p - \frac{3\left(g_X+\frac{g_{12}}{2}\right)^2 g_X^2}{3g_X^4+4\lambda_p^2-\sum_k y_{\psi_k}^4}\left(\lambda_\Phi+\sum_k\left\{\frac{y_{\psi_k}^4}{16\pi^2}\left[\frac{2}{3}+\ln\left(\frac{2g_X^2}{y_{\psi_k}^2}\right)\right]\right\}\right)\right]\Phi_0^2H_b^2 \\ +\frac{\lambda_p\lambda_H}{16\pi^2}\left[...\right]\Phi_0^2H_b^2, \tag{6.20}$$

where we dropped terms proportional to the $\lambda_p\lambda_H/(16\pi^2)$ factor. For small g_{12} and small y_ψ, this is approximated by $\approx 2(\lambda_p-\lambda_\Phi)\Phi_0^2H_b^2$. Custodial symmetry ensures that $\lambda_p-\lambda_\Phi$ remains small. Crucially, the custodial symmetry violation from SM interactions (EW gauge couplings and top Yukawa coupling) does not show up in Eq. (6.20). Despite the $\mathcal{O}(1)$ top Yukawa coupling, the Higgs mass is protected by the pNGB nature.

Eq. (6.20) is obtained without assuming a specific value for the RG scale μ. The only requirement is, that μ should be close to the physical scales (for example Φ_0). It turns out, that $V_{\rm EFT}$ takes a particularly convenient form if we choose $\mu=\mu_0 := \sqrt{2}g_X\Phi_0e^{-1/6}$. With this choice, the quadratic term in $V_{\rm EFT}$ is given by

$$V_{\rm EFT} \supset 2\lambda_p\left\{1+\frac{\left[4\lambda_p+6\lambda_H\right]\left[\ln\left(\frac{2\lambda_p\Phi_0^2}{\mu_0^2}\right)-1\right]}{16\pi^2}\right\}H_b^2\Phi_0^2. \tag{6.21}$$

At $\mu=\mu_0$,

$$\lambda_\Phi\big|_{\mu=\mu_0} = \frac{\sum_k y_\psi^4\left[\ln\left(\frac{y_\psi}{\sqrt{2}g_X}\right)-\frac{1}{3}\right]-2\lambda_p^2\left[\ln\left(\frac{\lambda_p}{g_X^2}\right)-\frac{2}{3}\right]}{8\pi^2}, \tag{6.22}$$

and therefore $|\lambda_\Phi| \ll |\lambda_p|$. The mass term of the Higgs field is well approximated by $2\lambda_p\Phi_0^2$ at μ_0.

The expansion $H_b \ll \Phi_0$ implicitly treats $2\lambda_p\Phi_0^2$ as large. This is not necessarily in issue. In the following, we propose a slightly different expansion that takes into account that $2\lambda_p\Phi_0^2$ is roughly of order of the EW scale. This new expansion scheme will allow us to make a precise connection to the SM effective potential.

Instead of expanding in powers of H_b/Φ_0, we introduce an artificial expansion parameter ϵ defined as

$$\frac{H_b}{\Phi_0} \to \epsilon\frac{H_b}{\Phi_0}, \quad \lambda_p \to \epsilon^2\lambda_p. \tag{6.23}$$

This definition is similar to the 't Hooft-Veneziano limit [186, 187] with $\epsilon \to 0$ corresponding to

$$\frac{\Phi_0}{H_b} \to \infty, \quad \frac{\lambda_p}{\lambda_H} \to 0, \quad \lambda_p\Phi_0^2 = \lambda_H H_b^2 \text{ (fixed)}. \tag{6.24}$$

This limit also aligns with the flat direction of the Gildener Weinberg approximation given by

$$\lambda_H H^2 = -\lambda_p\Phi^2. \tag{6.25}$$

Now we expand $V_{\rm EFT}$ in powers of ϵ and at up to $\mathcal{O}(\epsilon^4)$, we find at $\mu = \mu_0$

$$\begin{aligned} V_{\rm EFT} =& \frac{-3g_X^4 + \sum_k y_{\psi_k}^4}{32\pi^2}\Phi_0^4 + 2\lambda_p\Phi_0^2 H_b^2 + \lambda_H H_b^4 \\ &+ \sum_i \frac{n_i(-1)^{2s_i}}{64\pi^2} m_{i,\rm eff}^4\left[\ln\left(\frac{m_{i,\rm eff}^2}{\mu_0^2}\right) - C_i\right] - \frac{3\left(\frac{g_{12}}{2}+g_X\right)^4\left(\sum_k y_{\psi_k}^4\right)}{16\pi^2\left(3g_X^4 - \sum_k y_{\psi_k}^4\right)}H_b^4, \end{aligned} \tag{6.26}$$

where the sum over i runs over the gauge bosons in the SM, and the top quark effective mass. The sum also includes scalar mass terms given by $\{2\lambda_p\Phi_0^2 + 6\lambda_H H_b^2, 2\lambda_p\Phi_0^2 + 2\lambda_H H_b^2, 2\lambda_p\Phi_0^2 + 2\lambda_H H_b^2, 2\lambda_p\Phi_0^2 + 2\lambda_H H_b^2\}$. These are the effective masses one obtains from a tree level potential given by $V_{\rm tree} = 2\lambda_p\Phi_0^2|H|^2 + \lambda_H|H|^4$. Essentially, we find that Eq. (6.26) is the one-loop effective potential of the SM [188] up to the last term. This term gives a small corrections to the Higgs quartic coupling. We checked that the difference of the expansion in powers of ϵ compared to powers of H_b/Φ_0 is small. Explicitly, the terms quadratic in H_b differ by terms $\propto \lambda_p^2 H_b^2\Phi_0^2$ and for the quartic terms by terms $\propto \lambda_p H_b^4$.

6.1.4 Vector boson masses

The VEVs of H and Φ spontaneously break the gauge symmetry and give rise to the masses of the gauge bosons. The mass matrix for the neutral gauge bosons is given by Eq. (6.14) evaluated at $\Phi_b = \langle\Phi\rangle$ and $H_b = \langle H\rangle$. This matrix is diagonalized by two rotations, explicitly $U^T M_V U$ with

$$U = \begin{pmatrix} c & -sc' & ss' \\ s & cc' & -cs' \\ 0 & s' & c' \end{pmatrix}, \tag{6.27}$$

where $c = \cos\theta_W, s = \sin\theta_W$ and $c' = \cos\theta', s' = \sin\theta'$. θ_W is the weak mixing angle given by $\theta_W = \arctan\left(\frac{g_Y}{g_L}\right)$ and

$$\tan(2\theta') := -\frac{2(g_{12}+2g_X)\sqrt{g_L^2+g_Y^2}\langle H\rangle^2}{\left[g_L^2+g_Y^2-(g_{12}+2g_X)^2\right]\langle H\rangle^2 - 4\,g_X^2\langle\Phi\rangle^2}\,. \tag{6.28}$$

The eigenvalues of the vector boson mass matrix i.e. the masses of the neutral gauge bosons Z and Z' are given by

$$m_Z^2 = \frac{1}{2}(g_L^2+g_Y^2)\langle H\rangle^2 - \frac{(g_{12}+2g_X)^2(g_L^2+g_Y^2)}{8g_X^2}\frac{\langle H\rangle^4}{\langle\Phi\rangle^2} + \mathcal{O}\left(\frac{\langle H\rangle^6}{\langle\Phi\rangle^4}\right), \tag{6.29}$$

$$m_{Z'}^2 = 2g_X^2\langle\Phi\rangle^2 + \frac{1}{2}(g_{12}+2g_X)^2\langle H\rangle^2 + \frac{(g_{12}+2g_X)^2(g_L^2+g_Y^2)}{8g_X^2}\frac{\langle H\rangle^4}{\langle\Phi\rangle^2} + \mathcal{O}\left(\frac{\langle H\rangle^6}{\langle\Phi\rangle^4}\right), \tag{6.30}$$

while the third eigenvalue vanishes and the photon does not obtain a mass. The mass of the Z boson slightly different compared to the SM prediction. The new $\mathrm{U}(1)_X$ gauge group explicitly breaks the SO(4) custodial symmetry of the SM (similar to hypercharge), therefore modifying the predictions for m_W/m_Z. Keeping all SM couplings fixed, the shift in the Z mass remains in the 2σ range [189], if $\langle\Phi\rangle \gtrsim 18\,\mathrm{TeV}$. Direct Z' searches typically constrain $\langle\Phi\rangle$ to be larger than this limit.

6.1.5 Scalar masses

The scalar masses are obtained from the curvature of the effective potential at the minimum, i.e. $m_{ab}^2 = \partial_{\phi_a}\partial_{\phi_b}V_{\text{eff}}$ evaluated at $H_b = \langle H\rangle =$ and $\Phi_b = \langle\Phi\rangle$. The full expression for the mass matrix is quite unwieldy, however an approximate expression can be found. We checked numerically that these expressions give a somewhat reasonable approximation. For the Higgs boson we find

$$m_h^2 \approx \left[-\lambda_p + \frac{3\left(g_X+\frac{g_{12}}{2}\right)^2 g_X^2}{3g_X^4+4\lambda_p^2-\sum_k y_{\psi_k}^4}\left(\lambda_\Phi + \sum_k\left\{\frac{y_{\psi_k}^4}{16\pi^2}\left[\frac{2}{3}+\ln\left(\frac{2g_X^2}{y_{\psi_k}^2}\right)\right]\right\}\right)\right]\langle\Phi\rangle^2. \tag{6.31}$$

Approximating for small g_{12} and small y_ψ, this simplifies to

$$m_h^2 \approx (-\lambda_p + \lambda_\Phi)\,\langle\Phi\rangle^2, \tag{6.32}$$

illustrating the nature of the Higgs boson as a pNGB associated with spontaneous breaking of SO(6) custodial symmetry. The radial excitation, i.e. the dilaton obtains a mass given by

$$m_{h_\Phi}^2 \approx \frac{3g_X^4 - \sum_k y_{\psi_k}^4 + 4\lambda_p^2}{4\pi^2}\langle\Phi\rangle^2 \approx 2\beta_{\lambda_\Phi}\langle\Phi\rangle^2. \tag{6.33}$$

This relation illustrates the suppression of the dilaton mass by the beta functions, i.e. the scale anomaly. This is understood since the dilaton is the pNGB associated with spontaneous breaking of scale symmetry. The mixing angle θ between the dilaton and the Higgs boson is approximated by

$$\begin{aligned}\tan\theta \approx\ & \frac{\left[\lambda_p - \frac{3\left(g_X+\frac{g_{12}}{2}\right)^2 g_X^2}{3g_X^4+4\lambda_p^2-\sum_k y_\psi^4}\left(\lambda_\Phi + \sum_k\left\{\frac{y_\psi^4}{16\pi^2}\left[\frac{2}{3}+\ln\left(\frac{2g_X^2}{y_\psi^2}\right)\right]\right\}\right)\right]\langle\Phi\rangle\langle H\rangle}{m_h^2 - m_{h_\Phi}^2} \\ &+ \frac{\left[\frac{3\left(g_X+\frac{g_{12}}{2}\right)^2 g_X^2}{16\pi^2}\right]\langle\Phi\rangle\langle H\rangle}{m_h^2 - m_{h_\Phi}^2}.\end{aligned} \tag{6.34}$$

The value of this mixing angle is proportional to custodial symmetry violation and typically $\tan\theta \lesssim 10^{-2}$.

6.2 Models realizing Custodial Naturalness

6.2.1 Minimal model

The particle content of the minimal model that realizes Custodial Naturalness is given in Tab. 6.1 (top). No new fermions apart from the right-handed neutrinos are introduced. The parameter q_Φ is set to $q_\Phi = -\frac{1}{3}$. Along the RG flow towards the IR, the gauge kinetic mixing parameter g_{12} runs towards $g_{12} = \frac{14}{41}g_X$ at one-loop. In Sec. 6.1.2 we find that small positive values of g_{12} are required for EWSB. We will see below that, in the minimal model, the boundary condition $g_{12}\big|_{M_{\text{Pl}}} = 0$ leads to EWSB since g_{12} runs towards small positive values. Such a boundary condition is justified since it enhances custodial symmetry at the high scale. The scalar sector of the minimal model has only one free parameter, the SO(6) custodially symmetric coupling λ. In the new gauge sector we have another new parameter

g_X. If we do not impose $g_{12}\big|_{M_{\rm Pl}} = 0$, the model is slightly less minimal and g_{12} becomes a free parameter. In summary, we trade the two parameters of the SM Higgs potential $(m_H^{\rm SM}, \lambda_H^{\rm SM})$ for λ and g_X and the minimal model has the same number of parameters as the SM.

Since the minimal model is as predictive as the SM, in principle one should perform a fit of the model parameters to the experimental measurements. In this work we restrict ourselves to a parameter scan. Below we will see, that due to experimental uncertainties (mostly on the top pole mass), we are not able to give a single value as prediction for the Z' mass and the dilaton mass.

For our parameter scan, we will do the following: We randomly select input values at the low scale and these couplings are then run up to $M_{\rm Pl}$. At $M_{\rm Pl}$ we impose SO(6) custodial symmetry. Then we use these values that now obey SO(6) custodial symmetry as a reasonable starting point at $M_{\rm Pl}$ and run the couplings down to the intermediate scale where we calculate the effective potential and match to the SM.

In more detail, we start by choosing a random value for the top pole mass M_t in the 3σ range $M_t \in [170.4, 174.6]$ GeV. Using the formulas in Ref. [16], we obtain the values for the SM gauge and Yukawa couplings in $\overline{\rm MS}$. We fix $\lambda_H^{\rm SM}$ and $m_H^{\rm SM}$, i.e. the parameters of the SM Higgs potential by requiring that the one-loop effective potential of the SM at $\mu = M_t$ has a minimum at 246.22 GeV and the Higgs mass obtained from second derivative matches the central value of the measured Higgs mass. Using the two-loop SM RGEs, we run these couplings up to $\tilde{\mu}_0$ which is randomly chosen in the range $\tilde{\mu}_0 \in [500, 10^6]$ GeV. Next we randomly choose $g_X\big|_{\tilde{\mu}_0} \in [0, 0.20]$. We now use $\tilde{\mu}_0 = \sqrt{2} g_X \Phi_0 e^{-1/6}$ where Φ_0 is given by Eq. (6.19) to determine $\lambda_\Phi\big|_{\tilde{\mu}_0}$ (λ_p can safely be neglected in Eq. (6.19)). For λ_H and λ_p the precise values will be fixed by custodial symmetry and we use $\lambda_H\big|_{\tilde{\mu}_0} = \lambda_H^{\rm SM}\big|_{\tilde{\mu}_0}$ and $\lambda_p\big|_{\tilde{\mu}_0} = \lambda_\Phi\big|_{\tilde{\mu}_0}$ as reasonable estimates. This set of couplings is then run up to $M_{\rm Pl}$ using the two-loop RGEs of the minimal model found using `PyR@TE` [190]. At $M_{\rm Pl}$ we impose SO(6) custodial symmetry. This is done by defining $\lambda := \lambda_\Phi\big|_{M_{\rm Pl}}$. This implicitly sets $\lambda_H, \lambda_p|_{M_{\rm Pl}} = \lambda$. For the minimal setup, we then impose $g_{12}\big|_{M_{\rm Pl}} = 0$. We also consider a scenario where we choose random values for g_{12} in the range $g_{12}\big|_{M_{\rm Pl}} \in [-0.1, 0.1] \cdot g_X\big|_{M_{\rm Pl}}$. Now all parameters at the high scale are fixed. Using the two-loop RGEs, we run this set of parameters down to μ_0 which is determined by iteratively using the definition $\mu_0 = \sqrt{2} g_X \Phi_0 e^{-1/6}$ and Eq. (6.19). At μ_0 we determine the VEVs $\langle \Phi \rangle$, $\langle H \rangle$, and scalar masses m_{h_Φ} and m_h numerically from the full one-loop effective potential. In order to match to the SM, we choose $\lambda_H^{\rm SM}\big|_{\mu_0}$

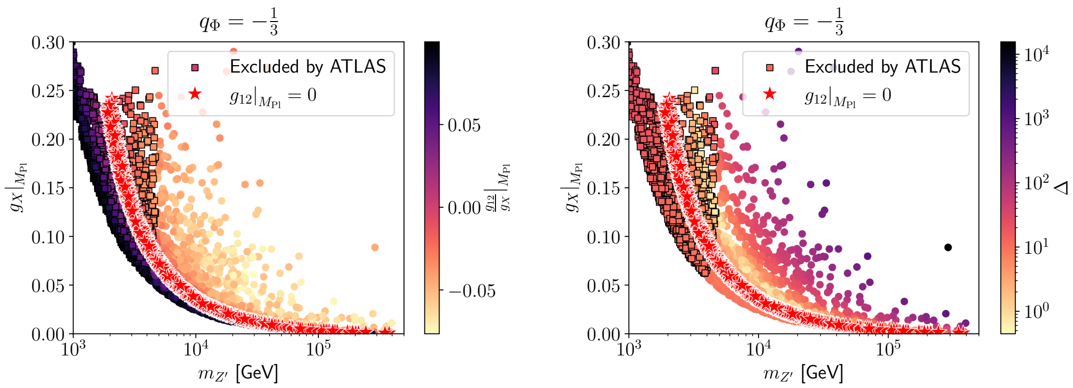

Figure 6.4: Parameter points in the minimal model that yield the correct EW scale in the $m_{Z'} - g_X$ plane. The left plot shows the amount of custodial symmetry violation given by $g_{12}/g_X\big|_{M_{\rm Pl}}$ and the right plot shows the amount of fine tuning. These figures are published in Ref. [2].

and $m_H^{\rm SM}\big|_{\mu_0}$ in such a way that the SM one-loop effective potential gives the same Higgs VEV and Higgs mass as the full effective potential Eq. (6.13), where both effective potentials are evaluated at μ_0. We then run the SM couplings down to M_t using the two-loop RGEs of the SM where we obtain the Higgs VEV and Higgs mass from the SM one-loop effective potential (at $\mu = M_t$). From the inverted formulas in Ref. [16], we obtain the top pole mass. In our plots we show points for which the Higgs VEV lies within the ± 0.1 GeV interval of the experimental value. Unless stated otherwise, no constraint on the Higgs mass is used. We checked that the points with correct Higgs mass have a similar distribution in the scatter area as points with arbitrary Higgs mass. The numerical routine agrees with the one used in Refs. [1,2] and also the same datasets are used.

Figure 6.4 shows the results of our parameter scan. For $g_{12}\big|_{M_{\rm Pl}} = 0$ (red stars) there is a clear relation between $m_{Z'}$ and g_X. If we allow for $g_{12}\big|_{M_{\rm Pl}} \neq 0$, the parameter space opens up and the hierarchy between the EW scale and the intermediate scale is determined by the value of $g_{12}\big|_{M_{\rm Pl}}$. Positive values lead to more custodial symmetry violation and therefore to a larger separation of λ_p and λ_Φ and a smaller hierarchy between the intermediate scale and the EW scale. For $g_{12}\big|_{M_{\rm Pl}} \lesssim -0.075 \cdot g_X\big|_{M_{\rm Pl}}$, $\lambda_p > \lambda_\Phi$ at $\mu = \mu_0$ and therefore EWSB does not occur.

Custodial Naturalness is a mechanism to solve the hierarchy problem, which is a problem of fine tuning. Fine tuning is often quantified using the Barbieri-Giudice measure [191]. This measure does not actually measure fine tuning, but rather sensitivity on small changes in the parameters (see Ref. [192] for a discussion). Dimensional transmutation is exponentially sensitive to changes in the parameters but still not considered fine tuning. For our purpose, we use a fine tuning measure which is a modification of the original Barbieri-Giudice measure. We quantify fine tuning of the hierarchy between the intermediate scale and the EW scale with

$$\Delta := \max_{g_i} \left| \frac{g_i}{\frac{\langle H \rangle}{\langle \Phi \rangle}} \frac{\partial \frac{\langle H \rangle}{\langle \Phi \rangle}}{\partial g_i} \right| = \max_{g_i} \left| \frac{g_i}{\langle H \rangle} \frac{\partial \langle H \rangle}{\partial g_i} - \frac{g_i}{\langle \Phi \rangle} \frac{\partial \langle \Phi \rangle}{\partial g_i} \right| . \tag{6.35}$$

Defined in this way, the sensitivity from dimensional transmutation is automatically subtracted and the tuning required for the little hierarchy, i.e. the separation between the intermediate scale and the EW scale, is quantified. In practice, we calculated Δ by using small variation of the parameters at the high scale and then evaluate the changes of the VEVs at the low scale. We show the tuning required for our parameter points in Fig. 6.4 (right). For most of our parameter space the tuning Δ is well below 10^2 and these point are not fine tuned at all. For large values of $m_{Z'}$, Δ takes larger values since for these points, tuning between the SM contributions to $\lambda_p - \lambda_\Phi$ and the contributions from g_{12} is required. Further there seems to be a minimum (valley of minimal fine tuning) present. The physical meaning of this valley is unclear. At this valley, $\Delta \sim \mathcal{O}(1)$ while outside of the minimum, Δ is roughly around 10, which is still not considered fine tuned. We also checked that this minimum is not present if, in Eq. (6.35), we replace $\langle H \rangle$ by m_h. The order of magnitude for Δ outside of the valley does not change.

The strongest direct constraints on our model come from direct Z' searches. We calculate the Z' production cross section times branching ratio into dileptons (e^+e^- and $\mu^+\mu^-$) using `MadGraph5_aMC@NLO` [196]. The `UFO` file [197] was generated using `FeynRules` [198]. We show the fiducial cross section times branching ratio for our parameter points and the comparison to the current limits for dilepton searches at ATLAS [193] and CMS [194] in Fig. 6.5 (left). We use the same fiducial cuts as in Ref. [193]. We also calculate the fiducial cross section times branching ratio for different values of $m_{Z'}$ and g_X (see Fig. 6.5 (right)). This allows us to recast the limits from Ref. [193] by finding the value of $m_{Z'}$ for which the line with constant g_X intersects the 95% C.L. exclusion limit from ATLAS. If there a two intersections of these lines, we take the lower value. Interpolating then yields the limits in the $m_{Z'} - g_X$ plane.

The minimal setup with $g_{12}\big|_{M_{\rm Pl}} = 0$ has the same number of parameters as the SM. In principle this allows us to fix all the parameters by the measurements of

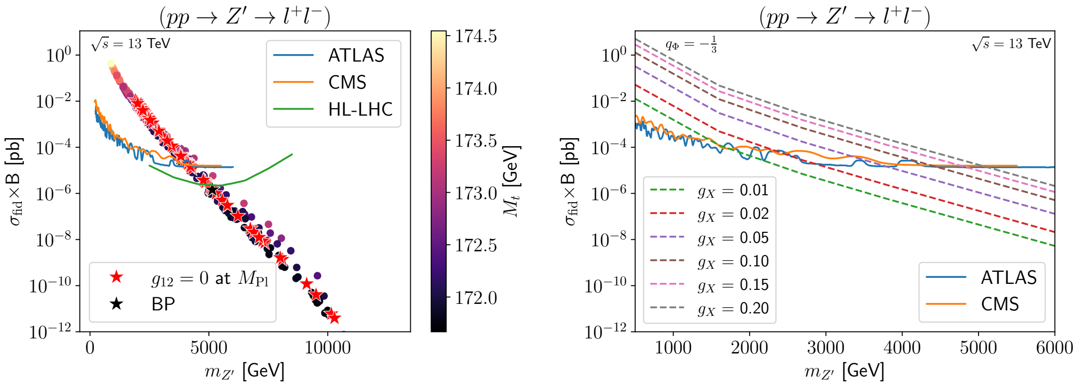

Figure 6.5: Left: Production cross section times branching ratio ($Z' \to l^+l^-$ for $l = e, \mu$) for the parameter points of the minimal model with correct Higgs mass and the limits from dilepton searches at ATLAS [193] and CMS [194] at 95% C.L. Also shown are expected limits at HL-LHC at 14 TeV [195]. Right: Production cross section times branching ratio for different values of $m_{Z'}$ and g_X for $q_\Phi = -\frac{1}{3}$. The same cuts as in Ref. [193] are used. These figures are published in Ref. [2].

the masses and interactions of the SM fields, and the Z' mass and dilaton mass are predictions. However, in practice a large range of values for these two masses is possible. This is mainly due to the experimental uncertainty on the top mass. The top Yukawa coupling gives a large contribution in the running of λ_H. The uncertainty is magnified by the running over orders of magnitude and manifests as an uncertainty in the prediction of the Higgs mass. We show the relation between the Higgs mass and the top quark mass in Fig. 6.6 (top left) for all points not excluded by direct Z' searches. In the minimal setup, there is an approximately linear relation and the measurement of the Higgs mass constrains the top pole mass to lie at the lower end of the 1σ range of the current measurement. In order to fix the Z' mass, the top quark mass needs to be measured with permille level accuracy. For $g_{12}\big|_{M_{\rm Pl}} \neq 0$, most points still obey the same linear relation as in the minimal setup while a few points reach to larger values of M_t and there are no points with correct Higgs mass and $M_t \lesssim 171.5\,\text{GeV}$.

The mass of the dilaton, given by Eq. (6.33), is suppressed by β_{λ_Φ} compared to the intermediate scale. We show the numerical results for m_{h_Φ} in Fig. 6.6 (top right). The points with $g_{12}\big|_{M_{\rm Pl}} = 0$ (red stars) give a dilaton mass of $\approx 70\,\text{GeV}$ and therefore, in the minimal scenario, the dilaton is always lighter than the Higgs

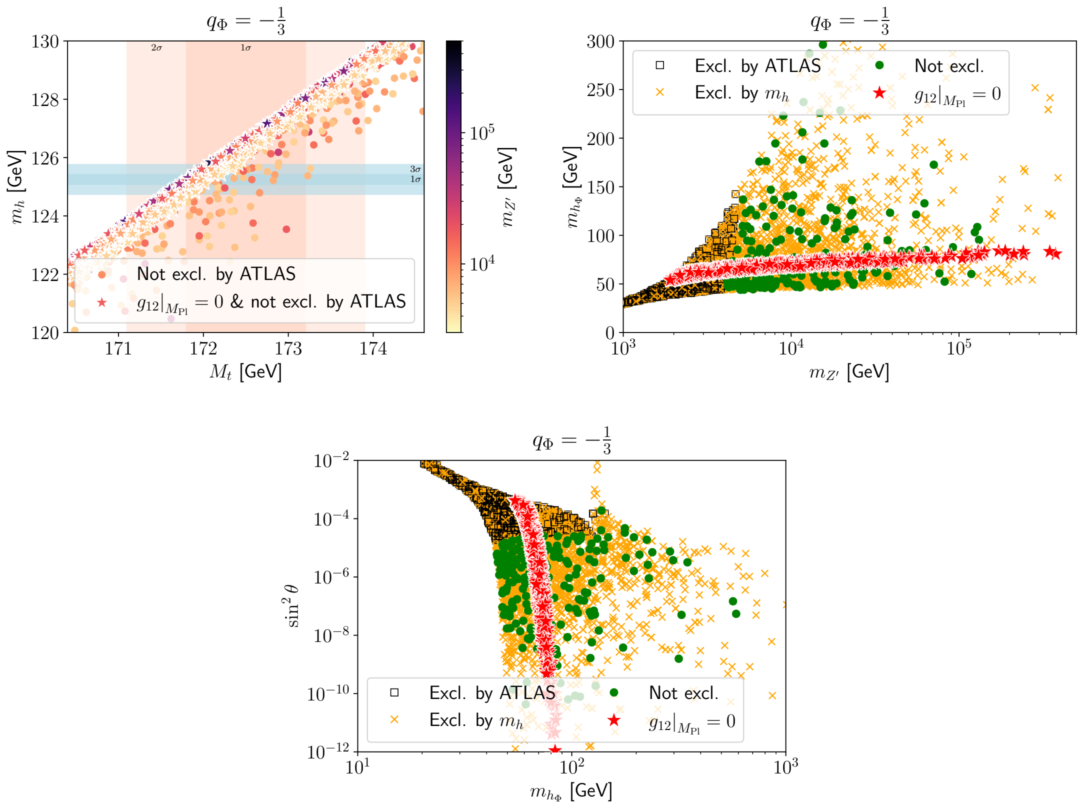

Figure 6.6: The top pole mass vs the Higgs mass for parameter points not excluded by dilepton searches in the minimal model (top left). White bordered stars indicate points with $g_{12}\big|_{M_{\rm Pl}} = 0$. Parameter points of the minimal model in the $m_{Z'} - m_{h_\Phi}$ plane (top right) and the mixing angle θ vs the dilaton mass m_{h_Φ} (bottom). The points marked with orange crosses have a Higgs mass outside of the 3σ range and the black squares indicate points excluded by dilepton searches. These figures are published in Ref. [2].

boson. With $g_{12}\big|_{M_{\rm Pl}} \neq 0$, the dilaton mass varies between 40 GeV and a few 100 GeV.

The Higgs dilaton mixing angle, given by Eq. (6.34), is suppressed by $\langle H\rangle/\langle\Phi\rangle$ and typically $\sin^2\theta \lesssim 10^{-5}$ for viable points (see Fig. 6.6). Experimental constraints on the Higgs-scalar mixing angle [199–201] are therefore avoided. If $m_h \approx m_{h_\Phi}$, the mixing angle is much larger reaching values up to $\sin^2\theta \sim \mathcal{O}(1)$.

6.2.2 Neutrino portal model

The minimal fermionic extension is given in Tab. 6.1 (middle). The charges of ψ_L and ψ_R are chosen in such a way that there is a Yukawa interaction involving Φ (see Eq. (6.6)). This Yukawa interaction automatically involves the right-handed neutrinos. We further choose $q_\Phi = -\frac{3}{8}$. For this choice, along the RG flow towards the IR, the gauge kinetic mixing parameter g_{12} runs towards $g_{12} = \frac{10}{123} g_X$ at one-loop. If g_{12} is set to zero at Planck scale, the contributions of gauge kinetic mixing to $\lambda_p - \lambda_\Phi$ are too small to overcome the SM contributions. We need to introduce additional sources of custodial symmetry violation in order to obtain EWSB. This is achieved by considering non vanishing Yukawa interaction involving Φ, i.e. $y_\psi \neq 0$ or simply taking $g_{12}\big|_{M_{\rm Pl}} > 0$.

The VEVs of the scalar field generate Dirac mass terms for the neutral fermions given by

$$\begin{aligned}
\mathcal{L}_{\rm mass} &\supset y_\nu^{\alpha\beta}\langle H\rangle \overline{\nu}_L^\alpha \nu_R^\beta + y_\psi^\beta \langle\Phi\rangle \overline{\psi}_L \nu_R^\beta + \text{h.c.} \\
&= \begin{pmatrix} \overline{\nu}_L^\alpha & \overline{\psi}_L \end{pmatrix} \begin{pmatrix} y_\nu^{\alpha\beta}\langle H\rangle & 0 \\ y_\psi^\beta\langle\Phi\rangle & 0 \end{pmatrix} \begin{pmatrix} \nu_R^\beta \\ \psi_R \end{pmatrix} + \text{h.c.} \\
&=: \begin{pmatrix} \overline{\nu}_L^\alpha & \overline{\psi}_L \end{pmatrix} M_N \begin{pmatrix} \nu_R^\beta \\ \psi_R \end{pmatrix} + \text{h.c.}
\end{aligned} \tag{6.36}$$

After symmetry breaking there remains an accidental global lepton number symmetry and Majorana mass terms are not generated. ψ_R does not have a Yukawa interaction and therefore ψ_R remains a massless Weyl spinor due to unbroken chiral symmetry. This implies that there also will be a massless left handed Weyl spinor. We can obtain the masses of the neutral fermions by the eigenvalues of

$$M_N M_N^\dagger = \begin{pmatrix} y_\nu^{\alpha\beta}(y_\nu^\dagger)^{\beta\alpha'}\langle H\rangle^2 & y_\nu^{\alpha\beta}(y_\psi^*)^\beta\langle H\rangle\langle\Phi\rangle \\ y_\psi^\beta(y_\nu^\dagger)^{\beta\alpha'}\langle H\rangle\langle\Phi\rangle & y_\psi^\beta(y_\psi^*)^\beta\langle\Phi\rangle^2 \end{pmatrix}. \tag{6.37}$$

The lower left entry of this matrix dominates and the mass of the heavy eigenstate is, assuming real Yukawa couplings, given by $m_\psi \approx \sqrt{y_\psi^\beta y_\psi^\beta}\langle\Phi\rangle = \bar{y}_\psi\langle\Phi\rangle$. The Dirac spinor corresponding to this heavy eigenstate can be written as

$$\Psi \sim \begin{pmatrix} \cos(\alpha_\psi)\psi_L + \sin(\alpha_\psi)\nu_L \\ \nu_R' \end{pmatrix}, \tag{6.38}$$

for a linear combination of the right-handed neutrinos ν_R'. The mixing angle α_ψ between ψ_L and the active neutrinos is approximately given by $\sin(\alpha_\psi) \approx y_\nu\langle H\rangle/\langle\Phi\rangle$ where y_ν denotes a typical entry of the neutrino Yukawa matrix $y_\nu^{\alpha\beta}$. The two light but massive eigenstates have a mass of approximately $y_\nu\langle H\rangle$ and therefore $y_\nu \sim 10^{-11}$. This implies that $\sin(\alpha_\psi) \ll 10^{-11}$. Since the matrix Eq. (6.37) has rank three, the remaining state is a massless Weyl spinor given by an active left handed neutrino. While the addition of the minimal set of new fermions populates the neutrino portal, we do not explain the smallness of neutrino masses.

We study the parameter space of the neutrino portal model using a parameter scan with the same setup as in the minimal model. We perform two scans, one where we randomly sample $\bar{y}_\psi = 0$ and $g_{12}\big|_{M_{\text{Pl}}} \in [0, 0.2] \cdot g_X\big|_{M_{\text{Pl}}}$ and one with $\bar{y}_\psi\big|_{\tilde{\mu}_0} \in [0, 0.9] \cdot g_X\big|_{\tilde{\mu}_0}$ and $g_{12}\big|_{M_{\text{Pl}}} = 0$ while all other parameters are sampled in the same range as in the minimal model. The same dataset has been used in Ref. [2].

As discussed earlier, in models with $q_\Phi = -\frac{3}{8}$, additional sources of custodial symmetry violation are required to overcome the SM contributions to $\lambda_p - \lambda_\Phi$ and ensure that the Higgs field obtains a VEV. In Fig. 6.7 (top) we illustrate how this can be achieved by $g_{12}\big|_{M_{\text{Pl}}} > 0$ and by $\bar{y}_\psi \neq 0$. For large values of g_{12} or $\bar{y}_\psi$, custodial symmetry violation is large and the hierarchy between the EW and the intermediate scale is small. We also show the fine tuning required for each parameter point in Fig. 6.7 (bottom).

We also recast the Z' limits from dilepton searches for models with $q_\Phi = -\frac{3}{8}$. We use the same setup as for the minimal model and we do not include the effects of the new fermions as final states. This does affect the width of the Z' boson, however, we checked that the effect on our results is negligible. The fiducial cross section times branching ratio for different values of $m_{Z'}$ and g_X are shown in Fig. 6.8. The recast limits obtained for $q_\Phi = -\frac{3}{8}$ are very similar to the limits obtained for $q_\Phi = -\frac{1}{3}$ and in all plots in this chapter, points excluded by these limits are again marked by black squares.

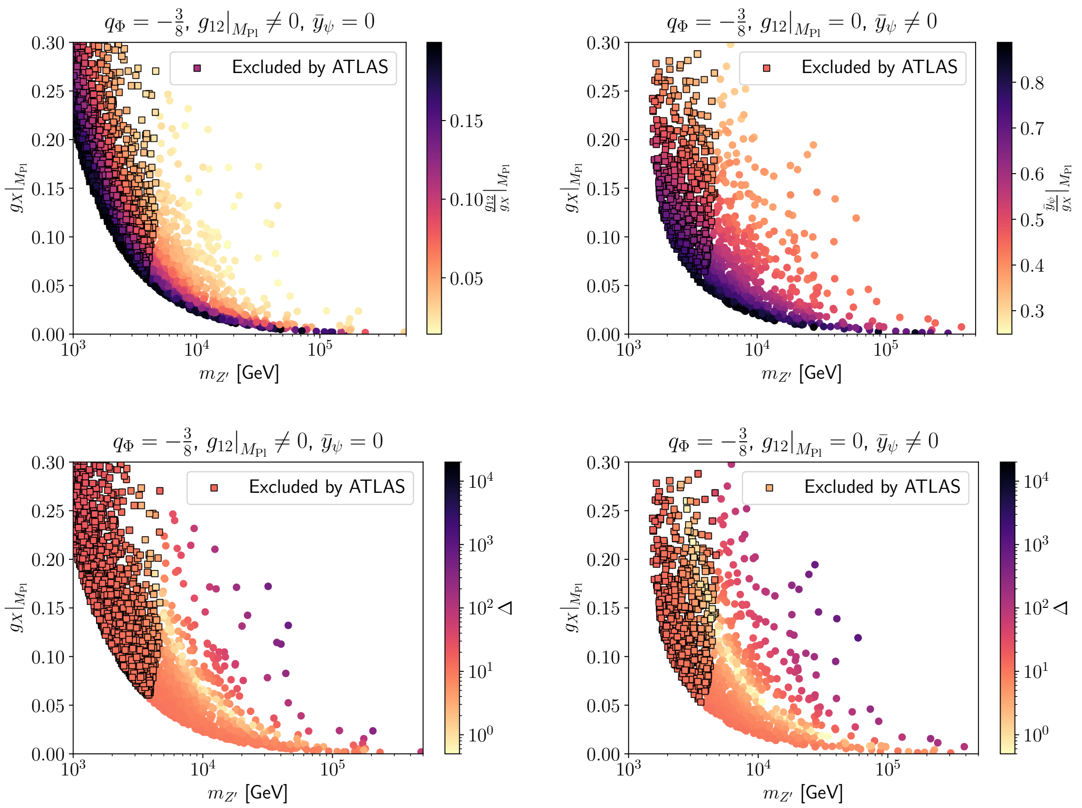

Figure 6.7: Parameter points in the neutrino portal model that yield the correct EW scale. The top plots show the custodial symmetry violation and the bottom plots show the amount of fine tuning. The plots on the left have $\bar{y}_\psi^\alpha = 0$ and $g_{12}\big|_{M_{\rm Pl}} \neq 0$ and the plots on the right have $\bar{y}_\psi^\alpha \neq 0$, $g_{12}\big|_{M_{\rm Pl}} = 0$. These figures are published in Ref. [2].

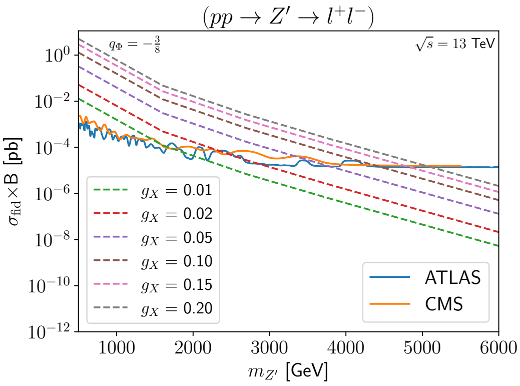

Figure 6.8: Production cross section times branching ratio for different values of $m_{Z'}$ and g_X for $q_\Phi = -\frac{3}{8}$ and the 95% C.L. limits from ATLAS [193] and CMS [194]. The same cuts as in Ref. [193] are used.

The top pole mass and the Higgs mass have a similar linear relation as in the minimal model while a few points with correct Higgs mass reach the upper end of the 3σ range for the top mass uncertainty (see Fig. 6.9 (top)). For $\bar{y}_\psi \neq 0$ the dilaton mass can reach small values if $3g_X^4 \approx \bar{y}_\psi^4$ (see Eq. (6.33)). The numerical results for the dilaton mass are shown Fig. 6.9 (middle). For $\bar{y}_\psi \neq 0$ the dilaton mass is limited by the scan range of $\bar{y}_\psi$ and for $\bar{y}_\psi = 0, g_{12}\big|_{M_{\rm Pl}} \neq 0$ the dilaton mass takes similar values as in the minimal model with $g_{12}\big|_{M_{\rm Pl}} \neq 0$. Also shown are the values for the Higgs dilaton mixing angle for our parameter points in Fig. 6.9 (bottom).

6.2.3 Dark matter model

In the DM model we introduce two vector like fermions that do not interact with the neutrino sector. The charges are chosen in such a way that Yukawa interactions involving Φ are possible (see Eq. (6.7)). The charges of these new fermions are found in Tab. 6.1 (bottom). The parameter α is only constrained by the requirement that the Yukawa interaction involving right-handed neutrinos is forbidden. For our parameter scans, we choose $\alpha = \frac{1}{2}$. Similar to the neutrino portal model, we choose $q_\Phi = -\frac{3}{8}$ which necessitates additional sources of custodial symmetry violation for realistic EWSB.

The VEV of Φ generates mass terms for the new fermions given by

$$\mathcal{L}_{\rm mass} \supset y_\psi \langle\Phi\rangle \bar{\psi}_L \psi_R + y_{\psi'} \langle\Phi\rangle \bar{\psi'}_L \psi'_R + \text{h.c.} =: m_\psi \bar{\psi}_L \psi_R + m_{\psi'} \bar{\psi'}_L \psi'_R + \text{h.c.} \quad (6.39)$$

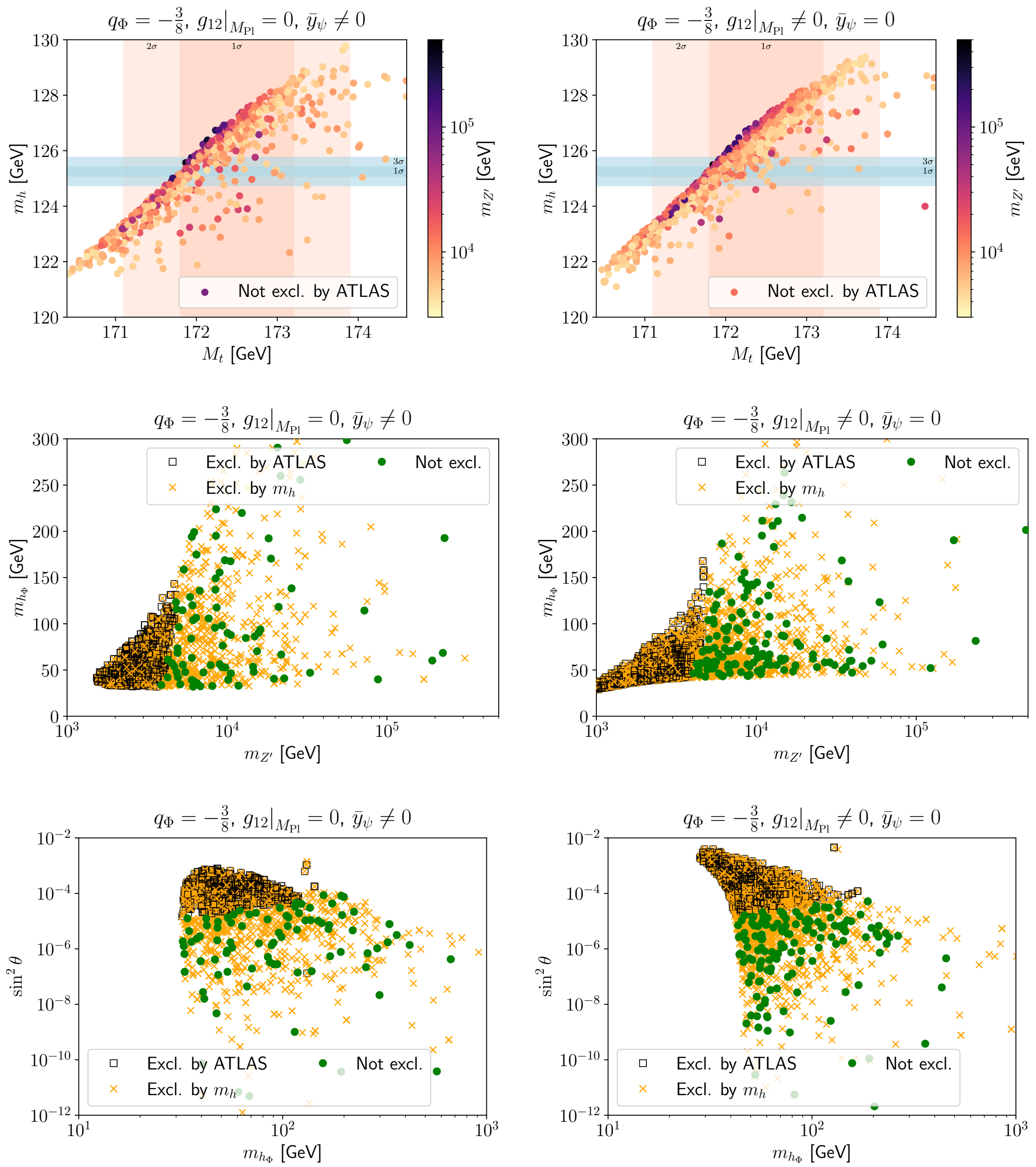

Figure 6.9: The top pole mass vs the Higgs mass for parameter points not excluded by dilepton searches in the neutrino portal model (top). Parameter points of the neutrino portal model in the $m_{Z'} - m_{h_\Phi}$ plane (middle) and the mixing angle θ vs the dilaton mass m_{h_Φ} (bottom). The points marked with orange crosses have a Higgs mass outside of the 3σ range and the black squares indicate points excluded by dilepton searches. The plots on the left have $\bar{y}^\alpha_\psi = 0$ and $g_{12}\big|_{M_{\rm Pl}} \neq 0$ and the plots on the right have $\bar{y}^\alpha_\psi \neq 0$, $g_{12}\big|_{M_{\rm Pl}} = 0$. These figures are published in Ref. [2].

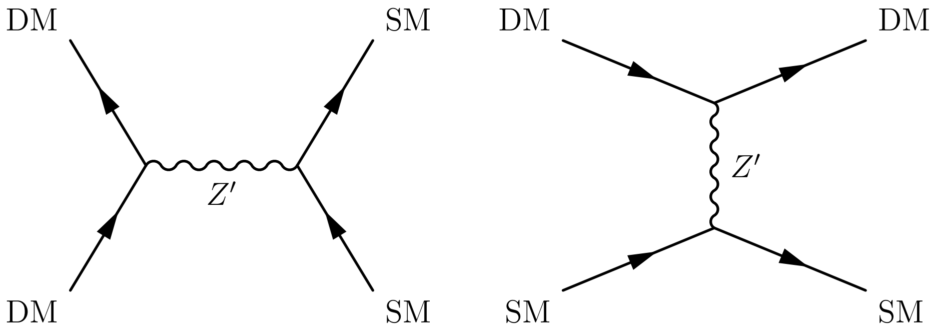

Figure 6.10: Feynman diagrams for the DM annihilation via the Z' channel (left) and the Feynman diagram for the spin independent DM nucleon scattering (right). These are the dominant diagrams for the respective process.

and we denote the two massive Dirac fermions as ψ and ψ'. After symmetry breaking the Lagrangian is symmetric under two global accidental U(1) symmetries under which only ψ and ψ' transform. This guarantees that ψ and ψ' are stable and therefore they constitute two-component DM candidates.

In this section, we assume that ψ and ψ' are in thermal equilibrium in the early universe. This assumption is only correct, if the reheating temperature after the phase transition to the $\mathrm{U}(1)_X$ breaking vacuum is high enough. In this case ψ and ψ' are produced via Z' decays. The thermal history of the Universe for models similar to ours in discussed in Sec. 6.3. We note that, if the reheating temperature is not high enough, then ψ and ψ' do not reach thermal equilibrium and the DM relic density needs to be reevaluated. Naively, we expect that in this case the relic is smaller compared to the results presented in this section, which in turn opens up the allowed parameter space [202].

The DM candidates ψ and ψ' form two-component DM and the total DM relic density is given by

$$\Omega h^2 = (\Omega h^2)_\psi + (\Omega h^2)_{\psi'}, \tag{6.40}$$

where $(\Omega h^2)_\psi$ and $(\Omega h^2)_{\psi'}$ denote the relic density of ψ and ψ' respectively. ψ and ψ' separately freeze out and the dominant DM annihilation channel is given in Fig. 6.10 (left) with SM fermions in the final state.

To study the allowed parameter space for the DM model, we conduct a parameter scan. We use the same basic setup as in the previous sections. We conduct two scans, one where we choose $g_{12}\big|_{M_{\mathrm{Pl}}} = 0$ and one with $g_{12}\big|_{M_{\mathrm{Pl}}} = -0.1 \cdot g_X\big|_{M_{\mathrm{Pl}}}$. For simplicity, we set $y_\psi = y_{\psi'}$ and randomly choose $y_\psi \in [0, 0.8] \cdot g_X\big|_{\tilde{\mu}_0}$. Similar to the neutrino portal model, non-zero values for y_ψ and y_ψ are required to cancel the SM contributions to $\lambda_p - \lambda_\Phi$ and lead to successful EWSB. For the scan with

$g_{12}\big|_{M_{\rm Pl}} = -0.1 \cdot g_X\big|_{M_{\rm Pl}}$, the Yukawa interaction also need to cancel the contributions from gauge kinetic mixing. The results of our parameter scan are shown in Fig. 6.11. Similar to the previous sections, the hierarchy between the intermediate and EW scale is smaller, if custodial symmetry violation in form of $y_\psi = y_\psi$ is larger (Fig. 6.11 (top)). The scan with $g_{12}\big|_{M_{\rm Pl}} = -0.1 \cdot g_X\big|_{M_{\rm Pl}}$ allows for larger values of m_ψ at fixed $m_{Z'}$ compared to the scan with $g_{12}\big|_{M_{\rm Pl}} = 0$. We also show the amount of fine tuning calculated from Eq. (6.35) in Fig. 6.11 (middle). For the scan with $g_{12}\big|_{M_{\rm Pl}} = -0.1 \cdot g_X\big|_{M_{\rm Pl}}$, the cancellation of the contributions to $\lambda_p - \lambda_\Phi$ from gauge kinetic mixing and the Yukawa couplings need to cancel and therefore the tuning is larger compared to the scan with $g_{12}\big|_{M_{\rm Pl}} = 0$. Assuming thermal equilibrium for ψ and ψ' we calculate the relic density via the freeze out process using `micrOMEGAs 6.0.5` [203]. The model files are generated with `SARAH-4.15.2` [204]. The results for the relic density is shown in Fig. 6.11 (bottom). Near the Z' resonance for DM annihilation (i.e. $m_\psi \approx m_{\psi'} \approx \frac{1}{2} m_{Z'}$), the relic density turns out to be close to and below the observed value of $\Omega h^2 = 0.12$ [205] while in the rest of the parameter space the relic density is too large. For our parameter scan we used $y_\psi = y_{\psi'}$. It turns out that this needs to hold up to deviations of a few percent, in order for m_ψ and $m_{\psi'}$ to be close to the Z' resonance simultaneously. The relation $y_\psi = y_{\psi'}$ can be imposed by a parity-like symmetry that exchanges $\psi_L \leftrightarrow \psi'_R$ and $\psi'_L \leftrightarrow \psi_R$. In Fig. 6.11, all points that overproduce DM are marked with gray bordered plus symbols. For the scan with $g_{12}\big|_{M_{\rm Pl}} = 0$, only few points are not excluded by ATLAS and yield $\Omega h^2 \leq 0.12$. For the scan $g_{12}\big|_{M_{\rm Pl}} = -0.1 \cdot g_X\big|_{M_{\rm Pl}}$ the parameter space opens up since for fixed $m_{Z'}$ the ratio $m_\psi / m_{Z'}$ is larger. Thus points with $m_\psi \approx m_{\psi'} \approx \frac{1}{2} m_{Z'}$ have larger values of $m_{Z'}$ where ATLAS is less sensitive.

The scattering cross section for DM scattering off nucleons can be calculated using `micrOMEGAs 6.0.5`. The dominant contribution to WIMP nucleon scattering is given by the t-channel Z' exchange (see Fig. 6.10 (right)). Assuming $m_\psi = m_{\psi'}$, the spin independent scattering cross section $\sigma_{\rm SI}$ for both ψ and ψ' is identical ($\sigma_{\rm SI} = \sigma_{\rm SI}(\psi) = \sigma_{\rm SI}(\psi')$). We show the spin independent scattering cross section for our parameter points in Fig. 6.12. The ATLAS limits on the Z' boson already exclude all points accessible by XENONnT. The sensitivity of the DARWIN experiment will reach the neutrino floor and probe parts of our parameter space [208]. Fermionic DM with a heavy Z' mediator have been widely studied in the literature, see e.g. Refs. [209–214].

We show the relation between the top pole mass and the Higgs mass in Fig. 6.13 (top). The results are very similar to the behavior found in the previous sections. The points for which DM is not overproduced seem to be evenly distributed in

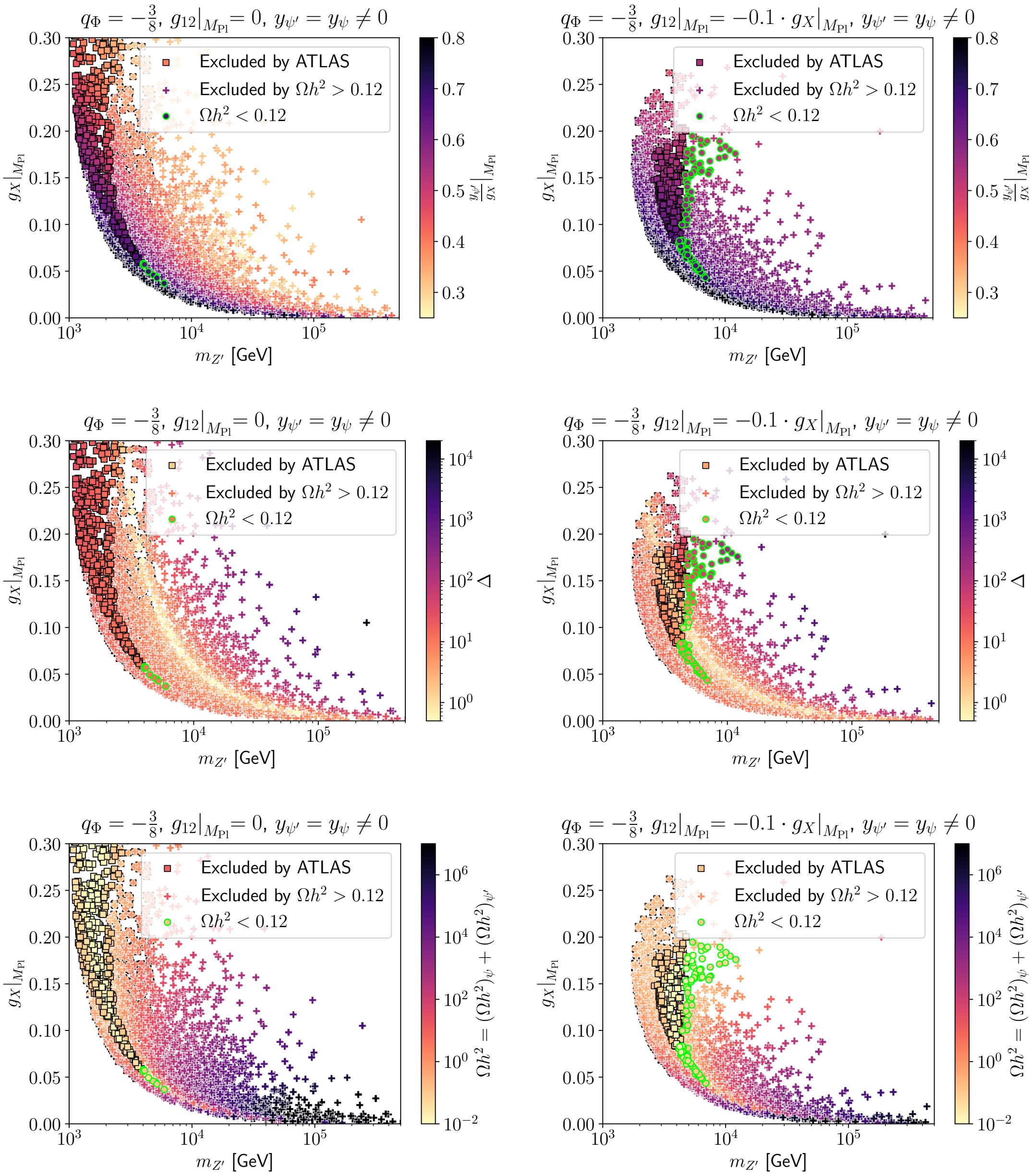

Figure 6.11: Parameter points in the DM model that yield the correct EW scale. Shown are the amount of custodial symmetry violation (top) and the amount of fine tuning (middle) and the DM relic density (bottom) for the scans with $g_{12}\big|_{M_{\rm Pl}} = 0$ (left) and $g_{12}\big|_{M_{\rm Pl}} = -0.1 \cdot g_X\big|_{M_{\rm Pl}}$ (right). All plots assume $y_\psi = y_{\psi'}$. Points excluded by ATLAS searches are marked with black squares and point for which DM is overproduced are marked with gray plus symbols while the remaining points are marked by a bright green border. These figures are published in Ref. [2].

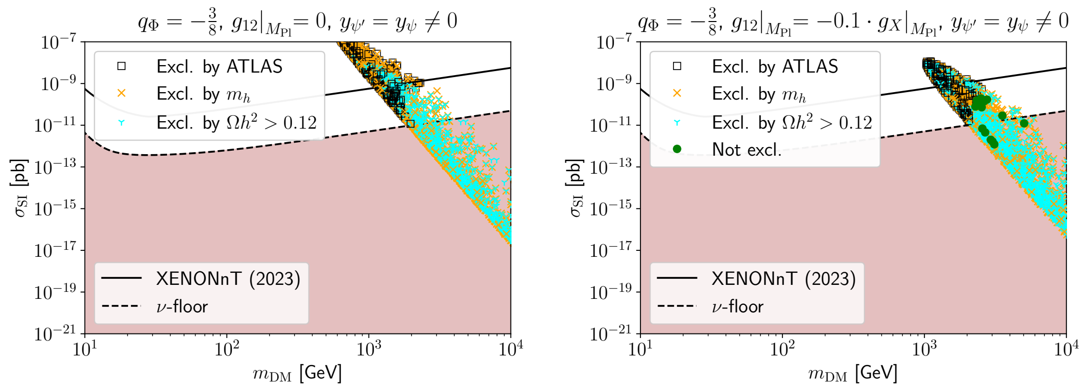

Figure 6.12: Spin independent DM nucleon scattering cross section for the DM model. Also shown are the XENONnT limits [206] (black line) and neutrino floor [207] (black dashed line). Points excluded by ATLAS are marked with black squares, points where the Higgs mass is outside of its 3σ range are marked by orange crosses and the cyan "tri-down" points are used to indicate points which yield a relic density $\Omega h^2 > 0.12$. The green points are not excluded. These figures are published in Ref. [2].

the scatter area. We also show the dilaton mass as a function of $m_{Z'}$ in Fig. 6.13 (middle) and the Higgs dilation mixing angle in Fig. 6.13 (bottom). The results agree with those for the neutrino model with $\bar{y}_\psi \neq 0$.

6.3 Experimental signatures

The massive Z' boson in our models has couplings to all SM fermions and can be searched for at colliders. We already discussed the current limits from dilepton searches [193, 194] which exclude $m_{Z'} \lesssim 4\,\text{TeV}$. The reach to higher masses is limited since at LHC, a heavy on-shell Z'-boson can only be produced from the high momentum tail of the parton distribution function. We show the limits recast from ATLAS and projections for proposed future colliders in Fig. 6.14. The projections, taken from Ref. [215, Fig. 8.3], assume hypercharge-universal couplings of the Z' boson. The couplings of the Z' boson in our models differ by an $\mathcal{O}(1)$ factor compared to the hypercharge-universal Z' boson. Large parts of our parameter space can be probed by these proposed future colliders. In the DM model, all viable points found in our scans can be tested by HE-LHC, FCC-$hh/ee/eh$ or a 10 TeV muon collider.

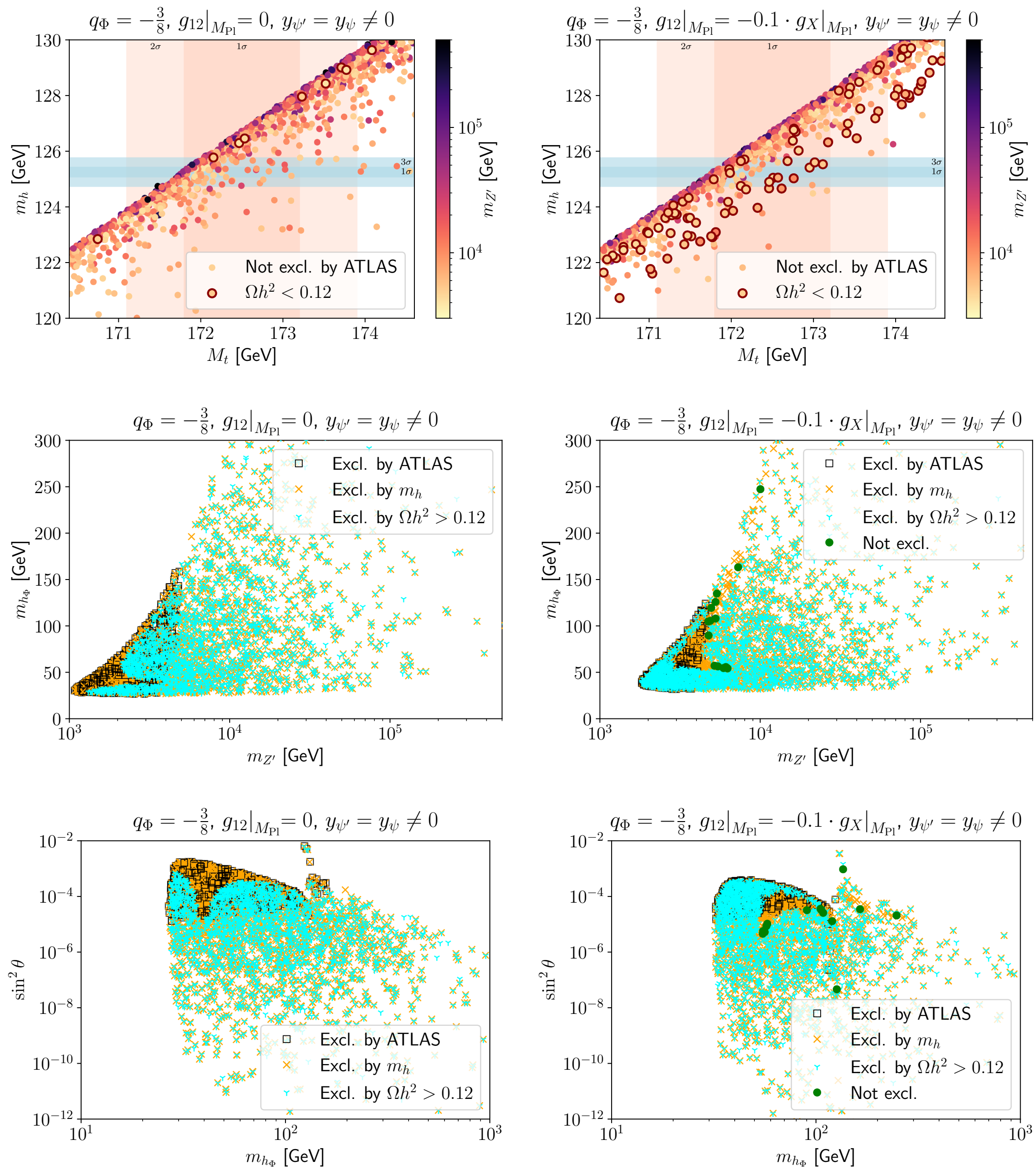

Figure 6.13: The relation of the top pole mass and the Higgs mass for points not excluded by ATLAS (top). Points with $\Omega h^2 < 0.12$ are dark bordered. Parameter points of the DM model in the $m_{Z'} - m_{h_\Phi}$ plane (middle) and the mixing angle θ vs the dilaton mass m_{h_Φ} (bottom). Points excluded by the ATLAS are marked with black squares, points where the Higgs mass is outside of its 3σ range are marked by orange crosses and the cyan “tri-down” points are used to indicate points which yield a relic density $\Omega h^2 > 0.12$. The green points are not excluded. These figures are published in Ref. [2].

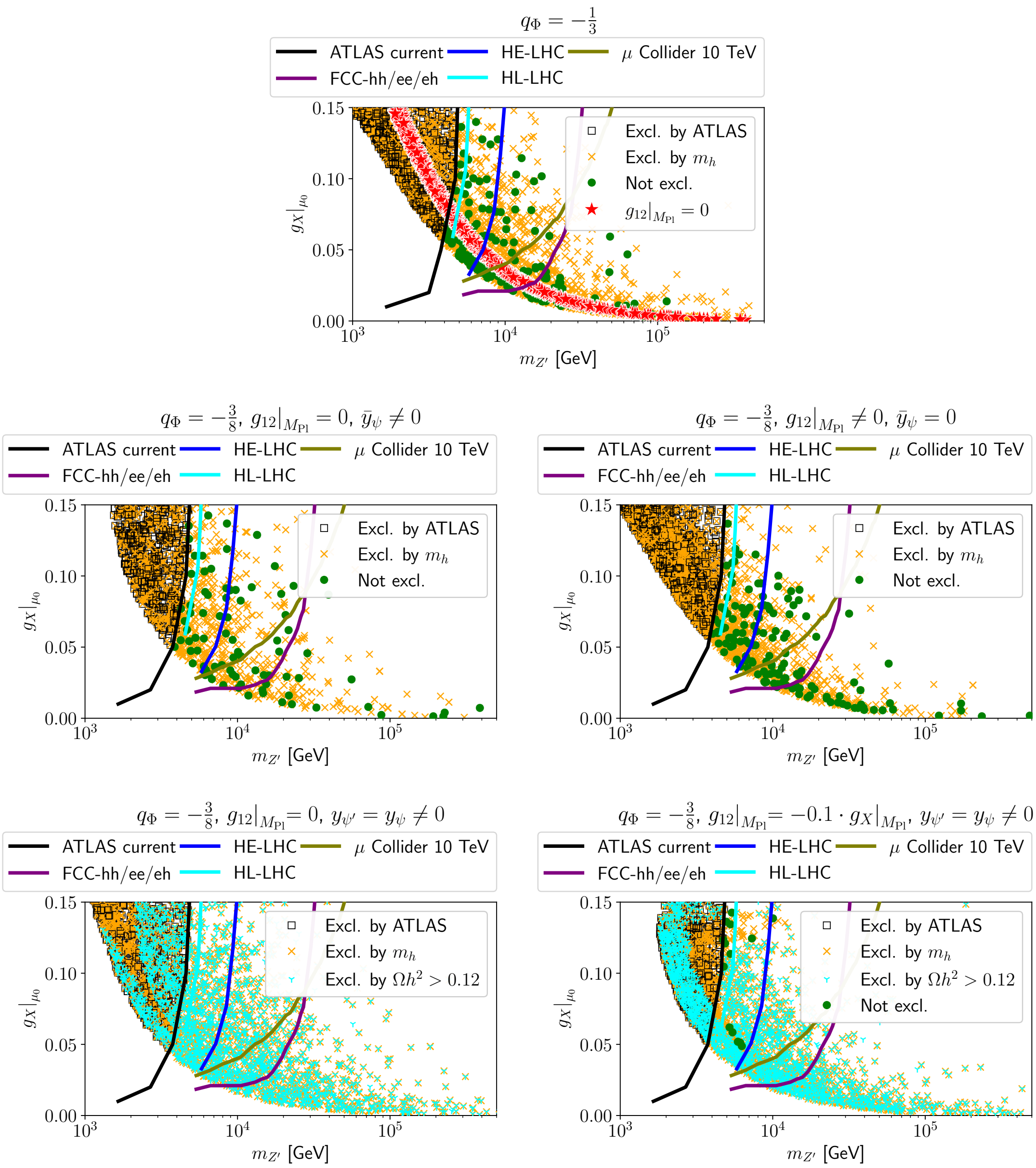

Figure 6.14: Parameter points in the $m_{Z'} - g_X\big|_{\mu 0}$ plane for the minimal model (top), the neutrino portal model (middle) and the DM model (bottom). Points excluded by the ATLAS are marked with black squares, points where the Higgs mass is outside of its 3σ range are marked by orange crosses and, for the DM model, the cyan "tri-down" points are used to indicate points which yield a relic density $\Omega h^2 > 0.12$. The green points are not excluded. Explicitly shown are the recast ATLAS limits [193] and the projections Z' searches at future colliders (assuming hypercharge universal couplings) Ref. [215]. These figures are published in Ref. [2].

The dilaton typically has a mass roughly in the 40 − 400 GeV range and a mixing angle with the Higgs boson $\sin^2\theta \lesssim 10^{-5}$. The Higgs-dilaton mixing induces a coupling of the dilaton to the SM fields given by $\mathcal{O}_{h_\Phi} \approx \sin\theta \times \mathcal{O}^{\rm SM}_{h\to h_\Phi}$ where $\mathcal{O}^{\rm SM}_{h\to h_\Phi}$ are the SM operators involving the Higgs boson h where h is replaced by the dilaton h_Φ. Further interactions of the dilaton could originate from the trace anomaly [216–218]. These interaction involve pairs of gauge boson and are suppressed by h_Φ/v_Φ and therefore easily avoided [219, 220].

Dilaton production at colliders is possible through the Higgs mixing with an estimated efficiency of one dilaton per 10^5 Higgs bosons assuming $\sin^2\theta \sim \mathcal{O}(10^{-5})$. With smaller mixing angles, the production is further suppressed. However for such small mixing angles, the dilaton becomes long lived. For example, with $\sin^2\theta \sim \mathcal{O}(10^{-7})$ we expect one dilaton with a lifetime of $\tau_{h_\Phi\to \rm SM} \sim \mathcal{O}(10^{-15}\,\text{s})$ per 10^7 Higgs bosons. This opens up the possibility for displaced vertex searches at Higgs factories [221–223].

The three-scalar vertices in the limit ($g_{12} \ll 1$, $y_\psi \ll 1$ and $\lambda_\Phi - \lambda_p \ll 1$) are approximated by

$$\frac{\partial^3 V_{\rm eff}}{\partial h^3} \approx 6\lambda_H \sqrt{2}\langle H\rangle, \tag{6.41}$$

$$\frac{\partial^3 V_{\rm eff}}{\partial h^2 \partial h_\Phi} \approx \left(m^2_{h_\Phi} - m^2_h\right) \frac{1}{\sqrt{2}\langle\Phi\rangle}, \tag{6.42}$$

$$\frac{\partial^3 V_{\rm eff}}{\partial h \partial h^2_\Phi} \approx \left(3m^2_{h_\Phi} - m^2_h\right) \frac{\langle H\rangle}{\sqrt{2}\langle\Phi\rangle^2}. \tag{6.43}$$

If $2m_{h_\Phi} < m_h$, the Higgs decay to two dilatons is kinematically allowed, however strongly suppressed with a branching ratio of roughly $\Gamma_{h\to h_\Phi h_\Phi}/\Gamma_{h,\rm tot} \sim \mathcal{O}(10^{-8})$. The dilaton emission from a virtual Higgs $h \to h h_\Phi$ is also highly suppressed.

6.4 Finite temperature effects

In the cosmological evolution of the Universe one needs to include temperature corrections to the effective potential. It turns out that models with Coleman-Weinberg symmetry breaking generically have a first order phase transition (FOPT) [23, 224, 225].

The models discussed in this chapter are very similar to the classically conformal $B - L$ model. In particular, the minimal model that realizes Custodial Naturalness has the same particle content as the classically conformal $B - L$ model. The differences are that in the minimal model Φ has a charge of $q_\Phi = -\frac{1}{3}$ in the

$B-L$ basis compared to the value $q_\Phi = 2$ in the classically conformal $B-L$ model and that we impose SO(6) custodial symmetry. Refs. [226–230] investigate the thermal history of the Universe in the classically conformal $B-L$ model. We note that Ref. [228] considers different values for the gauge kinetic mixing parameter showing that the qualitative results are fairly independent of this parameter. Therefore, we expect the cosmological evolution of the Universe in our models to closely resemble the evolution in the classically conformal $B-L$ model. The different values of q_Φ can be largely compensated by rescaling of the gauge coupling. In this section we briefly summarize the main findings of Refs. [226–230]. A detailed analysis of the finite temperature potential and the phase transitions should be conducted in future work.

For a sufficiently high temperature T, the effective potential has a minimum at $\Phi = 0$ and $H = 0$. During the expansion of the Universe, the temperature drops and the potential develops a second minimum. At a critical temperature $T_c \sim m_{Z'}$, this second minimum becomes the global minimum however the fields Φ and H remain trapped at $(\Phi, H) = (0, 0)$ due to a thermal barrier which does not disappear at low temperatures. The fields can tunnel to the global minimum which leads to the formation of bubbles. In the classically conformal $B-L$ model, the percolation temperature T_p, i.e. the temperature where the formation and expansion of bubbles becomes efficient, is $T_p \ll T_c$. Since the fields are trapped in the false vacuum, this leads to a period of thermal inflation with $N \sim 10$ [228] where N is the number of e-folds. For large parts of the parameter space, percolation is inefficient for temperatures down to the QCD scale. Ref. [227] finds that this happens if $g_{\mathrm{B-L}} \lesssim 0.2$ at $\mu = m_{Z'}$. Taking into account the different charge of Φ in the $B-L$ model compared to the models discussed in this chapter, we rescale this bound and find that for $g_X \lesssim 0.4$ percolation remains inefficient. With $N_f = 6$ massless quarks, QCD undergoes a FOPT with a critical temperature of $T_c^{\mathrm{QCD}} \approx 85\,\mathrm{MeV}$ [231, 232] and no strong supercooling. After the QCD phase transition, a linear term in the Higgs potential is generated from the top quark condensate which in turn induces a Higgs VEV of [227, 230]

$$v_{H,\mathrm{QCD}} = \left| y_t/(\sqrt{2}\lambda_H)\langle t\bar{t}\rangle \right|^{1/3} \approx 100\,\mathrm{MeV}. \tag{6.44}$$

For the parameters space relevant in our model, Ref. [227] finds that the fields are trapped at $(\Phi, H) = (0, v_{H,\mathrm{QCD}}/\sqrt{2})$ followed by an FOPT to the realistic $B-L$ breaking vacuum. In contrast, Ref. [230] finds that QCD induces a tachyonic instability and the transition to the $B-L$ breaking vacuum happens without a FOPT. We stress that in both cases, the QCD phase transition is first order.

Gravitational wave signals originating from bubble collisions can be probed by future gravitational wave observatories [226–230, 233–237].

The decay $h_\Phi \to hh$ can reheat the SM thermal bath if $m_{h_\Phi} > 2m_h$ and the reheating temperature $T_{\rm rh}$ is found to be roughly of $\sim \mathcal{O}(\text{TeV})$ [230]. For $m_{h_\Phi} < 2m_h$ scalar mixing might provide a reheating mechanism [238]. A more detailed analysis of the reheating process is required to find out whether QCD and EW symmetry is restored after reheating and, in case of our DM model, whether the DM candidates are in thermal equilibrium after reheating.

Our model introduces new light degrees of freedom given by the right-handed components of the Dirac neutrinos. If these new light degrees of freedom are produced after the period of thermal inflation, they contribute to $\Delta N_{\rm eff}$ and this contribution can potentially be detected in future CMB measurements [239–241].

6.5 Future directions

The models constructed in this chapter assume family universal $\mathrm{U}(1)_\mathrm{X}$ charges and therefore the new charges are required to be a linear combination of the $B-L$ charge and hypercharge. Non-universal U(1) charge assignments such as $\mathrm{U}(1)_{\mathrm{L}_\mu-\mathrm{L}_\tau}$ can potentially connect "Custodial Naturalness" to flavor anomalies for example the muon anomalous magnetic moment [242–247]. One can also consider $B-L$ charge assignments where the right-handed neutrinos have the charges $\nu_R \sim (-4,-4,5)$. For such a charge assignment, gauge anomalies cancel and the Yukawa interaction of the lepton doublet with the right-handed neutrinos and the Higgs doublet is forbidden. This setup is often used to explain the smallness of neutrino masses [248–251].

In order for λ_Φ to reach critical values, bosonic loops need to contribute to β_{λ_Φ}. In the models presented in this chapter, these contribution come from the $\mathrm{U}(1)_X$ gauge group. One can also consider the case where these contributions come from an additional scalar field S which is a singlet under enhanced custodial symmetry. In this case Φ and S can be real fields and, at the high scale, the potential is given by

$$V = \lambda\left(|H|^2+\frac{1}{2}\Phi^2\right)^2 + \frac{\lambda_{HS}}{2}\left(|H|^2+\frac{1}{2}\Phi^2\right)S^2 + \frac{\lambda_S}{4!}S^4 \qquad \text{at } \mu = M_{\rm Pl}. \quad (6.45)$$

This potential has a SO(5) symmetry where Φ and the real components of H form a **5**-plet. If we include right-handed neutrinos ν_R, then the Yukawa interaction

$$\mathcal{L}_{\rm Yuk} \supset y_N^{\alpha\beta}\Phi\bar{\nu}_R^\alpha\nu_R^\beta, \quad (6.46)$$

can contribute as additional custodial symmetry violation, similar to the Yukawa interactions discussed in Sec. 6.1.2. After spontaneous symmetry breaking where Φ obtains a VEV, a Majorana mass for ν_R is generated and the low-scale type I seesaw scenario is realized. The scalar field S is odd under an accidental unbroken $\mathbb{Z}_2$ symmetry and therefore a stable DM candidate. A setup with similar particle content but without enhanced custodial symmetry has been considered in Ref. [178]. In this reference the DM relic density has been calculated using the freeze out scenario. Ref. [252] discusses Coleman-Weinberg symmetry breaking induced by scalar loops and finds that the reheating temperature ranges from $\sim 10 - 10^4$ GeV. This suggests that for parts of the parameter space, S is not thermalized after the phase transition and the relic density is lower then expected from the freeze out mechanism [253]. A detailed study of this realization of Custodial Naturalness is currently ongoing in collaboration with *Manfred Lindner* and *Andreas Trautner*. A publication is planned in Ref. [3].

In this chapter, SO(6) custodial symmetry is imposed at the Planck scale. In Sec. 6.1.2 we discuss that the SM contributions to $\beta_{\lambda_p} - \beta_{\lambda_\Phi}$ change sign around 10^{11} GeV. If the scale where custodial symmetry is restored is lowered, then the integrated effect of the SM contribution to $\lambda_p - \lambda_\Phi$ can be sufficient to trigger EWSB. In this case no additional sources of custodial symmetry breaking are required. In such a setting, the charge assignment $q_\Phi = -\frac{16}{41}$ seems particularly interesting, since g_{12} remains zero at one-loop and thus only contributes to custodial symmetry violation at two-loop. Such a charge assignment and the lower scale of custodial symmetry might originate from a grand unified theory (GUT). Similar to the way the SM custodial symmetry is embedded in Pati-Salam unification [254] (SO(4) $\subset$ SO(10)), SO(6) custodial symmetry is expected to be embedded in the GUT group.

Future work should also consider the inclusion of baryo- or leptogenesis [202, 235, 236, 255–260] or include different DM production mechanisms [202, 261]. One should also investigate the possibility for inflation where Φ takes the role of the inflaton [238, 262, 263].

Chapter 7

Symmetries of beta functions

Outer automorphisms can be understood as the non-trivial symmetries of a symmetry group. Acting as transformation of the fields, these outer automorphisms are not symmetries, but the transformation can be absorbed into the couplings [86]. For example the CP transformation in the SM is an outer automorphism [81, 82] which maps the couplings to their complex conjugate.

In this chapter, we derive how the beta function functions transform under outer automorphisms. We show that the beta functions, seen as a set of partial differential equation, have a symmetry given by the transformations of couplings under the outer automorphism.[1] This allows us to derive general constraints on the form of the beta functions. The transformation of beta functions under the outer automorphisms can be used to validate the argument on which t'Hooft naturalness is based. We also briefly discuss scale transformation as an outer automorphism of the Poincarè group.

The results presented in this chapter are part of ongoing work in collaboration with *Andreas Trautner* and a publication is planned in Ref. [4].

7.1 Outer automorphism

Say we have a symmetry group G. Automorphisms are bijective homomorphisms from the group to itself, i.e. $u : G \to G$ where u preserves the group structure. The maps u form a group, namely the automorphism group $\mathrm{Aut}(G)$. Some elements

[1] By symmetry we mean a transformation g, and for any for any solution $x(t)$ to a differential equation $\dot{x} = F(x)$, $g(x(t))$ is also a solution. This agrees with the definition given for example in Ref. [264, Definition 2.23].

$u \in \text{Aut}(G)$ can be written as multiplication with group elements, i.e. there exist a group element $h \in G$ such that $u(g) = h \cdot g \cdot h^{-1}$ for all $g \in G$. These automorphisms are called inner. Any automorphism which is not inner, is an **outer automorphism**.[2]

The symmetry transformations under a group element $g \in G$ act on a field $\phi^{(\boldsymbol{r})}$ in the $\boldsymbol{r}$ representation as

$$\phi^{(\boldsymbol{r})} \to \rho_{\boldsymbol{r}}(g)\phi^{(\boldsymbol{r})}, \tag{7.1}$$

where $\rho_{\boldsymbol{r}}(g)$ is the matrix representation of the group element g. The action is symmetric, if

$$S\left[\phi^{(\boldsymbol{r})}\right] = S\left[\rho_{\boldsymbol{r}}(g)\phi^{(\boldsymbol{r})}\right]. \tag{7.2}$$

In this chapter, we consider more general transformations given by

$$\phi^{(\boldsymbol{r}_i)} \xrightarrow{u} \tilde{\phi}^{(\boldsymbol{r}_i)} := \mathcal{F}(\phi^{(\boldsymbol{r}_i)}) = U\phi^{(\boldsymbol{r}'_i)}, \tag{7.3}$$

where the field $\phi^{(\boldsymbol{r}_i)}$ in the $\boldsymbol{r}_i$ representation is mapped to a field $\phi^{(\boldsymbol{r}'_i)}$ in the $\boldsymbol{r}'_i$ representation. The matrix U is defined as a solution to

$$\rho_{\boldsymbol{r}_i}(u(g)) = U\rho_{\boldsymbol{r}'_i}(g)U^{-1}. \tag{7.4}$$

In Ref [87] (see also Refs. [83, 84, 86, 265]) it is shown that a solution to Eq. (7.4) exists if and only if u is an automorphism. The solutions to Eq. (7.4) are not unique. For example for any solution U, $e^{i\alpha}U$ for some phase α is also a solution. For each solution to Eq. (7.4), we have a corresponding transformation acting on the fields via Eq. (7.3). Sometimes one refers to the transformation in Eq. (7.3) as the transformation under the (outer) automorphism. All possible transformations that fulfill Eq. (7.4) form a group which we denote by H. Since $U = \rho_{\boldsymbol{r}}(h)$ for any $h \in G$ is a solution to Eq. (7.4), the symmetry group G is a subgroup of H. Further, H contains the automorphism group $\text{Aut}(G)$ and the phase rotations of U as subgroups.

The transformation in Eq. (7.3) is not a symmetry of the action, however, the following statement is true:

Finding 1 *If for every field $\phi^{(\boldsymbol{r}_i)}$, also $\phi^{(\boldsymbol{r}'_i)}$ is part of the particle content*[3] *then following relation holds:*

$$S[\phi, \lambda_n] = S[\tilde{\phi}, f_n(\lambda)], \tag{7.5}$$

[2] We clarify that the outer automorphism group is defined differently. In this chapter, we are only concerned with outer automorphism in the sense that they are not inner.

[3] This is equivalent to demanding that the particle content of the model can be written in representations of the group H (or more precisely of the subgroup generated by U). If this is not the case, the "possible" symmetry is maximally broken by the particle content.

for some function $f_n(\lambda)$ determined by the transformation in Eq. (7.3) i.e. the outer automorphisms transformation.

This statement has been shown in Ref. [86] and we repeat the arguments below.

We write the Lagrangian in terms of operators $\mathcal{O}_n[\phi]$

$$\mathcal{L}[\phi, \lambda_n] = \sum_n \lambda_n \mathcal{O}_n[\phi], \tag{7.6}$$

where each operator is invariant under the symmetry transformations Eq. (7.1) and λ_n are independent couplings. This sum must include every independent operator consistent with all symmetries, as expected from renormalizability. Now we write

$$\mathcal{L}[\phi, \lambda_n] = \mathcal{L}[\mathcal{F}^{-1}(\tilde{\phi}), \lambda_n] := \tilde{\mathcal{L}}[\tilde{\phi}, \lambda_n] = \sum_k \tilde{f}_k(\lambda_m)\tilde{\mathcal{O}}_k[\tilde{\phi}], \tag{7.7}$$

where we decomposed $\tilde{\mathcal{L}}$ in a similar way as we decomposed $\mathcal{L}$. Under the symmetry transformation Eq. (7.1), $\tilde{\phi}^{(\boldsymbol{r}_i)}$ transforms as

$$\tilde{\phi}^{(\boldsymbol{r}_i)} = U\phi^{(\boldsymbol{r}_i')} \to U\rho_{\boldsymbol{r}_i'}(g)\phi^{(\boldsymbol{r}_i')} = \rho_{\boldsymbol{r}_i}(u(g))U\phi^{(\boldsymbol{r}_i')} = \rho_{\boldsymbol{r}_i}(u(g))\tilde{\phi}^{(\boldsymbol{r}_i)}, \tag{7.8}$$

i.e. $\tilde{\phi}^{(\boldsymbol{r}_i)}$ transforms in the $\rho_{\boldsymbol{r}_i}$ representations (of a different group element). As the operator decomposition Eq. (7.6) includes all operators invariant under symmetry transformations, there exists an operator $\mathcal{O}_{n_m}$ such that[4]

$$\mathcal{O}_{n_m}[\tilde{\phi}] = \tilde{\mathcal{O}}_m[\tilde{\phi}]. \tag{7.9}$$

Therefore we have

$$\tilde{\mathcal{L}}[\tilde{\phi}, \lambda_n] = \sum_k \tilde{f}_k(\lambda_m)\tilde{\mathcal{O}}_k[\tilde{\phi}] = \sum_k \tilde{f}_k(\lambda_m)\mathcal{O}_{n_m}[\tilde{\phi}] := \sum_n f_n(\lambda_m)\mathcal{O}_n[\tilde{\phi}] = \mathcal{L}[\tilde{\phi}, f_n(\lambda_m)], \tag{7.10}$$

which implies Eq. (7.5).

Observation 1 *If the operators in Eq. (7.6) are monomials in the fields, then Eq. (7.5) is given by*

$$S[\phi, \lambda_n] = S[\tilde{\phi}, \tilde{U}\lambda], \tag{7.11}$$

for some matrix $\tilde{U}$ determined by the transformation in Eq. (7.3). Since the transformation in Eq. (7.3) form the group H, the matrices $\tilde{U}$ also form a group, which we denote as $\tilde{H}$. The couplings λ_n transform under representations of $\tilde{H}$.

[4] Technically this might be a linear combination, however the argument still holds.

If the operators $\mathcal{O}_n$ are monomials in the fields, then we can write

$$\lambda_n \mathcal{O}^n[\phi] = \lambda_n T^n_{ab...} \phi_a \phi_b ..., \tag{7.12}$$

where the indices $a, b, ...$ run over all fields and $T^n_{ab...}$ is some tensor. Eq. (7.6) acts on ϕ_a as a matrix multiplication $\phi_a \to U^{aa'} \phi_{a'}$. Then we have

$$\lambda_n T^n_{ab...} \phi_a \phi_b ... \to \lambda_n T^n_{ab...} U^{aa'} U^{bb'} \phi_{a'} \phi_{b'} ... =: \lambda_n (T')^n_{ab...} \phi_a \phi_b ... \tag{7.13}$$

Since we have a complete set of operators $\mathcal{O}[\phi]$, $(T')^n$ is simply a linear combination of T^n and therefore the transformation of λ_n is described by a matrix multiplication.

Observation 2 *Say the couplings fulfill $f_n(\lambda) = \lambda_n$. Then the transformation $\phi \to \tilde{\phi}$ leaves the Lagrangian invariant. u is then part of the symmetry group.*

Finding 2 *If the outer automorphism transformation (Eq. (7.3)) leaves the path integral measure invariant, then $S[\phi, \lambda_n]$ and $S[\phi, f_n(\lambda)]$ lead to the same physical predictions. Therefore these parts of the parameter space are redundant.*

Consider the generating functional

$$Z[J] = \int \mathcal{D}\phi \exp\left(i \int d^4x \; \mathcal{L}[\phi, \lambda_n] + J\phi\right). \tag{7.14}$$

By field redefinition invariance, we know that

$$Z'[J] = \int \mathcal{D}\phi \exp\left(i \int d^4x \; \mathcal{L}[\phi, \lambda_n] + J\tilde{\phi}\right), \tag{7.15}$$

gives the same predictions as $Z[J]$.[5] Using Eq. (7.5) we can rewrite this to

$$\begin{aligned} Z'[J] &= \int \mathcal{D}\phi \exp\left(i \int d^4x \; \mathcal{L}[\tilde{\phi}, f_n(\lambda)] + J\tilde{\phi}\right) \\ &= \int \mathcal{D}\phi \det\left[\frac{\delta \mathcal{F}^{-1}[\phi]}{\delta\phi}\right] \exp\left(i \int d^4x \; \mathcal{L}[\phi, f_n(\lambda)] + J\phi\right) \\ &= \int \mathcal{D}\phi \exp\left(i \int d^4x \; \mathcal{L}[\phi, f_n(\lambda)] + J\phi\right). \end{aligned} \tag{7.16}$$

where we assumed $\det\left[\frac{\delta\mathcal{F}[\phi]}{\delta\phi}\right] = 1$ in the final equality.[6] As Eq. (7.14) and Eq. (7.16) give the same predictions, the function f_n maps redundant parts of the parameter space to one another.

[5] By same predictions, we mean same S-matrix elements [266, 267]. A modern derivation of field redefinition invariance is given in Ref. [268].

[6] This is the same requirement as anomaly freedom.

Finding 3 *The redundancy in parameter space also manifests itself in the structure of the RGEs. If we consider the beta functions as functions with the couplings as arguments (i.e.* $\beta_{\lambda_n}(\ .\ )$*) then*

$$\beta_{\lambda_n}(f_k(\lambda)) = \frac{\partial f_n(\lambda)}{\partial \lambda_m}\beta_{\lambda_m}(\lambda_k). \tag{7.17}$$

Therefore the transformation $\lambda \to f(\lambda)$ *is a symmetry of the beta functions.*

The generating functionals in Eq. (7.14) and Eq. (7.16) have the same functional form and therefore the beta functions we calculate with these two theories have the same functional form, i.e.

$$\mu\frac{\partial}{\partial\mu}\lambda_n := \beta_{\lambda_n}(\lambda_k), \tag{7.18}$$

$$\mu\frac{\partial}{\partial\mu}f_n(\lambda) := \beta_{f_n(\lambda)}(f_k(\lambda)) = \beta_{\lambda_n}(f_k(\lambda)). \tag{7.19}$$

Eq. (7.17) follows from the chain rule.

Observation 3 *With the assumption of the operators* $\mathcal{O}_n$ *being monomials, the couplings transform under representations of* $\tilde{H}$ *(see Observation 1). Eq. (7.17) implies that the beta functions transform under the same representations as the couplings. We write the couplings transforming in the* $\boldsymbol{r}_i$ *representation as* $\lambda_{\boldsymbol{r}_i}$*. Then expanding the beta function as a power series, we find*

$$\beta_{\lambda_{\boldsymbol{r}_i}} = \sum_{j,k} c_{jk}\left[\lambda_{\boldsymbol{r}_j}\otimes\lambda_{\boldsymbol{r}_k}\right]_{\boldsymbol{r}_i} + \sum_{j,k,l} c_{jkl}\left[\lambda_{\boldsymbol{r}_j}\otimes\lambda_{\boldsymbol{r}_k}\otimes\lambda_{\boldsymbol{r}_l}\right]_{\boldsymbol{r}_i} + \ldots \tag{7.20}$$

where $\left[\lambda_{\boldsymbol{r}_j}\otimes\lambda_{\boldsymbol{r}_k}\right]_{\boldsymbol{r}_i}$ *is the tensor product of* $\lambda_{\boldsymbol{r}_j}$ *and* $\lambda_{\boldsymbol{r}_k}$ *projected onto* $\boldsymbol{r}_i$*.*

A similar to approach is used for the two Higgs doublet model (2HDM) in Refs. [269–271] where the tensor structure of the couplings under basis transformations is used to constrain the all-loop beta functions. For a discussion of the outer automorphisms in the 2HDM we refer to Ref. [91]. The tensor structure of the couplings is also used in high loop calculations as for example in Ref. [272].

Observation 4 ***t'Hooft naturalness:*** *The notion of t'Hooft naturalness states that a set of couplings can be naturally small, if and only if the symmetries of* *the model are enhanced by setting this set of couplings to zero. If the (approximate) symmetry transformation is an outer automorphism, i.e. can be written as Eq. (7.3), then Observation 3 implies t'Hooft naturalness.*[7]

Any coupling that preserves the symmetry, transforms trivially under $f_n(\lambda)$. For couplings that violate the symmetry explicitly, Eq. (7.20) implies that the beta function transforms covariantly and therefore the beta function of symmetry violating couplings must be proportional to symmetry violating couplings.

7.2 Example I: Cyclic group of order three

As a first example, we consider a model with the symmetry group $\mathbb{Z}_3 = \langle a | a^3 = e \rangle$. This group has three irreducible representations all of which are one-dimensional. They are given by the trivial representation, $\rho_{\boldsymbol{r}}(a) = \omega$ and $\rho_{\overline{\boldsymbol{r}}}(a) = \omega^2$ with $\omega = e^{i\frac{2\pi}{3}}$. The group $\mathbb{Z}_3$ has a non-trivial outer automorphism given by the $\mathbb{Z}_2$ group that exchanges a and a^2. For this outer automorphism u, we evaluate Eq. (7.4) and find

$$\rho_{\boldsymbol{r}}(u(a)) = \rho_{\boldsymbol{r}}(a^2) = \omega^2 = \rho_{\overline{\boldsymbol{r}}}(a). \tag{7.21}$$

Thus u maps the representation $\boldsymbol{r}$ to the conjugate representation $\overline{\boldsymbol{r}}$. We start by considering the case $U = 1$. Now consider a single scalar field ϕ which transforms in the $\boldsymbol{r}$ representation. The most general renormalizable potential is given by

$$V = m^2|\phi|^2 + (\kappa\phi^3 + \text{h.c.}) + \lambda|\phi|^4. \tag{7.22}$$

The conjugate field ϕ^* transforms in the conjugate representation $\overline{\boldsymbol{r}}$ and the outer automorphism maps $\phi \to \phi^*$. Therefore the outer automorphism is the CP-transformation. However all couplings in Eq. (7.22) are real up to unphysical phases. Thus CP is already a symmetry of the theory and nothing is gained by the outer automorphism.

Another solution to Eq. (7.4) is the phase rotation $U = e^{i\alpha}$. The couplings transform as

$$m^2 \to m^2, \qquad \kappa \to e^{3i\alpha}\kappa, \qquad \lambda \to \lambda, \tag{7.23}$$

and $\kappa = 0$ enhances the symmetry to a global U(1).

[7] Ref. [80] assumes, without proof, that the beta function for a coupling a is proportional to a, if $a = 0$ enhances a symmetry. To our knowledge, our argument here gives the first strict derivation of this proportionality.

At this point, we could use Eq. (7.17) to constrain the form of the beta functions. However due to the different mass dimensions of the couplings, the beta functions are already tightly constrained and no new insight is gained. We now consider another example where we can constrain the form of the beta functions.

7.3 Example II: Dihedral group of order eight

Consider the dihedral group of order eight, $D_8 = \langle a, b | a^4 = b^2 = abab = e \rangle$. It turns out to be more convenient to choose $s = b$ and $t = ab$ as generating elements which implies $D_8 = \langle s, t | s^2 = t^2 = (st)^4 = e \rangle$. There are five irreducible representations of D_8. The representations map the generating elements as follows

	I	s	t
$\mathbf{1}_{++}$	1	1	1
$\mathbf{1}_{+-}$	1	1	-1
$\mathbf{1}_{-+}$	1	-1	1
$\mathbf{1}_{--}$	1	-1	-1
$\mathbf{2}$	1	σ_3	σ_1

where σ_i are the Pauli matrices. D_8 has an outer automorphism given by the $\mathbb{Z}_2$ operation which exchanges $s \leftrightarrow t$. Consequently this exchanges the $\mathbf{1}_{+-} \leftrightarrow \mathbf{1}_{-+}$ representations while it leaves the other representations invariant. For the one-dimensional representation, Eq. (7.4) is solved by $U = \pm 1$,[8] while for the $\mathbf{2}$ representation, we find

$$U_{\mathbf{2}} = \begin{pmatrix} \frac{1}{\sqrt{2}} & \frac{1}{\sqrt{2}} \\ \frac{1}{\sqrt{2}} & -\frac{1}{\sqrt{2}} \end{pmatrix}. \tag{7.24}$$

Now consider a real field in the $\mathbf{2}$ representation

$$\Phi = \begin{pmatrix} \phi_1 \\ \phi_2 \end{pmatrix}. \tag{7.25}$$

The most general renomalizable potential is given by

$$V = m^2 \left(\phi_1^2 + \phi_2^2\right) + \lambda \left(\phi_1^4 + \phi_2^4\right) + 2\lambda_p \phi_1^2 \phi_2^2, \tag{7.26}$$

[8] A complex phase is only allowed if we consider complex fields.

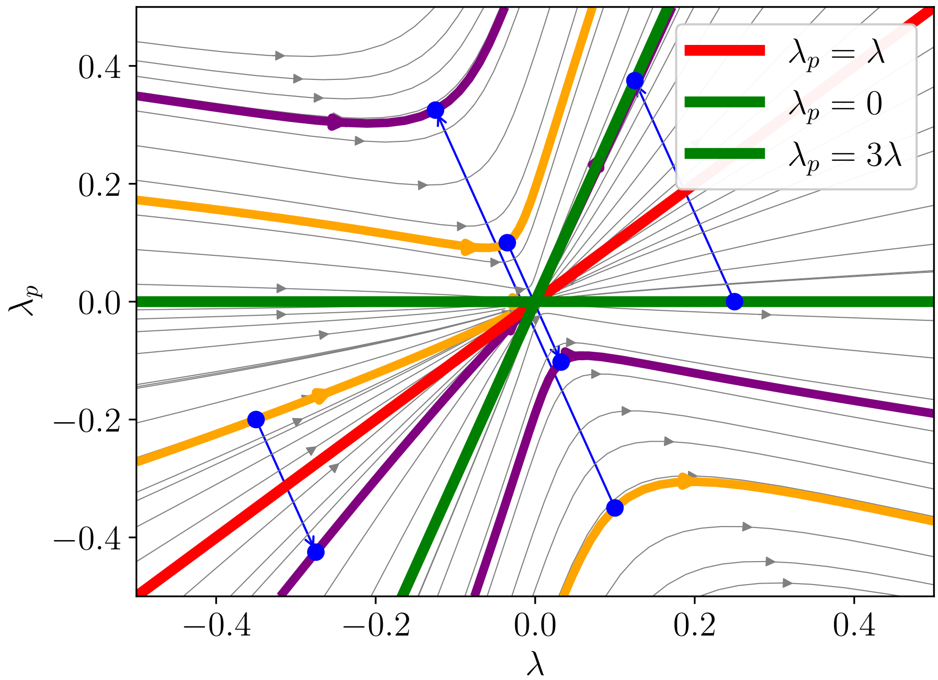

Figure 7.1: RG flow for Example II in the λ-λ_p plane. The red line corresponds to the enhanced outer automorphism symmetry. Green lines correspond to decoupling limits. Mapping of parameter points under the outer automorphism is shown (blue points and arrows). Trajectories through these points are highlighted.

and the action of the outer automorphism $\Phi \to U_{\mathbf{2}}\Phi$ maps the couplings to

$$m'^2 = m^2, \qquad \lambda' = \frac{\lambda + \lambda_p}{2}, \qquad \lambda'_p = \frac{3\lambda - \lambda_p}{2}. \tag{7.27}$$

At the point of enhanced symmetry, $\lambda = \lambda_p$, the theory has a D_{16} symmetry (which turns out to be an accidental O(2) symmetry). In Fig. 7.1, we show the RG flow and the symmetry enhanced line with $\lambda_p = \lambda$. We also show how different parts of the parameter space are mapped onto each other by the outer automorphism. These parts of the parameter space are redundant.

The transformation in Eq. (7.27) is a $\mathbb{Z}_2$ transformations. We can write the couplings in terms of irreducible representations as

$$\lambda_{\mathbf{1}} = 3\lambda + \lambda_p, \qquad \lambda_{\mathbf{1}'} = \lambda - \lambda_p. \tag{7.28}$$

These couplings transform under the $\mathbb{Z}_2$ transformation as

$$\lambda_{\mathbf{1}} \to \lambda_{\mathbf{1}}, \qquad \lambda_{\mathbf{1}'} \to -\lambda_{\mathbf{1}'}. \tag{7.29}$$

Observation 3 then implies that the one-loop beta functions are given by

$$\beta_{\lambda_{\mathbf{1}}} = c_1 \lambda_{\mathbf{1}}^2 + c_2 \lambda_{\mathbf{1}'}^2, \tag{7.30}$$

$$\beta_{\lambda_{\mathbf{1}}'} = c_3 \lambda_{\mathbf{1}} \lambda_{\mathbf{1}'}. \tag{7.31}$$

Non-zero values of $\lambda_{\mathbf{1}'}$ explicitly break the $\mathbb{Z}_2$ outer automorphism. We explicitly see that $\beta_{\lambda_{\mathbf{1}}'} \propto \lambda_{\mathbf{1}'}$ and therefore $\lambda_{\mathbf{1}'}$ can be naturally small.

In terms of λ and λ_p, the beta functions are given by

$$\beta_\lambda = \frac{1}{4}(9c_1 + c_2 + 3c_3)\lambda^2 + \frac{1}{4}(6c_1 - 2c_2 - 2c_3)\lambda\lambda_p + \frac{1}{4}(c_1 + c_2 - c_3)\lambda_p^2, \tag{7.32}$$

$$\beta_{\lambda_p} = \frac{1}{4}(9c_1 + c_2 - 9c_3)\lambda^2 + \frac{1}{4}(6c_1 - 2c_2 + 6c_3)\lambda\lambda_p + \frac{1}{4}(c_1 + c_2 + 3c_3)\lambda_p^2. \tag{7.33}$$

Setting $\lambda_p = 0$ leads to the decoupling of ϕ_1 and ϕ_2 and the beta function β_{λ_p} should reflect that. Therefore $c_3 = c_1 + \frac{1}{9}c_2$ and

$$\beta_\lambda = \frac{1}{3}(9c_1 + c_2)\lambda^2 + \left(c_1 - \frac{5}{9}c_2\right)\lambda\lambda_p + \frac{2}{9}c_2\lambda_p^2, \tag{7.34}$$

$$\beta_{\lambda_p} = \left(3c_1 - \frac{1}{3}c_2\right)\lambda\lambda_p + \left(c_1 + \frac{1}{3}c_2\right)\lambda_p^2. \tag{7.35}$$

An explicit calculation of the beta functions yields

$$c_1 = \frac{5}{4\pi^2}, \qquad c_2 = \frac{9}{4\pi^2}. \tag{7.36}$$

7.4 Example III: Pauli Group

Consider the Pauli Group $G_{C_4 \circ D_4}$, i.e. the group generated by the Pauli matrices $\sigma_1, \sigma_2, \sigma_3$. The field

$$\Phi = \begin{pmatrix} \phi_1 \\ \phi_2 \end{pmatrix}, \tag{7.37}$$

transforms in the **2** representation. Then the most general renomalizable potential is given by

$$\begin{aligned} V =& m^2 \left(|\phi_1|^2 + |\phi_2|^2\right) + \lambda_1 \left(|\phi_1|^2 + |\phi_2|^2\right)^2 \\ &+ \lambda_{\mathbf{2}_1} \left(|\phi_1|^4 - 4|\phi_1|^2|\phi_2|^2 + |\phi_2|^4\right) + \lambda_{\mathbf{2}_2} \left(\phi_1^2(\phi_2^\dagger)^2 + (\phi_1^\dagger)^2\phi_2^2\right) \\ &+ \lambda_{\mathbf{4}_1} \left(\phi_1^4 + \phi_2^4\right) + \text{h.c.} + \lambda_{\mathbf{4}_2}\phi_1^2\phi_2^2 + \text{h.c.} \end{aligned} \tag{7.38}$$

Now consider the following transformations on the fields

$$\begin{aligned}
\text{(I)}: &\quad \begin{pmatrix}\phi_1\\ \phi_2\end{pmatrix} \to \begin{pmatrix}0 & i\\ -1 & 0\end{pmatrix}\begin{pmatrix}\phi_1\\ \phi_2\end{pmatrix},\\
\text{(II)}: &\quad \begin{pmatrix}\phi_1\\ \phi_2\end{pmatrix} \to \frac{1}{\sqrt{2}}\begin{pmatrix}1 & 1\\ 1 & -1\end{pmatrix}\begin{pmatrix}\phi_1\\ \phi_2\end{pmatrix},\\
\text{(III)}: &\quad \begin{pmatrix}\phi_1\\ \phi_2\end{pmatrix} \to \begin{pmatrix}\phi_1^\dagger\\ \phi_2^\dagger\end{pmatrix},\\
\text{(IV)}: &\quad \begin{pmatrix}\phi_1\\ \phi_2\end{pmatrix} \to \begin{pmatrix}i^{\frac{1}{4}} & 0\\ 0 & i^{\frac{1}{4}}\end{pmatrix}\begin{pmatrix}\phi_1\\ \phi_2\end{pmatrix}.
\end{aligned} \tag{7.39}$$

The first three transformations are outer automorphism with the fourth one is the trivial automorphism with a phase. The couplings transform (i.e. $\lambda \to f(\lambda)$) as follows under these outer automorphisms

$$\begin{aligned}
\text{(I)}: &\quad \lambda_{\mathbf{2}_2} \to -\lambda_{\mathbf{2}_2}, \quad \lambda_{\mathbf{4}_2} \to -\lambda_{\mathbf{4}_2},\\
\text{(II)}: &\quad \lambda_{\mathbf{2}_1} \to \frac{1}{2}\left(\lambda_{\mathbf{2}_2} - \lambda_{\mathbf{2}_1}\right), \quad \lambda_{\mathbf{2}_2} \to \frac{1}{2}\left(3\lambda_{\mathbf{2}_1} + \lambda_{\mathbf{2}_2}\right),\\
&\quad \lambda_{\mathbf{4}_1} \to \left(\frac{1}{2}\lambda_{\mathbf{4}_1} + \frac{1}{4}\lambda_{\mathbf{4}_2}\right), \quad \lambda_{\mathbf{4}_2} \to \left(3\lambda_{\mathbf{4}_1} - \frac{1}{2}\lambda_{\mathbf{4}_2}\right),\\
\text{(III)}: &\quad \lambda_{\mathbf{4}_1} \to \lambda^*_{\mathbf{4}_1}, \quad \lambda_{\mathbf{4}_2} \to \lambda^*_{\mathbf{4}_2},\\
\text{(IV)}: &\quad \lambda_{\mathbf{4}_1} \to -i\lambda_{\mathbf{4}_1}, \quad \lambda_{\mathbf{4}_2} \to -i\lambda_{\mathbf{4}_2},
\end{aligned} \tag{7.40}$$

These coupling transformations generate the group $D_4 \times S_3$ and the couplings transform under the following irreducible representations:

$$\begin{aligned}
&\lambda_1 && \mathbf{1}_1 \ \text{trivial representation},\\
&\begin{pmatrix}\lambda_{\mathbf{2}_1}\\ \lambda_{\mathbf{2}_2}\end{pmatrix} && \mathbf{2} \ \text{lifted from } S_3,\\
&\begin{pmatrix}\mathrm{Re}(\lambda_{\mathbf{4}_1})\\ \mathrm{Re}(\lambda_{\mathbf{4}_2})\\ \mathrm{Im}(\lambda_{\mathbf{4}_1})\\ \mathrm{Im}(\lambda_{\mathbf{4}_2})\end{pmatrix} && \mathbf{4} \ \text{faithful}.
\end{aligned} \tag{7.41}$$

The beta functions at one-loop are then given by

$$\beta_{\lambda_1} = \frac{1}{16\pi^2}\left(c_{\mathbf{1}_1}\left[\mathbf{1}\otimes\mathbf{1}\right]_{\mathbf{1}} + c_{\mathbf{1}_2}\left[\mathbf{2}\otimes\mathbf{2}\right]_{\mathbf{1}} + c_{\mathbf{1}_3}\left[\mathbf{4}\otimes\mathbf{4}\right]_{\mathbf{1}}\right), \tag{7.42}$$

$$\begin{pmatrix}\beta_{\lambda_{\mathbf{2}_1}}\\ \beta_{\lambda_{\mathbf{2}_2}}\end{pmatrix} = \frac{1}{16\pi^2}\left(c_{\mathbf{2}_1}\left[\mathbf{1}\otimes\mathbf{2}\right]_{\mathbf{2}} + c_{\mathbf{2}_2}\left[\mathbf{2}\otimes\mathbf{2}\right]_{\mathbf{2}} + c_{\mathbf{2}_3}\left[\mathbf{4}\otimes\mathbf{4}\right]_{\mathbf{2}}\right), \tag{7.43}$$

$$\begin{pmatrix}\beta_{\lambda_{\mathbf{4}_1}}\\ \beta_{\lambda_{\mathbf{4}_2}}\end{pmatrix} = \frac{1}{16\pi^2}\left(c_{\mathbf{4}_1}\left[\mathbf{1}\otimes\mathbf{4}\right]_{\mathbf{4}} + c_{\mathbf{4}_2}\left[\mathbf{2}\otimes\mathbf{4}\right]_{\mathbf{4}}\right), \tag{7.44}$$

or explicitly

$$\beta_{\lambda_1} = \frac{1}{16\pi^2}\left[c_{\mathbf{1}_1}\lambda_1^2 + c_{\mathbf{1}_2}\left(\lambda_{\mathbf{2}_1}^2 + \frac{1}{3}\lambda_{\mathbf{2}_2}^2\right) + c_{\mathbf{1}_3}\left(|\lambda_{\mathbf{4}_1}|^2 + \frac{1}{12}|\lambda_{\mathbf{4}_2}|^2\right)\right], \tag{7.45}$$

$$\begin{pmatrix}\beta_{\lambda_{\mathbf{2}_1}}\\ \beta_{\lambda_{\mathbf{2}_2}}\end{pmatrix} = \frac{1}{16\pi^2}\left[c_{\mathbf{2}_1}\begin{pmatrix}\lambda_1\lambda_{\mathbf{2}_1}\\ \lambda_1\lambda_{\mathbf{2}_2}\end{pmatrix} + c_{\mathbf{2}_2}\begin{pmatrix}\lambda_{\mathbf{2}_1}^2 - \frac{1}{3}\lambda_{\mathbf{2}_2}^2\\ -2\lambda_{\mathbf{2}_1}\lambda_{\mathbf{2}_2}\end{pmatrix} + c_{\mathbf{2}_3}\begin{pmatrix}|\lambda_{\mathbf{4}_1}|^2 - \frac{1}{12}|\lambda_{\mathbf{4}_2}|^2\\ \frac{1}{2}\left(\lambda_{\mathbf{4}_1}\lambda_{\mathbf{4}_2}^* + \lambda_{\mathbf{4}_1}^*\lambda_{\mathbf{4}_2}\right)\end{pmatrix}\right], \tag{7.46}$$

$$\begin{pmatrix}\beta_{\lambda_{\mathbf{4}_1}}\\ \beta_{\lambda_{\mathbf{4}_2}}\end{pmatrix} = \frac{1}{16\pi^2}\left[c_{\mathbf{4}_1}\begin{pmatrix}\lambda_1\lambda_{\mathbf{4}_1}\\ \lambda_1\lambda_{\mathbf{4}_2}\end{pmatrix} + c_{\mathbf{4}_2}\begin{pmatrix}\lambda_{\mathbf{2}_1}\lambda_{\mathbf{4}_1} + \frac{1}{6}\lambda_{\mathbf{2}_2}\lambda_{\mathbf{4}_2}\\ 2\lambda_{\mathbf{2}_2}\lambda_{\mathbf{4}_1} - \lambda_{\mathbf{2}_1}\lambda_{\mathbf{4}_2}\end{pmatrix}\right]. \tag{7.47}$$

There are three interesting decoupling limits: We can decouple the two sectors consisting of ϕ_1 and ϕ_2 by setting

$$\lambda_{\mathbf{2}_1} = \frac{1}{2}\lambda_1, \quad \lambda_{\mathbf{2}_2} = 0, \quad \lambda_{\mathbf{4}_2} = 0. \tag{7.48}$$

By setting

$$\begin{aligned}\lambda_{\mathbf{2}_2} &= \frac{1}{2}\lambda_1 - \lambda_{\mathbf{2}_1}, \quad \mathrm{Re}(\lambda_{\mathbf{4}_1}) = \frac{1}{6}\left(\lambda_1 + \lambda_{\mathbf{2}_1}\right),\\ \mathrm{Re}(\lambda_{\mathbf{4}_2}) &= \frac{1}{2}\lambda_1 - \lambda_{\mathbf{2}_1}, \quad \mathrm{Im}(\lambda_{\mathbf{4}_1}) = \mathrm{Im}(\lambda_{\mathbf{4}_2}) = 0,\end{aligned} \tag{7.49}$$

the sectors containing $\{\mathrm{Re}(\phi_1), \mathrm{Re}(\phi_2)\}$ and $\{\mathrm{Im}(\phi_1), \mathrm{Im}(\phi_2)\}$ decouple. We can also decouple a singe real field (e.g. $\mathrm{Re}(\phi_1)$) by setting

$$\lambda_{\mathbf{2}_1} = \frac{1}{2}\lambda_1, \quad \mathrm{Re}(\lambda_{\mathbf{4}_1}) = \frac{1}{4}\lambda_1, \quad \lambda_{\mathbf{2}_2} = 0, \quad \mathrm{Im}(\lambda_{\mathbf{4}_1}) = 0, \quad \lambda_{\mathbf{4}_2} = 0. \tag{7.50}$$

The RG flow should respect the decoupling limits. This constrains

$$\begin{aligned}c_{\mathbf{2}_1} &= c_{\mathbf{1}_1} + \frac{1}{8}c_{\mathbf{1}_2} - \frac{1}{32}c_{\mathbf{1}_3}, \quad c_{\mathbf{2}_2} = \frac{1}{4}c_{\mathbf{1}_2} + \frac{1}{16}c_{\mathbf{1}_3}, \quad c_{\mathbf{2}_3} = \frac{1}{2}c_{\mathbf{1}_3},\\ c_{\mathbf{4}_1} &= c_{\mathbf{1}_1} - \frac{1}{8}c_{\mathbf{1}_2} + \frac{1}{32}c_{\mathbf{1}_3}, \quad c_{\mathbf{4}_2} = \frac{3}{4}c_{\mathbf{1}_2} + \frac{1}{16}c_{\mathbf{1}_3},\end{aligned} \tag{7.51}$$

leaving three coefficients that need to be determined. An explicit calculation of the one-loop beta functions gives

$$c_{\mathbf{1}_1} = 24, \quad c_{\mathbf{1}_2} = 24, \quad c_{\mathbf{1}_3} = 96. \tag{7.52}$$

7.5 Four scalar fields without symmetries

We have seen how the outer automorphisms constrain the shape of the beta functions. If the group of outer automorphisms is large, we will find many constraints on the shape of the beta functions. For a model with no symmetry, all fields transform under the trivial representation $\rho_{\boldsymbol{r}} = \rho_{\boldsymbol{r}'} = I$ and Eq. (7.4) is solved by any invertible matrix U. Taking into account that the kinetic terms should remain invariant, for N real scalar fields, the group of outer automorphism transformations H is given by $\mathrm{O}(N)$. We will now discuss a model with four reals scalar fields and no symmetry imposed. The most general potential can be written as

$$V = m^2_{ij}\phi_i\phi_j + \kappa_{ijk}\phi_i\phi_j\phi_k + \lambda_{ijkl}\phi_i\phi_j\phi_k\phi_l, \tag{7.53}$$

with $1 \leq i \leq j \leq k \leq l \leq 4$. Since we can reorder the fields in each operator (for example $\phi_1\phi_2 = \phi_2\phi_1$), there are 10 independent mass parameters, 20 cubic couplings and 35 quartic couplings. As there is no symmetry present, the group of outer automorphism transformations H is given by $\mathrm{O}(4)$. We will focus on $\mathrm{SO}(4) \cong \mathrm{SU}(2) \times \mathrm{SU}(2)$ and the four reals scalar fields transform under the $\phi \sim (\mathbf{2}, \mathbf{2})$ representation of $\mathrm{SU}(2) \times \mathrm{SU}(2)$. The couplings can be decomposed into irreducible representations as[9]

$$m^2 \sim (\mathbf{1},\mathbf{1}) \oplus (\mathbf{3},\mathbf{3}) =: m^2_{(\mathbf{1},\mathbf{1})} + m^2_{(\mathbf{3},\mathbf{3})}, \tag{7.54}$$

$$\kappa \sim (\mathbf{2},\mathbf{2}) \oplus (\mathbf{4},\mathbf{4}) =: \kappa_{(\mathbf{2},\mathbf{2})} + \kappa_{(\mathbf{4},\mathbf{4})}, \tag{7.55}$$

$$\lambda \sim (\mathbf{1},\mathbf{1}) \oplus (\mathbf{3},\mathbf{3}) \oplus (\mathbf{5},\mathbf{5}) =: \lambda_{(\mathbf{1},\mathbf{1})} + \lambda_{(\mathbf{3},\mathbf{3})} + \lambda_{(\mathbf{5},\mathbf{5})}. \tag{7.56}$$

In this section we focus on the quartic couplings. Similar calculations can be done for the cubic couplings and masses. Since beta functions transform in a covariant way, we again write them in terms of tensor products. At quadratic order in couplings (one-loop) we find

$$\beta_{\lambda_{(\mathbf{1},\mathbf{1})}} = c^{(1)}_{\mathbf{1}} \left[\lambda_{(\mathbf{1},\mathbf{1})} \otimes \lambda_{(\mathbf{1},\mathbf{1})}\right]_{(\mathbf{1},\mathbf{1})} + c^{(2)}_{\mathbf{1}} \left[\lambda_{(\mathbf{3},\mathbf{3})} \otimes \lambda_{(\mathbf{3},\mathbf{3})}\right]_{(\mathbf{1},\mathbf{1})} + c^{(3)}_{\mathbf{1}} \left[\lambda_{(\mathbf{5},\mathbf{5})} \otimes \lambda_{(\mathbf{5},\mathbf{5})}\right]_{(\mathbf{1},\mathbf{1})}, \tag{7.57}$$

$$\begin{aligned}\beta_{\lambda_{(\mathbf{3},\mathbf{3})}} =& c^{(1)}_{\mathbf{3}} \left[\lambda_{(\mathbf{1},\mathbf{1})} \otimes \lambda_{(\mathbf{3},\mathbf{3})}\right]_{(\mathbf{3},\mathbf{3})} + c^{(2)}_{\mathbf{3}} \left[\lambda_{(\mathbf{3},\mathbf{3})} \otimes \lambda_{(\mathbf{3},\mathbf{3})}\right]_{(\mathbf{3},\mathbf{3})} \\ &+ c^{(3)}_{\mathbf{3}} \left[\lambda_{(\mathbf{5},\mathbf{5})} \otimes \lambda_{(\mathbf{5},\mathbf{5})}\right]_{(\mathbf{3},\mathbf{3})} + c^{(4)}_{\mathbf{3}} \left[\lambda_{(\mathbf{3},\mathbf{3})} \otimes \lambda_{(\mathbf{5},\mathbf{5})}\right]_{(\mathbf{3},\mathbf{3})}, \end{aligned}\tag{7.58}$$

$$\begin{aligned}\beta_{\lambda_{(\mathbf{5},\mathbf{5})}} =& c^{(1)}_{\mathbf{5}} \left[\lambda_{(\mathbf{1},\mathbf{1})} \otimes \lambda_{(\mathbf{5},\mathbf{5})}\right]_{(\mathbf{5},\mathbf{5})} + c^{(2)}_{\mathbf{5}} \left[\lambda_{(\mathbf{3},\mathbf{3})} \otimes \lambda_{(\mathbf{3},\mathbf{3})}\right]_{(\mathbf{5},\mathbf{5})} \\ &+ c^{(3)}_{\mathbf{5}} \left[\lambda_{(\mathbf{5},\mathbf{5})} \otimes \lambda_{(\mathbf{5},\mathbf{5})}\right]_{(\mathbf{5},\mathbf{5})} + c^{(4)}_{\mathbf{5}} \left[\lambda_{(\mathbf{3},\mathbf{3})} \otimes \lambda_{(\mathbf{5},\mathbf{5})}\right]_{(\mathbf{5},\mathbf{5})}. \end{aligned}\tag{7.59}$$

[9] Antisymmetric tensor products such as $\left[\phi_{(\mathbf{2},\mathbf{2})} \otimes \phi_{(\mathbf{2},\mathbf{2})}\right]_{(\mathbf{3},\mathbf{1})}$ vanish.

We know that the decoupling limit exists and is stable under the RG flow. All the possible decoupling limits (decoupling one scalar field or decoupling into two sectors each with two real scalar fields) constrains the coefficients as

$$\begin{aligned}
c_{\mathbf{1}}^{(3)} =& -20c_{\mathbf{1}}^{(1)} + 15c_{\mathbf{1}}^{(2)}, \quad c_{\mathbf{3}}^{(1)} = \frac{5}{3}c_{\mathbf{1}}^{(1)}, \quad c_{\mathbf{3}}^{(2)} = \frac{2}{3}c_{\mathbf{1}}^{(1)} + \frac{1}{4}c_{\mathbf{1}}^{(2)}, \\
c_{\mathbf{3}}^{(3)} =& -15c_{\mathbf{1}}^{(1)} + \frac{45}{4}c_{\mathbf{1}}^{(2)}, \quad c_{\mathbf{3}}^{(4)} = -\frac{25}{3}c_{\mathbf{1}}^{(1)} + \frac{15}{2}c_{\mathbf{1}}^{(2)}, \\
c_{\mathbf{5}}^{(1)} =& c_{\mathbf{1}}^{(1)}, \quad c_{\mathbf{5}}^{(2)} = \frac{1}{4}c_{\mathbf{1}}^{(2)}, \quad c_{\mathbf{5}}^{(3)} = -7c_{\mathbf{1}}^{(1)} + \frac{21}{4}c_{\mathbf{1}}^{(2)}, \quad c_{\mathbf{5}}^{(4)} = -c_{\mathbf{1}}^{(1)} + \frac{3}{2}c_{\mathbf{1}}^{(2)}.
\end{aligned} \tag{7.60}$$

This leaves only two free coefficients in the one-loop beta functions,

$$\begin{aligned}
\beta_{\lambda_{(\mathbf{1},\mathbf{1})}} =& c_{\mathbf{1}}^{(1)} \left[\lambda_{(\mathbf{1},\mathbf{1})} \otimes \lambda_{(\mathbf{1},\mathbf{1})}\right]_{(\mathbf{1},\mathbf{1})} + c_{\mathbf{1}}^{(2)} \left[\lambda_{(\mathbf{3},\mathbf{3})} \otimes \lambda_{(\mathbf{3},\mathbf{3})}\right]_{(\mathbf{1},\mathbf{1})} \\
&+ \left(-20c_{\mathbf{1}}^{(1)} + 15c_{\mathbf{1}}^{(2)}\right) \left[\lambda_{(\mathbf{5},\mathbf{5})} \otimes \lambda_{(\mathbf{5},\mathbf{5})}\right]_{(\mathbf{1},\mathbf{1})},
\end{aligned} \tag{7.61}$$

$$\begin{aligned}
\beta_{\lambda_{(\mathbf{3},\mathbf{3})}} =& \frac{5}{3}c_{\mathbf{1}}^{(1)} \left[\lambda_{(\mathbf{1},\mathbf{1})} \otimes \lambda_{(\mathbf{3},\mathbf{3})}\right]_{(\mathbf{3},\mathbf{3})} + \left(\frac{2}{3}c_{\mathbf{1}}^{(1)} + \frac{1}{4}c_{\mathbf{1}}^{(2)}\right) \left[\lambda_{(\mathbf{3},\mathbf{3})} \otimes \lambda_{(\mathbf{3},\mathbf{3})}\right]_{(\mathbf{3},\mathbf{3})} \\
&+ \left(-15c_{\mathbf{1}}^{(1)} + \frac{45}{4}c_{\mathbf{1}}^{(2)}\right) \left[\lambda_{(\mathbf{5},\mathbf{5})} \otimes \lambda_{(\mathbf{5},\mathbf{5})}\right]_{(\mathbf{3},\mathbf{3})} \\
&+ \left(-\frac{25}{3}c_{\mathbf{1}}^{(1)} + \frac{15}{2}c_{\mathbf{1}}^{(2)}\right) \left[\lambda_{(\mathbf{3},\mathbf{3})} \otimes \lambda_{(\mathbf{5},\mathbf{5})}\right]_{(\mathbf{3},\mathbf{3})},
\end{aligned} \tag{7.62}$$

$$\begin{aligned}
\beta_{\lambda_{(\mathbf{5},\mathbf{5})}} =& c_{\mathbf{1}}^{(1)} \left[\lambda_{(\mathbf{1},\mathbf{1})} \otimes \lambda_{(\mathbf{5},\mathbf{5})}\right]_{(\mathbf{5},\mathbf{5})} + \frac{1}{4}c_{\mathbf{1}}^{(2)} \left[\lambda_{(\mathbf{3},\mathbf{3})} \otimes \lambda_{(\mathbf{3},\mathbf{3})}\right]_{(\mathbf{5},\mathbf{5})} \\
&+ \left(-7c_{\mathbf{1}}^{(1)} + \frac{21}{4}c_{\mathbf{1}}^{(2)}\right) \left[\lambda_{(\mathbf{5},\mathbf{5})} \otimes \lambda_{(\mathbf{5},\mathbf{5})}\right]_{(\mathbf{5},\mathbf{5})} \\
&+ \left(-c_{\mathbf{1}}^{(1)} + \frac{3}{2}c_{\mathbf{1}}^{(1)}\right) \left[\lambda_{(\mathbf{3},\mathbf{3})} \otimes \lambda_{(\mathbf{5},\mathbf{5})}\right]_{(\mathbf{5},\mathbf{5})}.
\end{aligned} \tag{7.63}$$

Note how this are fewer free coefficients as in Sec. 7.4. Since we started with the general case, the group of potential symmetries is larger compared to the Pauli group example and therefore we have more constraints on the beta functions. Note that, if we now impose symmetries, the coefficients $c_{\mathbf{1}}^{(1)}, c_{\mathbf{1}}^{(2)}$ do not change. With the structure of the beta function known in the general case, we could now impose the same symmetry as in Sec. 7.4 and obtain the beta functions for the Pauli group model.

We now impose decoupling of ϕ_3 and ϕ_4 together with parity and exchange symmetry. Then the potential for ϕ_1 and ϕ_2 can be written as

$$V = \lambda \left(\phi_1^4 + \phi_2^4\right) + 2\lambda_p\, \phi_1^2\phi_2^2. \tag{7.64}$$

In this case the beta functions are given by

$$\begin{aligned}\beta_\lambda =&\left(-\frac{1}{2}c_{\mathbf{1}}^{(1)}+\frac{3}{4}c_{\mathbf{1}}^{(2)}\right)\lambda^2+\left(\frac{5}{6}c_{\mathbf{1}}^{(1)}-\frac{1}{2}c_{\mathbf{1}}^{(2)}\right)\lambda\lambda_p+\left(-\frac{1}{3}c_{\mathbf{1}}^{(1)}+\frac{1}{4}c_{\mathbf{1}}^{(2)}\right)\lambda_p^2\\ \beta_{\lambda_p} =&\frac{1}{2}c_{\mathbf{1}}^{(1)}\lambda\lambda_p+\left(-\frac{1}{2}c_{\mathbf{1}}^{(1)}+\frac{1}{2}c_{\mathbf{1}}^{(2)}\right)\lambda_p^2\end{aligned} \tag{7.65}$$

and comparing to the known beta function we find

$$c_{\mathbf{1}}^{(1)}=\frac{96}{16\pi^2},\qquad c_{\mathbf{1}}^{(2)}=\frac{160}{16\pi^2}, \tag{7.66}$$

which fixes all the one-loop beta functions for the four scalar system.

7.6 Dilations

One of the main topics of this thesis are models with classical scale invariance. It turns out that scale transformations are outer automorphisms the of Poincarè group [82]. At the level of the classical action, scale transformations simply transform the dimensionful couplings (see Eq. (7.5)). For example consider the following action

$$S[\phi,\{m^2,\lambda\}]=\int d^4x\,\frac{1}{2}\partial_\mu\phi(x)\partial^\mu\phi(x)-\frac{1}{2}m^2\phi(x)^2-\frac{\lambda}{4!}\phi(x)^4. \tag{7.67}$$

For the scale transformation we have $\phi'(x)=e^\sigma\phi(e^\sigma x)$ and for the action we then find

$$\begin{aligned}S[\phi,\{m^2,\lambda\}]=&\int d^4x\,\frac{1}{2}\partial_\mu\phi(x)\partial^\mu\phi(x)-\frac{1}{2}m^2\phi^2(x)-\frac{\lambda}{4!}\phi^4(x)\\ =&\int d^4x'\,\frac{1}{2}\partial'_\mu\phi(x')\partial'^\mu\phi(x')-\frac{1}{2}m^2\phi^2(x')-\frac{\lambda}{4!}\phi^4(x')\\ =&\int d^4x\,e^{4\sigma}\left[e^{-2\sigma}\frac{1}{2}\partial_\mu\phi(e^\sigma x')\partial^\mu\phi(e^\sigma x)-\frac{1}{2}m^2\phi^2(e^\sigma x)-\frac{\lambda}{4!}\phi^4(e^\sigma x)\right]\\ =&\int d^4x\,\frac{1}{2}\partial_\mu\phi'(x)\partial^\mu\phi'(x)-\frac{1}{2}e^{2\sigma}m^2\phi'^2(x)-\frac{\lambda}{4!}\phi'^4(x)\\ =&S[\phi',\{e^{2\sigma}m^2,\lambda\}].\end{aligned} \tag{7.68}$$

In the derivation of Finding 3, we assumed that the functional measure transforms trivially, i.e. the outer automorphism transformation is anomaly free. As discussed in Chap. 2, this does not hold for dilations. Scale transformations map the marginal couplings $\lambda \to \lambda + \sigma\beta_\lambda$. Repeating the calculation of the scale anomaly, we find that for the ϕ^4 model, Eq. (7.16) should read

$$\begin{aligned} Z'[J] &= \int \mathcal{D}\phi \, \exp\left\{ iS\left[\phi, \left\{\left[1+\sigma\left(2+\frac{\lambda}{16\pi^2}\right)\right] m^2, \left[\lambda+\sigma\frac{3\lambda^2}{16\pi^2}\right]\right\}\right] + \int d^4x \, J\phi \right\} \\ &= \int \mathcal{D}\phi \, \exp\left\{ iS\left[\phi, \left\{m^2 + \sigma\left(2m^2 + \beta_{m^2}\right), \lambda + \sigma\beta_\lambda\right\}\right] + \int d^4x \, J\phi \right\}, \end{aligned} \tag{7.69}$$

where we assumed infinitesimal scale transformations and generalized the anomaly calculation in Chap. 2 to include the mass term. This is a remarkable result. Despite the non-invariance of the measure, the outer automorphism transformations can be absorbed into couplings. However the transformation of the couplings differs from the classical result. Similar to the arguments in Finding 2, $Z[J]$ and $Z'[J]$ have the same functional form and the parameter points $\{m^2, \lambda\}$ and $\{m^2 + \sigma\left(2m^2 + \beta_{m^2}\right), \lambda + \sigma\beta_\lambda\}$ are physically redundant. A simple calculation shows that Eq. (7.17) trivially holds.

7.7 Outlook

In the previous section, we discussed an outer automorphism where the transformation does not leave the path integral measure invariant. We speculate that the findings of this example should generalize. The general argument should look as follows:

Consider the case where the symmetry G is anomaly free. Then the quantum effective action is symmetric, i.e. $\Gamma[\phi^{(\boldsymbol{r})}] = \Gamma[\rho_{\boldsymbol{r}}(g)\phi^{(\boldsymbol{r})}]$. It is typically assumed that the effective action contains all operators consistent with the symmetries of the action. Since the set of operators is complete, the arguments given for the classical action S in Finding 1 should also apply for the effective action Γ.[10] Then we would have, similar to Eq. (7.5),

$$\Gamma[\phi, \lambda] = \Gamma[\tilde{\phi}, f^{(\Gamma)}(\lambda)]. \tag{7.70}$$

It should be noted that this $f^{(\Gamma)}(\lambda)$ in general differs from the $f(\lambda)$ found from the classical action. If the outer automorphism transformation is anomalous, i.e.

[10] Subtleties might arise, since the couplings multiplying the operators are not necessarily independent.

the path integral measure is not invariant, then $f^{(\Gamma)}$ and f are expected to be different. We already saw this for dilations where classically

$$f(\lambda) = \lambda, \tag{7.71}$$

while the anomaly leads to

$$f^{(\Gamma)}(\lambda) = \lambda + \sigma\beta_\lambda. \tag{7.72}$$

Future work should also investigate whether our results can be used to constrain the all-loop beta functions similar to Refs. [270, 271]. In Refs. [270, 271] the tensor structure of the beta functions in the 2HDM is fixed by arguments using the Cayley-Hamilton theorem. In our case, one should be able to derive similar all-loop beta functions by using syzygies, i.e. a generalization of the Cayley-Hamilton theorem.

The arguments in this chapter are based on symmetries and outer automorphisms. They hold to all orders in perturbation theory. While we have presented the arguments for QFT, in principle they should generalize to other theories where the renormalization group is used.

Chapter 8

Conclusion and Outlook

In the SM, the fermions and gauge bosons obtain their masses via the Higgs mechanism and, at the classical level, Higgs mass parameter is the only dimensionful quantity. This mass parameter is not protected against corrections from potential UV completions of the SM giving rise to the hierarchy problem.

Scale transformations are space-time transformations that rescale each space-time point. Classically, fields transform according to their mass dimension and scale symmetry is realized if there are no dimensionful couplings. Scale invariance of the classical action does not imply scale invariance at the quantum level. The scale anomaly manifests itself as the non vanishing beta functions and scale symmetry is explicitly broken.

Scale invariance plays a crucial role in understanding the hierarchy problem. Bardeen argued that, in the absence of new scales, the Higgs mass term is protected against large corrections by scale invariance. The anomalous breaking of scale invariance does not lead to large corrections to the Higgs mass and the SM does not have a hierarchy problem. Once new physics, that comes with a new scale, is introduced, the Higgs mass receives corrections proportional to this new scale. This then leads to the hierarchy problem.

In classically scale invariant settings, the explicit breaking of scale invariance by the scale anomaly can be translated to a physical scale via dimensional transmutation. Coleman and Weinberg showed that, in the weak coupling regime, the gauge group of massless scalar electrodynamics is spontaneously broken. In order to obtain the VEV, one needs to consider loop contributions to the potential which is done by using the effective potential.

The effective potential is independent of the RG scale and therefore follows a Callan-Symanzik type equation. We used this Callan-Symanzik equation to write the effective potential in terms of beta functions. In the case of a single massless scalar field at one-loop, this can be done by integrating the RG equation. In case of multiple scalar fields, writing the effective potential in terms of beta functions is not so straightforward. We focused on the case with two massless scalar fields where the VEVs are hierarchical. In this setup, we wrote the effective potential in terms of beta functions and developed a procedure to approximate the effective potential of the light scalar field. We applied this procedure to models with an approximate symmetry of rotation between to two scalar fields. After spontaneous breaking of this approximate symmetry, we expect a pNGB and our procedure allowed us to identify which sources of symmetry breaking contribute to the mass of the pNGB at leading order.

The main result of this thesis is the concept of Custodial Naturalness which addresses the hierarchy problem. The idea is based on a combination of classical scale invariance together with a scalar sector which has an enhanced custodial symmetry at some high scale. Both symmetries are radiatively broken. At an intermediate scale, the enlarged custodial symmetry is spontaneously broken via the Coleman-Weinberg mechanism and the SM Higgs boson is a pNGB associated with this spontaneous breaking.

We realized Custodial Naturalness in models where the scalar sector consists of the SM Higgs doublet and an additional complex scalar field which is a singlet under the SM gauge group. At the Planck scale the scalar potential is symmetric under a SO(6) custodial symmetry. Both scalar fields have an identical charge under a new $\mathrm{U}(1)_X$ gauge group, which is a linear combination of $B-L$ and hypercharge. The contributions of the new gauge boson to the beta function of the scalar quartic couplings drive these couplings to critical values and the new scalar field obtains a VEV. This VEV spontaneously breaks the $\mathrm{U}(1)_X$ gauge group giving rise to a heavy Z' boson which typically has a mass of $\sim 4-100\,\mathrm{TeV}$. Simultaneously, SO(6) custodial symmetry is broken and the Higgs boson is the pNGB associated with this breaking. The VEV of the new scalar field also spontaneously breaks classical scale invariance giving rise to a dilaton with a mass typically in the range of $30-1000\,\mathrm{GeV}$.

The minimal realization, consisting of the SM fields including right-handed neutrinos, the new scalar field and the $\mathrm{U}(1)_X$ gauge boson, has the same number of parameters as the SM. Further, we showed that Custodial Naturalness can address the hierarchy problem even if the high scale boundary conditions are varied and additional sources of custodial symmetry violation are included. We presented models with additional fermions that populate the neutrino portal or are DM candidates.

Our models predict a thermal history of the Universe that includes a period of strong supercooling followed by a FOPT. Details of the cosmological evolution and potential gravitational wave signals should be explored in more detail in future work.

Another promising realization of Custodial Naturalness based on SO(5) custodial symmetry was briefly sketched. This realization introduces scalar DM and neutrino mass generation by a low-scale type I seesaw mechanism. This model and potential connections to leptogenesis should be studied in future work.

We have introduced outer automorphisms and showed how fields transform under these outer automorphisms. These transformations are not symmetries of the action but can be undone by a transformation of the couplings. We showed that the beta functions transform covariantly under these coupling transformations and illustrated how this constrains the structure of the beta functions in several examples. Connections to t'Hooft naturalness and scale transformations were discussed. Scale transformations served as an example to demonstrate how our results might generalize to the case where the outer automorphism transformation does not leave the path integral measure invariant. In case of anomalous outer automorphism transformations there should also exist a coupling transformation similar to the classical case. We presented some arguments why this should be the case, and the details need to be worked out in future work. Further investigation should also determine how outer automorphisms can fix the structure of the all-loop beta functions.

In summary, this thesis introduced the concept of Custodial Naturalness which is based on conformal symmetry combined with an enhanced custodial symmetry. The enhanced custodial symmetry is spontaneously broken via dimensional transmutation and the Higgs boson emerges as a pNGB, offering an explanation of both the little hierarchy and the separation of the EW and the Planck scale. Custodial Naturalness can be realized in minimal extensions of the SM and can be tested at future colliders and through by gravitational wave signatures originating from a FOPT.

Acknowledgments

I would like to express my gratitude to Manfred Lindner for the opportunity to pursue my doctoral research at Max Planck Institute for Kernphysik (MPIK), as well as for his supervision and guidance throughout my PhD studies.

I am also thankful to Joerg Jaeckel for serving as the second referee of my thesis, and to Björn Malte Schäfer and Loredana Gastaldo for being part of the PhD committee.

I am grateful to my collaborators at MPIK, particularly Andreas Trautner for the pleasant cooperation and our stimulating, fruitful discussions. Special thanks go to Willem Achtermann, Aqeel Ahmed, Tim Herbermann, Sophie Klett, Philipp Saake, Oliver Scholer and Andreas Trautner for their valuable comments on early versions of this thesis.

Further, I would like to thank everyone at MPIK for such a pleasant and inspiring environment, as well as for the many interesting conversations shared over coffee.

Finally, I thank my friends and family who supported my during the time of my PhD studies

Disclaimer

This thesis is based on several published papers or planned publications. In particular, Chapter 6 is based on work in collaboration with *Manfred Lindner* and *Andreas Trautner* published in

[1] T. de Boer, M. Lindner, and A. Trautner, "Electroweak hierarchy from conformal and custodial symmetry," *Phys. Lett. B* **861** (2025) 139241, `arXiv:2407.15920 [hep-ph]`

[2] T. de Boer, M. Lindner, and A. Trautner, "Custodial Naturalness," *accepted for publication in JHEP* (2025) , `arXiv:2502.09699 [hep-ph]`

Further the main idea of ongoing work in collaboration with *Manfred Lindner* and *Andreas Trautner* is sketched in Chapter 6. A publication is planned in

[3] T. de Boer, M. Lindner, and A. Trautner, "Hidden Sector Custodial Naturalness," *in preparation* (2025)

Chapter 7 is part of ongoing research together with *Andreas Trautner* and the results will be published in

[4] T. de Boer and A. Trautner, "RG flow constraints from outer automorphisms," *in preparation* (2025)

Bibliography

[1] T. de Boer, M. Lindner, and A. Trautner, "Electroweak hierarchy from conformal and custodial symmetry," *Phys. Lett. B* **861** (2025) 139241, arXiv:2407.15920 [hep-ph].

[2] T. de Boer, M. Lindner, and A. Trautner, "Custodial Naturalness," *accepted for publication in JHEP* (2025) , arXiv:2502.09699 [hep-ph].

[3] T. de Boer, M. Lindner, and A. Trautner, "Hidden Sector Custodial Naturalness," *in preparation* (2025) .

[4] T. de Boer and A. Trautner, "RG flow constraints from outer automorphisms," *in preparation* (2025) .

[5] F. Englert and R. Brout, "Broken Symmetry and the Mass of Gauge Vector Mesons," *Phys. Rev. Lett.* **13** (1964) 321–323.

[6] P. W. Higgs, "Broken symmetries, massless particles and gauge fields," *Phys. Lett.* **12** (1964) 132–133.

[7] P. W. Higgs, "Broken Symmetries and the Masses of Gauge Bosons," *Phys. Rev. Lett.* **13** (1964) 508–509.

[8] **ATLAS** Collaboration, G. Aad *et al.*, "Observation of a new particle in the search for the Standard Model Higgs boson with the ATLAS detector at the LHC," *Phys. Lett. B* **716** (2012) 1–29, arXiv:1207.7214 [hep-ex].

[9] **CMS** Collaboration, S. Chatrchyan *et al.*, "Observation of a New Boson at a Mass of 125 GeV with the CMS Experiment at the LHC," *Phys. Lett. B* **716** (2012) 30–61, arXiv:1207.7235 [hep-ex].

[10] M. Lindner, "Implications of Triviality for the Standard Model," *Z. Phys. C* **31** (1986) 295.

[11] N. Cabibbo, L. Maiani, G. Parisi, and R. Petronzio, "Bounds on the Fermions and Higgs Boson Masses in Grand Unified Theories," *Nucl. Phys. B* **158** (1979) 295–305.

[12] P. Q. Hung, "Vacuum Instability and New Constraints on Fermion Masses," *Phys. Rev. Lett.* **42** (1979) 873.

[13] M. Sher, "Electroweak Higgs Potentials and Vacuum Stability," *Phys. Rept.* **179** (1989) 273–418.

[14] M. Holthausen, K. S. Lim, and M. Lindner, "Planck scale Boundary Conditions and the Higgs Mass," *JHEP* **02** (2012) 037, `arXiv:1112.2415 [hep-ph]`.

[15] G. Degrassi, S. Di Vita, J. Elias-Miro, J. R. Espinosa, G. F. Giudice, G. Isidori, and A. Strumia, "Higgs mass and vacuum stability in the Standard Model at NNLO," *JHEP* **08** (2012) 098, `arXiv:1205.6497 [hep-ph]`.

[16] D. Buttazzo, G. Degrassi, P. P. Giardino, G. F. Giudice, F. Sala, A. Salvio, and A. Strumia, "Investigating the near-criticality of the Higgs boson," *JHEP* **12** (2013) 089, `arXiv:1307.3536 [hep-ph]`.

[17] W. A. Bardeen, "On naturalness in the standard model," in *Ontake Summer Institute on Particle Physics*. 8, 1995.

[18] K.-y. Oda and M. Yamada, "Non-minimal coupling in Higgs–Yukawa model with asymptotically safe gravity," *Class. Quant. Grav.* **33** no. 12, (2016) 125011, `arXiv:1510.03734 [hep-th]`.

[19] C. Wetterich and M. Yamada, "Gauge hierarchy problem in asymptotically safe gravity–the resurgence mechanism," *Phys. Lett. B* **770** (2017) 268–271, `arXiv:1612.03069 [hep-th]`.

[20] Y. Hamada and M. Yamada, "Asymptotic safety of higher derivative quantum gravity non-minimally coupled with a matter system," *JHEP* **08** (2017) 070, `arXiv:1703.09033 [hep-th]`.

[21] A. Eichhorn, Y. Hamada, J. Lumma, and M. Yamada, "Quantum gravity fluctuations flatten the Planck-scale Higgs potential," *Phys. Rev. D* **97** no. 8, (2018) 086004, `arXiv:1712.00319 [hep-th]`.

[22] S. R. Coleman and E. J. Weinberg, "Radiative Corrections as the Origin of Spontaneous Symmetry Breaking," *Phys. Rev. D* **7** (1973) 1888–1910.

[23] S. Weinberg, "Mass of the Higgs Boson," *Phys. Rev. Lett.* **36** (1976) 294–296.

[24] E. Gildener and S. Weinberg, "Symmetry Breaking and Scalar Bosons," *Phys. Rev. D* **13** (1976) 3333.

[25] R. Hempfling, "The Next-to-minimal Coleman-Weinberg model," *Phys. Lett. B* **379** (1996) 153–158, `arXiv:hep-ph/9604278`.

[26] K. A. Meissner and H. Nicolai, "Conformal Symmetry and the Standard Model," *Phys. Lett. B* **648** (2007) 312–317, `arXiv:hep-th/0612165`.

[27] R. Foot, A. Kobakhidze, and R. R. Volkas, "Electroweak Higgs as a pseudo-Goldstone boson of broken scale invariance," *Phys. Lett. B* **655** (2007) 156–161, `arXiv:0704.1165 [hep-ph]`.

[28] J. R. Espinosa and M. Quiros, "Novel Effects in Electroweak Breaking from a Hidden Sector," *Phys. Rev. D* **76** (2007) 076004, `arXiv:hep-ph/0701145`.

[29] W.-F. Chang, J. N. Ng, and J. M. S. Wu, "Shadow Higgs from a scale-invariant hidden U(1)(s) model," *Phys. Rev. D* **75** (2007) 115016, `arXiv:hep-ph/0701254`.

[30] L. Alexander-Nunneley and A. Pilaftsis, "The Minimal Scale Invariant Extension of the Standard Model," *JHEP* **09** (2010) 021, `arXiv:1006.5916 [hep-ph]`.

[31] C. Englert, J. Jaeckel, V. V. Khoze, and M. Spannowsky, "Emergence of the Electroweak Scale through the Higgs Portal," *JHEP* **04** (2013) 060, `arXiv:1301.4224 [hep-ph]`.

[32] A. Farzinnia, H.-J. He, and J. Ren, "Natural Electroweak Symmetry Breaking from Scale Invariant Higgs Mechanism," *Phys. Lett. B* **727** (2013) 141–150, `arXiv:1308.0295 [hep-ph]`.

[33] A. J. Helmboldt, P. Humbert, M. Lindner, and J. Smirnov, "Minimal conformal extensions of the Higgs sector," *JHEP* **07** (2017) 113, `arXiv:1603.03603 [hep-ph]`.

[34] E. Gabrielli, M. Heikinheimo, K. Kannike, A. Racioppi, M. Raidal, and C. Spethmann, "Towards Completing the Standard Model: Vacuum Stability, EWSB and Dark Matter," *Phys. Rev. D* **89** no. 1, (2014) 015017, arXiv:1309.6632 [hep-ph].

[35] T. Hambye and M. H. G. Tytgat, "Electroweak symmetry breaking induced by dark matter," *Phys. Lett. B* **659** (2008) 651–655, arXiv:0707.0633 [hep-ph].

[36] T. Hambye and A. Strumia, "Dynamical generation of the weak and Dark Matter scale," *Phys. Rev. D* **88** (2013) 055022, arXiv:1306.2329 [hep-ph].

[37] C. D. Carone and R. Ramos, "Classical scale-invariance, the electroweak scale and vector dark matter," *Phys. Rev. D* **88** (2013) 055020, arXiv:1307.8428 [hep-ph].

[38] W. Altmannshofer, W. A. Bardeen, M. Bauer, M. Carena, and J. D. Lykken, "Light Dark Matter, Naturalness, and the Radiative Origin of the Electroweak Scale," *JHEP* **01** (2015) 032, arXiv:1408.3429 [hep-ph].

[39] A. Karam and K. Tamvakis, "Dark matter and neutrino masses from a scale-invariant multi-Higgs portal," *Phys. Rev. D* **92** no. 7, (2015) 075010, arXiv:1508.03031 [hep-ph].

[40] A. Ahriche, K. L. McDonald, and S. Nasri, "The Scale-Invariant Scotogenic Model," *JHEP* **06** (2016) 182, arXiv:1604.05569 [hep-ph].

[41] A. Ahriche, A. Manning, K. L. McDonald, and S. Nasri, "Scale-Invariant Models with One-Loop Neutrino Mass and Dark Matter Candidates," *Phys. Rev. D* **94** no. 5, (2016) 053005, arXiv:1604.05995 [hep-ph].

[42] A. Lewandowski, K. A. Meissner, and H. Nicolai, "Conformal Standard Model, Leptogenesis and Dark Matter," *Phys. Rev. D* **97** no. 3, (2018) 035024, arXiv:1710.06149 [hep-ph].

[43] S. Iso, N. Okada, and Y. Orikasa, "Classically conformal B^{-} L extended Standard Model," *Phys. Lett. B* **676** (2009) 81–87, arXiv:0902.4050 [hep-ph].

[44] S. Iso, N. Okada, and Y. Orikasa, “The minimal B-L model naturally realized at TeV scale,” *Phys. Rev. D* **80** (2009) 115007, arXiv:0909.0128 [hep-ph].

[45] S. Oda, N. Okada, and D.-s. Takahashi, “Classically conformal U(1)’ extended standard model and Higgs vacuum stability,” *Phys. Rev. D* **92** no. 1, (2015) 015026, arXiv:1504.06291 [hep-ph].

[46] A. Das, N. Okada, and N. Papapietro, “Electroweak vacuum stability in classically conformal B-L extension of the Standard Model,” *Eur. Phys. J. C* **77** no. 2, (2017) 122, arXiv:1509.01466 [hep-ph].

[47] A. Das, S. Oda, N. Okada, and D.-s. Takahashi, “Classically conformal U(1)’ extended standard model, electroweak vacuum stability, and LHC Run-2 bounds,” *Phys. Rev. D* **93** no. 11, (2016) 115038, arXiv:1605.01157 [hep-ph].

[48] M. Holthausen, M. Lindner, and M. A. Schmidt, “Radiative Symmetry Breaking of the Minimal Left-Right Symmetric Model,” *Phys. Rev. D* **82** (2010) 055002, arXiv:0911.0710 [hep-ph].

[49] R. Foot, A. Kobakhidze, K. L. McDonald, and R. R. Volkas, “Neutrino mass in radiatively-broken scale-invariant models,” *Phys. Rev. D* **76** (2007) 075014, arXiv:0706.1829 [hep-ph].

[50] M. Lindner, S. Schmidt, and J. Smirnov, “Neutrino Masses and Conformal Electro-Weak Symmetry Breaking,” *JHEP* **10** (2014) 177, arXiv:1405.6204 [hep-ph].

[51] P. Humbert, M. Lindner, and J. Smirnov, “The Inverse Seesaw in Conformal Electro-Weak Symmetry Breaking and Phenomenological Consequences,” *JHEP* **06** (2015) 035, arXiv:1503.03066 [hep-ph].

[52] P. Humbert, M. Lindner, S. Patra, and J. Smirnov, “Lepton Number Violation within the Conformal Inverse Seesaw,” *JHEP* **09** (2015) 064, arXiv:1505.07453 [hep-ph].

[53] V. Brdar, Y. Emonds, A. J. Helmboldt, and M. Lindner, “Conformal Realization of the Neutrino Option,” *Phys. Rev. D* **99** no. 5, (2019) 055014, arXiv:1807.11490 [hep-ph].

[54] V. Brdar, A. J. Helmboldt, S. Iwamoto, and K. Schmitz, "Type-I Seesaw as the Common Origin of Neutrino Mass, Baryon Asymmetry, and the Electroweak Scale," *Phys. Rev. D* **100** (2019) 075029, arXiv:1905.12634 [hep-ph].

[55] D. B. Kaplan and H. Georgi, "SU(2) x U(1) Breaking by Vacuum Misalignment," *Phys. Lett. B* **136** (1984) 183–186.

[56] D. B. Kaplan, H. Georgi, and S. Dimopoulos, "Composite Higgs Scalars," *Phys. Lett. B* **136** (1984) 187–190.

[57] H. Georgi and D. B. Kaplan, "Composite Higgs and Custodial SU(2)," *Phys. Lett. B* **145** (1984) 216–220.

[58] M. J. Dugan, H. Georgi, and D. B. Kaplan, "Anatomy of a Composite Higgs Model," *Nucl. Phys. B* **254** (1985) 299–326.

[59] H. Georgi and A. Pais, "Calculability and Naturalness in Gauge Theories," *Phys. Rev. D* **10** (1974) 539.

[60] H. Georgi and A. Pais, "Vacuum Symmetry and the PseudoGoldstone Phenomenon," *Phys. Rev. D* **12** (1975) 508.

[61] N. Arkani-Hamed, A. G. Cohen, and H. Georgi, "Electroweak symmetry breaking from dimensional deconstruction," *Phys. Lett. B* **513** (2001) 232–240, arXiv:hep-ph/0105239.

[62] N. Arkani-Hamed, A. G. Cohen, T. Gregoire, and J. G. Wacker, "Phenomenology of electroweak symmetry breaking from theory space," *JHEP* **08** (2002) 020, arXiv:hep-ph/0202089.

[63] N. Arkani-Hamed, A. G. Cohen, E. Katz, and A. E. Nelson, "The Littlest Higgs," *JHEP* **07** (2002) 034, arXiv:hep-ph/0206021.

[64] N. Arkani-Hamed, A. G. Cohen, E. Katz, A. E. Nelson, T. Gregoire, and J. G. Wacker, "The Minimal moose for a little Higgs," *JHEP* **08** (2002) 021, arXiv:hep-ph/0206020.

[65] Z. Chacko, H.-S. Goh, and R. Harnik, "The Twin Higgs: Natural electroweak breaking from mirror symmetry," *Phys. Rev. Lett.* **96** (2006) 231802, arXiv:hep-ph/0506256.

[66] R. Barbieri, T. Gregoire, and L. J. Hall, "Mirror world at the large hadron collider," arXiv:hep-ph/0509242.

[67] Z. Chacko, Y. Nomura, M. Papucci, and G. Perez, "Natural little hierarchy from a partially goldstone twin Higgs," *JHEP* **01** (2006) 126, arXiv:hep-ph/0510273.

[68] J. Goldstone, "Field Theories with Superconductor Solutions," *Nuovo Cim.* **19** (1961) 154–164.

[69] Y. Nambu and G. Jona-Lasinio, "Dynamical Model of Elementary Particles Based on an Analogy with Superconductivity. 1.," *Phys. Rev.* **122** (1961) 345–358.

[70] J. Goldstone, A. Salam, and S. Weinberg, "Broken Symmetries," *Phys. Rev.* **127** (1962) 965–970.

[71] T. Alanne, H. Gertov, F. Sannino, and K. Tuominen, "Elementary Goldstone Higgs boson and dark matter," *Phys. Rev. D* **91** no. 9, (2015) 095021, arXiv:1411.6132 [hep-ph].

[72] H. Gertov, A. Meroni, E. Molinaro, and F. Sannino, "Theory and phenomenology of the elementary Goldstone Higgs boson," *Phys. Rev. D* **92** no. 9, (2015) 095003, arXiv:1507.06666 [hep-ph].

[73] A. Davidson, "$B-L$ as the fourth color within an $\mathrm{SU}(2)_L \times \mathrm{U}(1)_R \times \mathrm{U}(1)$ model," *Phys. Rev. D* **20** (1979) 776.

[74] R. E. Marshak and R. N. Mohapatra, "Quark - Lepton Symmetry and $B-L$ as the U(1) Generator of the Electroweak Symmetry Group," *Phys. Lett. B* **91** (1980) 222–224.

[75] R. N. Mohapatra and R. E. Marshak, "Local $B-L$ Symmetry of Electroweak Interactions, Majorana Neutrinos and Neutron Oscillations," *Phys. Rev. Lett.* **44** (1980) 1316–1319. [Erratum: Phys.Rev.Lett. 44, 1643 (1980)].

[76] C. Wetterich, "Neutrino Masses and the Scale of $B-L$ Violation," *Nucl. Phys. B* **187** (1981) 343–375.

[77] E. E. Jenkins, "Searching for a $(B-L)$ Gauge Boson in $p\bar{p}$ Collisions," *Phys. Lett. B* **192** (1987) 219–222.

[78] W. Buchmuller, C. Greub, and P. Minkowski, "Neutrino masses, neutral vector bosons and the scale of $B - L$ breaking," *Phys. Lett. B* **267** (1991) 395–399.

[79] S. Khalil, "Low scale $B - L$ extension of the Standard Model at the LHC," *J. Phys. G* **35** (2008) 055001, arXiv:hep-ph/0611205.

[80] G. 't Hooft, "Naturalness, chiral symmetry, and spontaneous chiral symmetry breaking," *NATO Sci. Ser. B* **59** (1980) 135–157.

[81] W. Grimus and M. N. Rebelo, "Automorphisms in gauge theories and the definition of CP and P," *Phys. Rept.* **281** (1997) 239–308, arXiv:hep-ph/9506272.

[82] I. L. Buchbinder, D. M. Gitman, and A. L. Shelepin, "Discrete symmetries as automorphisms of the proper Poincare group," *Int. J. Theor. Phys.* **41** (2002) 753–790, arXiv:hep-th/0010035.

[83] M. Holthausen, M. Lindner, and M. A. Schmidt, "CP and Discrete Flavour Symmetries," *JHEP* **04** (2013) 122, arXiv:1211.6953 [hep-ph].

[84] M.-C. Chen, M. Fallbacher, K. T. Mahanthappa, M. Ratz, and A. Trautner, "CP Violation from Finite Groups," *Nucl. Phys. B* **883** (2014) 267–305, arXiv:1402.0507 [hep-ph].

[85] M. Fallbacher, *Discrete Groups in Model Building and the Definition of CP*. PhD thesis, Munich, Tech. U., 8, 2015.

[86] M. Fallbacher and A. Trautner, "Symmetries of symmetries and geometrical CP violation," *Nucl. Phys. B* **894** (2015) 136–160, arXiv:1502.01829 [hep-ph].

[87] A. Trautner, *CP and other Symmetries of Symmetries*. PhD thesis, Munich, Tech. U., Universe, 2016. arXiv:1608.05240 [hep-ph].

[88] A. Baur, H. P. Nilles, A. Trautner, and P. K. S. Vaudrevange, "Unification of Flavor, CP, and Modular Symmetries," *Phys. Lett. B* **795** (2019) 7–14, arXiv:1901.03251 [hep-th].

[89] B. Henning, X. Lu, T. Melia, and H. Murayama, "Outer automorphism anomalies," *JHEP* **02** (2022) 094, arXiv:2111.04728 [hep-th].

[90] I. Bischer, C. Döring, and A. Trautner, "Telling compositeness at a distance with outer automorphisms and CP," *J. Phys. A* **56** no. 28, (2023) 285401, arXiv:2212.07439 [hep-ph].

[91] C. Döring and A. Trautner, "Symmetries from outer automorphisms and unorthodox group extensions," arXiv:2410.11052 [hep-ph].

[92] E. Noether, "Invariant Variation Problems," *Gott. Nachr.* **1918** (1918) 235–257, arXiv:physics/0503066.

[93] C. G. Callan, Jr., S. R. Coleman, and R. Jackiw, "A New improved energy - momentum tensor," *Annals Phys.* **59** (1970) 42–73.

[94] G. Mack and A. Salam, "Finite component field representations of the conformal group," *Annals Phys.* **53** (1969) 174–202.

[95] D. J. Gross and J. Wess, "Scale invariance, conformal invariance, and the high-energy behavior of scattering amplitudes," *Phys. Rev. D* **2** (1970) 753–764.

[96] S. Coleman, *Aspects of Symmetry: Selected Erice Lectures*. Cambridge University Press, Cambridge, U.K., 1985.

[97] J. Polchinski, "Scale and Conformal Invariance in Quantum Field Theory," *Nucl. Phys. B* **303** (1988) 226–236.

[98] S. El-Showk, Y. Nakayama, and S. Rychkov, "What Maxwell Theory in D<>4 teaches us about scale and conformal invariance," *Nucl. Phys. B* **848** (2011) 578–593, arXiv:1101.5385 [hep-th].

[99] Y. Nakayama, "Scale invariance vs conformal invariance," *Phys. Rept.* **569** (2015) 1–93, arXiv:1302.0884 [hep-th].

[100] K. Fujikawa, "Path Integral Measure for Gauge Invariant Fermion Theories," *Phys. Rev. Lett.* **42** (1979) 1195–1198.

[101] M. Umezawa, "Regularization of the Path Integral Measure for Anomalies," *Phys. Rev. D* **39** (1989) 3672.

[102] F. Englert, C. Truffin, and R. Gastmans, "Conformal Invariance in Quantum Gravity," *Nucl. Phys. B* **117** (1976) 407–432.

[103] M. Shaposhnikov and D. Zenhausern, "Quantum scale invariance, cosmological constant and hierarchy problem," *Phys. Lett. B* **671** (2009) 162–166, arXiv:0809.3406 [hep-th].

[104] M. E. Shaposhnikov and F. V. Tkachov, "Quantum scale-invariant models as effective field theories," arXiv:0905.4857 [hep-th].

[105] C. Tamarit, "Running couplings with a vanishing scale anomaly," *JHEP* **12** (2013) 098, arXiv:1309.0913 [hep-th].

[106] F. Gretsch and A. Monin, "Perturbative conformal symmetry and dilaton," *Phys. Rev. D* **92** no. 4, (2015) 045036, arXiv:1308.3863 [hep-th].

[107] S. Mooij, M. Shaposhnikov, and T. Voumard, "Hidden and explicit quantum scale invariance," *Phys. Rev. D* **99** no. 8, (2019) 085013, arXiv:1812.07946 [hep-th].

[108] S. Weinberg, "Implications of Dynamical Symmetry Breaking," *Phys. Rev. D* **13** (1976) 974–996. [Addendum: Phys.Rev.D 19, 1277–1280 (1979)].

[109] A. J. Buras, J. R. Ellis, M. K. Gaillard, and D. V. Nanopoulos, "Aspects of the Grand Unification of Strong, Weak and Electromagnetic Interactions," *Nucl. Phys. B* **135** (1978) 66–92.

[110] E. Gildener, "Gauge Symmetry Hierarchies," *Phys. Rev. D* **14** (1976) 1667.

[111] L. Susskind, "Dynamics of Spontaneous Symmetry Breaking in the Weinberg-Salam Theory," *Phys. Rev. D* **20** (1979) 2619–2625.

[112] S. Weinberg, "Gauge Hierarchies," *Phys. Lett. B* **82** (1979) 387–391.

[113] H. Aoki and S. Iso, "Revisiting the Naturalness Problem – Who is afraid of quadratic divergences? –," *Phys. Rev. D* **86** (2012) 013001, arXiv:1201.0857 [hep-ph].

[114] M. Yamada, "Gauge hierarchy problem and scalegenesis," *PoS* **CORFU2019** (2020) 077, arXiv:2004.00142 [hep-ph].

[115] S. Mooij and M. Shaposhnikov, "QFT without infinities and hierarchy problem," *Nucl. Phys. B* **990** (2023) 116172, arXiv:2110.05175 [hep-th].

[116] S. Mooij and M. Shaposhnikov, "Finite Callan-Symanzik renormalisation for multiple scalar fields," *Nucl. Phys. B* **990** (2023) 116176, arXiv:2110.15925 [hep-th].

[117] S. Mooij and M. Shaposhnikov, "Effective potential in finite formulation of QFT," *Nucl. Phys. B* **1006** (2024) 116642, arXiv:2408.00389 [hep-th].

[118] Y. Ageeva, P. Petrov, and M. Shaposhnikov, "Nonrenormalizable theories and finite formulation of QFT," *Phys. Rev. D* **111** no. 2, (2025) 025020, arXiv:2409.15036 [hep-th].

[119] C. Branchina, V. Branchina, F. Contino, and N. Darvishi, "Dimensional regularization, Wilsonian RG, and the naturalness and hierarchy problem," *Phys. Rev. D* **106** no. 6, (2022) 065007, arXiv:2204.10582 [hep-th].

[120] K.-S. Choi, "Renormalization, Decoupling and the Hierarchy Problem," arXiv:2408.06406 [hep-ph].

[121] R. R. Volkas, A. J. Davies, and G. C. Joshi, "NATURALNESS OF THE INVISIBLE AXION MODEL," *Phys. Lett. B* **215** (1988) 133–138.

[122] R. Foot, A. Kobakhidze, K. L. McDonald, and R. R. Volkas, "Poincaré protection for a natural electroweak scale," *Phys. Rev. D* **89** no. 11, (2014) 115018, arXiv:1310.0223 [hep-ph].

[123] R. Haag, J. T. Lopuszanski, and M. Sohnius, "All Possible Generators of Supersymmetries of the s Matrix," *Nucl. Phys. B* **88** (1975) 257.

[124] S. P. Martin, "A Supersymmetry primer," *Adv. Ser. Direct. High Energy Phys.* **18** (1998) 1–98, arXiv:hep-ph/9709356.

[125] J. Wess and B. Zumino, "Supergauge Transformations in Four-Dimensions," *Nucl. Phys. B* **70** (1974) 39–50.

[126] M. van Beekveld, S. Caron, and R. Ruiz de Austri, "The current status of fine-tuning in supersymmetry," *JHEP* **01** (2020) 147, arXiv:1906.10706 [hep-ph].

[127] R. Jackiw and K. Johnson, "Dynamical Model of Spontaneously Broken Gauge Symmetries," *Phys. Rev. D* **8** (1973) 2386–2398.

[128] J. M. Cornwall and R. E. Norton, “Spontaneous Symmetry Breaking Without Scalar Mesons,” *Phys. Rev. D* **8** (1973) 3338–3346.

[129] M. Weinstein, “CONSERVED CURRENTS, THEIR COMMUTATORS AND THE SYMMETRY STRUCTURE OF RENORMALIZABLE THEORIES OF ELECTROMAGNETIC, WEAK AND STRONG INTERACTIONS,” *Phys. Rev. D* **8** (1973) 2511.

[130] S. Dimopoulos and L. Susskind, “Mass Without Scalars,” *Nucl. Phys. B* **155** (1979) 237–252.

[131] E. Eichten and K. D. Lane, “Dynamical Breaking of Weak Interaction Symmetries,” *Phys. Lett. B* **90** (1980) 125–130.

[132] R. F. Dashen, “Chiral SU(3) x SU(3) as a symmetry of the strong interactions,” *Phys. Rev.* **183** (1969) 1245–1260.

[133] R. F. Dashen, “Some features of chiral symmetry breaking,” *Phys. Rev. D* **3** (1971) 1879–1889.

[134] K. D. Lane, “An Introduction to technicolor,” in *Theoretical Advanced Study Institute (TASI 93) in Elementary Particle Physics: The Building Blocks of Creation - From Microfermius to Megaparsecs*. 6, 1993. `arXiv:hep-ph/9401324`.

[135] T. Kaluza, “Zum Unitätsproblem der Physik,” *Sitzungsber. Preuss. Akad. Wiss. Berlin (Math. Phys.)* **1921** (1921) 966–972, `arXiv:1803.08616 [physics.hist-ph]`.

[136] O. Klein, “Quantum Theory and Five-Dimensional Theory of Relativity. (In German and English),” *Z. Phys.* **37** (1926) 895–906.

[137] V. A. Rubakov and M. E. Shaposhnikov, “Do We Live Inside a Domain Wall?,” *Phys. Lett. B* **125** (1983) 136–138.

[138] N. Arkani-Hamed, S. Dimopoulos, and G. R. Dvali, “The Hierarchy problem and new dimensions at a millimeter,” *Phys. Lett. B* **429** (1998) 263–272, `arXiv:hep-ph/9803315`.

[139] C. Csáki and P. Tanedo, “Beyond the Standard Model,” in *2013 European School of High-Energy Physics*, pp. 169–268. 2015. `arXiv:1602.04228 [hep-ph]`.

[140] L. Randall and R. Sundrum, “A Large mass hierarchy from a small extra dimension,” *Phys. Rev. Lett.* **83** (1999) 3370–3373, arXiv:hep-ph/9905221.

[141] P. W. Graham, D. E. Kaplan, and S. Rajendran, “Cosmological Relaxation of the Electroweak Scale,” *Phys. Rev. Lett.* **115** no. 22, (2015) 221801, arXiv:1504.07551 [hep-ph].

[142] N. Arkani-Hamed, T. Cohen, R. T. D’Agnolo, A. Hook, H. D. Kim, and D. Pinner, “Solving the Hierarchy Problem at Reheating with a Large Number of Degrees of Freedom,” *Phys. Rev. Lett.* **117** no. 25, (2016) 251801, arXiv:1607.06821 [hep-ph].

[143] G. Dvali, “Black Holes and Large N Species Solution to the Hierarchy Problem,” *Fortsch. Phys.* **58** (2010) 528–536, arXiv:0706.2050 [hep-th].

[144] G. Dvali and M. Redi, “Black Hole Bound on the Number of Species and Quantum Gravity at LHC,” *Phys. Rev. D* **77** (2008) 045027, arXiv:0710.4344 [hep-th].

[145] V. Agrawal, S. M. Barr, J. F. Donoghue, and D. Seckel, “Viable range of the mass scale of the standard model,” *Phys. Rev. D* **57** (1998) 5480–5492, arXiv:hep-ph/9707380.

[146] K. Agashe, R. Contino, and A. Pomarol, “The Minimal composite Higgs model,” *Nucl. Phys. B* **719** (2005) 165–187, arXiv:hep-ph/0412089.

[147] Z. Chacko, H.-S. Goh, and R. Harnik, “A Twin Higgs model from left-right symmetry,” *JHEP* **01** (2006) 108, arXiv:hep-ph/0512088.

[148] N. Craig, S. Knapen, and P. Longhi, “Neutral Naturalness from Orbifold Higgs Models,” *Phys. Rev. Lett.* **114** no. 6, (2015) 061803, arXiv:1410.6808 [hep-ph].

[149] N. Craig, A. Katz, M. Strassler, and R. Sundrum, “Naturalness in the Dark at the LHC,” *JHEP* **07** (2015) 105, arXiv:1501.05310 [hep-ph].

[150] R. Barbieri, L. J. Hall, and K. Harigaya, “Minimal Mirror Twin Higgs,” *JHEP* **11** (2016) 172, arXiv:1609.05589 [hep-ph].

[151] J. Serra and R. Torre, “Neutral naturalness from the brother-Higgs model,” *Phys. Rev. D* **97** no. 3, (2018) 035017, arXiv:1709.05399 [hep-ph].

[152] L.-X. Xu, J.-H. Yu, and S.-H. Zhu, "Minimal neutral naturalness model," *Phys. Rev. D* **101** no. 9, (2020) 095014, arXiv:1810.01882 [hep-ph].

[153] N. Craig, S. Koren, and T. Trott, "Cosmological Signals of a Mirror Twin Higgs," *JHEP* **05** (2017) 038, arXiv:1611.07977 [hep-ph].

[154] Z. Chacko, N. Craig, P. J. Fox, and R. Harnik, "Cosmology in Mirror Twin Higgs and Neutrino Masses," *JHEP* **07** (2017) 023, arXiv:1611.07975 [hep-ph].

[155] C. Csaki, E. Kuflik, and S. Lombardo, "Viable Twin Cosmology from Neutrino Mixing," *Phys. Rev. D* **96** no. 5, (2017) 055013, arXiv:1703.06884 [hep-ph].

[156] Z. Chacko, D. Curtin, M. Geller, and Y. Tsai, "Cosmological Signatures of a Mirror Twin Higgs," *JHEP* **09** (2018) 163, arXiv:1803.03263 [hep-ph].

[157] M. D. Schwartz, *Quantum Field Theory and the Standard Model*. Cambridge University Press, 3, 2014.

[158] R. Jackiw, "Functional evaluation of the effective potential," *Phys. Rev. D* **9** (1974) 1686.

[159] M. E. Peskin and D. V. Schroeder, *An Introduction to quantum field theory*. Addison-Wesley, Reading, USA, 1995.

[160] A. Andreassen, W. Frost, and M. D. Schwartz, "Consistent Use of Effective Potentials," *Phys. Rev. D* **91** no. 1, (2015) 016009, arXiv:1408.0287 [hep-ph].

[161] K. Symanzik, "Renormalizable models with simple symmetry breaking. 1. Symmetry breaking by a source term," *Commun. Math. Phys.* **16** (1970) 48–80.

[162] J. Iliopoulos, C. Itzykson, and A. Martin, "Functional Methods and Perturbation Theory," *Rev. Mod. Phys.* **47** (1975) 165.

[163] L. O'Raifeartaigh and G. Parravicini, "Effective Fields and Discontinuities in the Effective Potential," *Nucl. Phys. B* **111** (1976) 501–515.

[164] A. Dannenberg, "Dysfunctional Methods and the Effective Potential," *Phys. Lett. B* **202** (1988) 110–116.

[165] E. Gildener, "Radiatively Induced Spontaneous Symmetry Breaking for Asymptotically Free Gauge Theories," *Phys. Rev. D* **13** (1976) 1025.

[166] M. B. Einhorn and D. R. T. Jones, "A NEW RENORMALIZATION GROUP APPROACH TO MULTISCALE PROBLEMS," *Nucl. Phys. B* **230** (1984) 261–272.

[167] M. Bando, T. Kugo, N. Maekawa, and H. Nakano, "Improving the effective potential," *Phys. Lett. B* **301** (1993) 83–89, arXiv:hep-ph/9210228.

[168] M. Bando, T. Kugo, N. Maekawa, and H. Nakano, "Improving the effective potential: Multimass scale case," *Prog. Theor. Phys.* **90** (1993) 405–418, arXiv:hep-ph/9210229.

[169] H. Nakano and Y. Yoshida, "Improving the effective potential, multimass problem and modified mass dependent scheme," *Phys. Rev. D* **49** (1994) 5393–5407, arXiv:hep-ph/9309215.

[170] C. Ford and C. Wiesendanger, "A Multiscale subtraction scheme and partial renormalization group equations in the O(N) symmetric phi**4 theory," *Phys. Rev. D* **55** (1997) 2202–2217, arXiv:hep-ph/9604392.

[171] C. Ford and C. Wiesendanger, "Multiscale renormalization," *Phys. Lett. B* **398** (1997) 342–346, arXiv:hep-th/9612193.

[172] J. A. Casas, V. Di Clemente, and M. Quiros, "The Effective potential in the presence of several mass scales," *Nucl. Phys. B* **553** (1999) 511–530, arXiv:hep-ph/9809275.

[173] T. G. Steele, Z.-W. Wang, and D. G. C. McKeon, "Multiscale renormalization group methods for effective potentials with multiple scalar fields," *Phys. Rev. D* **90** no. 10, (2014) 105012, arXiv:1409.3489 [hep-ph].

[174] A. V. Manohar and E. Nardoni, "Renormalization Group Improvement of the Effective Potential: an EFT Approach," *JHEP* **04** (2021) 093, arXiv:2010.15806 [hep-ph].

[175] C. P. Burgess, "Introduction to Effective Field Theory," *Ann. Rev. Nucl. Part. Sci.* **57** (2007) 329–362, arXiv:hep-th/0701053.

[176] K. Kannike, L. Marzola, M. Raidal, and A. Strumia, "Light Higgs boson from multi-phase criticality in dynamical symmetry breaking," *Phys. Lett. B* **816** (2021) 136241, arXiv:2102.01084 [hep-ph].

[177] K. Huitu, K. Kannike, N. Koivunen, L. Marzola, S. Mondal, and M. Raidal, "Multiphase critical Higgs boson at colliders," *Phys. Rev. D* **105** no. 9, (2022) 095036, arXiv:2201.00824 [hep-ph].

[178] K. Kannike, N. Koivunen, A. Kubarski, L. Marzola, M. Raidal, A. Strumia, and V. Vipp, "Dark matter-induced multi-phase dynamical symmetry breaking," *Phys. Lett. B* **832** (2022) 137214, arXiv:2204.01744 [hep-ph].

[179] P. Galison and A. Manohar, "TWO Z's OR NOT TWO Z's?," *Phys. Lett. B* **136** (1984) 279–283.

[180] B. Holdom, "Two U(1)'s and Epsilon Charge Shifts," *Phys. Lett. B* **166** (1986) 196–198.

[181] J.-X. Pan, M. He, X.-G. He, and G. Li, "Scrutinizing a massless dark photon: basis independence," *Nucl. Phys. B* **953** (2020) 114968, arXiv:1807.11363 [hep-ph].

[182] C. D. Carone and H. Murayama, "Realistic models with a light U(1) gauge boson coupled to baryon number," *Phys. Rev. D* **52** (1995) 484–493, arXiv:hep-ph/9501220.

[183] L. N. Chang, O. Lebedev, W. Loinaz, and T. Takeuchi, "Constraints on gauged B - 3 L(tau) and related theories," *Phys. Rev. D* **63** (2001) 074013, arXiv:hep-ph/0010118.

[184] A. Aranda and C. D. Carone, "Orthogonal U(1) ' s, proton stability and extra dimensions," *Phys. Rev. D* **63** (2001) 075012, arXiv:hep-ph/0012092.

[185] W. Loinaz and T. Takeuchi, "Charge assignments in multiple U(1) gauge theories," *Phys. Rev. D* **60** (1999) 115008, arXiv:hep-ph/9903362.

[186] G. 't Hooft, "A Planar Diagram Theory for Strong Interactions," *Nucl. Phys. B* **72** (1974) 461.

[187] G. Veneziano, "Some Aspects of a Unified Approach to Gauge, Dual and Gribov Theories," *Nucl. Phys. B* **117** (1976) 519–545.

[188] S. P. Martin, "Two Loop Effective Potential for a General Renormalizable Theory and Softly Broken Supersymmetry," *Phys. Rev. D* **65** (2002) 116003, arXiv:hep-ph/0111209.

[189] **Particle Data Group** Collaboration, R. L. Workman *et al.*, "Review of Particle Physics," *PTEP* **2022** (2022) 083C01.

[190] L. Sartore and I. Schienbein, "PyR@TE 3," *Comput. Phys. Commun.* **261** (2021) 107819, arXiv:2007.12700 [hep-ph].

[191] R. Barbieri and G. F. Giudice, "Upper Bounds on Supersymmetric Particle Masses," *Nucl. Phys. B* **306** (1988) 63–76.

[192] G. W. Anderson and D. J. Castano, "Measures of fine tuning," *Phys. Lett. B* **347** (1995) 300–308, arXiv:hep-ph/9409419.

[193] **ATLAS** Collaboration, G. Aad *et al.*, "Search for high-mass dilepton resonances using 139 fb^{-1} of pp collision data collected at $\sqrt{s}$ =13 TeV with the ATLAS detector," *Phys. Lett. B* **796** (2019) 68–87, arXiv:1903.06248 [hep-ex].

[194] **CMS** Collaboration, A. M. Sirunyan *et al.*, "Search for resonant and nonresonant new phenomena in high-mass dilepton final states at $\sqrt{s} = 13$ TeV," *JHEP* **07** (2021) 208, arXiv:2103.02708 [hep-ex].

[195] **ATLAS** Collaboration, "Prospects for searches for heavy Z' and W' bosons in fermionic final states with the ATLAS experiment at the HL-LHC,".

[196] J. Alwall, R. Frederix, S. Frixione, V. Hirschi, F. Maltoni, O. Mattelaer, H. S. Shao, T. Stelzer, P. Torrielli, and M. Zaro, "The automated computation of tree-level and next-to-leading order differential cross sections, and their matching to parton shower simulations," *JHEP* **07** (2014) 079, arXiv:1405.0301 [hep-ph].

[197] C. Degrande, C. Duhr, B. Fuks, D. Grellscheid, O. Mattelaer, and T. Reiter, "UFO - The Universal FeynRules Output," *Comput. Phys. Commun.* **183** (2012) 1201–1214, arXiv:1108.2040 [hep-ph].

[198] N. D. Christensen and C. Duhr, "FeynRules - Feynman rules made easy," *Comput. Phys. Commun.* **180** (2009) 1614–1641, arXiv:0806.4194 [hep-ph].

[199] **ATLAS** Collaboration, G. Aad *et al.*, "Constraints on new phenomena via Higgs boson couplings and invisible decays with the ATLAS detector," *JHEP* **11** (2015) 206, arXiv:1509.00672 [hep-ex].

[200] T. Robens and T. Stefaniak, "Status of the Higgs Singlet Extension of the Standard Model after LHC Run 1," *Eur. Phys. J. C* **75** (2015) 104, arXiv:1501.02234 [hep-ph].

[201] A. Falkowski, C. Gross, and O. Lebedev, "A second Higgs from the Higgs portal," *JHEP* **05** (2015) 057, arXiv:1502.01361 [hep-ph].

[202] T. Konstandin and G. Servant, "Cosmological Consequences of Nearly Conformal Dynamics at the TeV scale," *JCAP* **12** (2011) 009, arXiv:1104.4791 [hep-ph].

[203] G. Alguero, G. Belanger, F. Boudjema, S. Chakraborti, A. Goudelis, S. Kraml, A. Mjallal, and A. Pukhov, "micrOMEGAs 6.0: N-component dark matter," *Comput. Phys. Commun.* **299** (2024) 109133, arXiv:2312.14894 [hep-ph].

[204] F. Staub, "SARAH 4 : A tool for (not only SUSY) model builders," *Comput. Phys. Commun.* **185** (2014) 1773–1790, arXiv:1309.7223 [hep-ph].

[205] **Planck** Collaboration, N. Aghanim *et al.*, "Planck 2018 results. VI. Cosmological parameters," *Astron. Astrophys.* **641** (2020) A6, arXiv:1807.06209 [astro-ph.CO]. [Erratum: Astron.Astrophys. 652, C4 (2021)].

[206] **XENON** Collaboration, E. Aprile *et al.*, "First Dark Matter Search with Nuclear Recoils from the XENONnT Experiment," *Phys. Rev. Lett.* **131** no. 4, (2023) 041003, arXiv:2303.14729 [hep-ex].

[207] C. A. J. O'Hare, "New Definition of the Neutrino Floor for Direct Dark Matter Searches," *Phys. Rev. Lett.* **127** no. 25, (2021) 251802, arXiv:2109.03116 [hep-ph].

[208] **DARWIN** Collaboration, J. Aalbers *et al.*, "DARWIN: towards the ultimate dark matter detector," *JCAP* **11** (2016) 017, arXiv:1606.07001 [astro-ph.IM].

[209] A. Alves, S. Profumo, and F. S. Queiroz, "The dark Z' portal: direct, indirect and collider searches," *JHEP* **04** (2014) 063, arXiv:1312.5281 [hep-ph].

[210] A. Alves, A. Berlin, S. Profumo, and F. S. Queiroz, "Dark Matter Complementarity and the Z′ Portal," *Phys. Rev. D* **92** no. 8, (2015) 083004, arXiv:1501.03490 [hep-ph].

[211] W. Wang and Z.-L. Han, "Radiative linear seesaw model, dark matter, and $U(1)_{B-L}$," *Phys. Rev. D* **92** (2015) 095001, arXiv:1508.00706 [hep-ph].

[212] A. Alves, A. Berlin, S. Profumo, and F. S. Queiroz, "Dirac-fermionic dark matter in $\mathrm{U}(1)_X$ models," *JHEP* **10** (2015) 076, arXiv:1506.06767 [hep-ph].

[213] T. Jacques, A. Katz, E. Morgante, D. Racco, M. Rameez, and A. Riotto, "Complementarity of DM searches in a consistent simplified model: the case of Z'," *JHEP* **10** (2016) 071, arXiv:1605.06513 [hep-ph]. [Erratum: JHEP 01, 127 (2019)].

[214] S. Okada, "Z' Portal Dark Matter in the Minimal $B-L$ Model," *Adv. High Energy Phys.* **2018** (2018) 5340935, arXiv:1803.06793 [hep-ph].

[215] R. K. Ellis *et al.*, "Physics Briefing Book: Input for the European Strategy for Particle Physics Update 2020," arXiv:1910.11775 [hep-ex].

[216] W. D. Goldberger, B. Grinstein, and W. Skiba, "Distinguishing the Higgs boson from the dilaton at the Large Hadron Collider," *Phys. Rev. Lett.* **100** (2008) 111802, arXiv:0708.1463 [hep-ph].

[217] Z. Chacko and R. K. Mishra, "Effective Theory of a Light Dilaton," *Phys. Rev. D* **87** no. 11, (2013) 115006, arXiv:1209.3022 [hep-ph].

[218] B. Bellazzini, C. Csaki, J. Hubisz, J. Serra, and J. Terning, "A Higgslike Dilaton," *Eur. Phys. J. C* **73** no. 2, (2013) 2333, arXiv:1209.3299 [hep-ph].

[219] A. Ahmed, B. M. Dillon, B. Grzadkowski, J. F. Gunion, and Y. Jiang, "Implications of the absence of high-mass radion signals," *Phys. Rev. D* **95** no. 9, (2017) 095019, arXiv:1512.05771 [hep-ph].

[220] A. Ahmed, A. Mariotti, and S. Najjari, "A light dilaton at the LHC," *JHEP* **05** (2020) 093, arXiv:1912.06645 [hep-ph].

[221] **ILD Concept Group** Collaboration, H. Abramowicz *et al.*, "International Large Detector: Interim Design Report," arXiv:2003.01116 [physics.ins-det].

[222] G. Ripellino, M. V. Voorde, A. Gallén, and R. Gonzalez Suarez, "Searching for long-lived dark scalars at the FCC-ee," arXiv:2412.10141 [hep-ex].

[223] B. Bhattacherjee, C. Bose, H. K. Dreiner, N. Ghosh, S. Matsumoto, and R. Sengupta, "Long-lived Light Mediators in a Higgs Portal Model at the FCC-ee," arXiv:2503.08780 [hep-ph].

[224] A. D. Linde, "Dynamical Symmetry Restoration and Constraints on Masses and Coupling Constants in Gauge Theories," *JETP Lett.* **23** (1976) 64–67.

[225] D. Litim, C. Wetterich, and N. Tetradis, "Nonperturbative analysis of the Coleman-Weinberg phase transition," *Mod. Phys. Lett. A* **12** (1997) 2287–2308, arXiv:hep-ph/9407267.

[226] R. Jinno and M. Takimoto, "Probing a classically conformal B-L model with gravitational waves," *Phys. Rev. D* **95** no. 1, (2017) 015020, arXiv:1604.05035 [hep-ph].

[227] S. Iso, P. D. Serpico, and K. Shimada, "QCD-Electroweak First-Order Phase Transition in a Supercooled Universe," *Phys. Rev. Lett.* **119** no. 14, (2017) 141301, arXiv:1704.04955 [hep-ph].

[228] C. Marzo, L. Marzola, and V. Vaskonen, "Phase transition and vacuum stability in the classically conformal B–L model," *Eur. Phys. J. C* **79** no. 7, (2019) 601, arXiv:1811.11169 [hep-ph].

[229] J. Ellis, M. Lewicki, and V. Vaskonen, "Updated predictions for gravitational waves produced in a strongly supercooled phase transition," *JCAP* **11** (2020) 020, arXiv:2007.15586 [astro-ph.CO].

[230] D. Schmitt and L. Sagunski, "QCD-sourced tachyonic phase transition in a supercooled Universe," arXiv:2409.05851 [hep-ph].

[231] J. Braun and H. Gies, "Chiral phase boundary of QCD at finite temperature," *JHEP* **06** (2006) 024, arXiv:hep-ph/0602226.

[232] F. Cuteri, O. Philipsen, and A. Sciarra, "On the order of the QCD chiral phase transition for different numbers of quark flavours," *JHEP* **11** (2021) 141, arXiv:2107.12739 [hep-lat].

[233] L. Marzola, A. Racioppi, and V. Vaskonen, "Phase transition and gravitational wave phenomenology of scalar conformal extensions of the Standard Model," *Eur. Phys. J. C* **77** no. 7, (2017) 484, arXiv:1704.01034 [hep-ph].

[234] T. Prokopec, J. Rezacek, and B. Świeżewska, "Gravitational waves from conformal symmetry breaking," *JCAP* **02** (2019) 009, arXiv:1809.11129 [hep-ph].

[235] A. Dasgupta, P. S. B. Dev, A. Ghoshal, and A. Mazumdar, "Gravitational wave pathway to testable leptogenesis," *Phys. Rev. D* **106** no. 7, (2022) 075027, arXiv:2206.07032 [hep-ph].

[236] P. Huang and K.-P. Xie, "Leptogenesis triggered by a first-order phase transition," *JHEP* **09** (2022) 052, arXiv:2206.04691 [hep-ph].

[237] L. Sagunski, P. Schicho, and D. Schmitt, "Supercool exit: Gravitational waves from QCD-triggered conformal symmetry breaking," *Phys. Rev. D* **107** no. 12, (2023) 123512, arXiv:2303.02450 [hep-ph].

[238] S. Kawai and N. Okada, "Reheating consistency condition on the classically conformal U(1)B–L Higgs inflation model," *Phys. Rev. D* **108** no. 1, (2023) 015013, arXiv:2303.00342 [hep-ph].

[239] J. Heeck, "Unbroken B − L symmetry," *Phys. Lett. B* **739** (2014) 256–262, arXiv:1408.6845 [hep-ph].

[240] K. N. Abazajian and J. Heeck, "Observing Dirac neutrinos in the cosmic microwave background," *Phys. Rev. D* **100** (2019) 075027, arXiv:1908.03286 [hep-ph].

[241] P. Adshead, P. Ralegankar, and J. Shelton, "Dark radiation constraints on portal interactions with hidden sectors," *JCAP* **09** (2022) 056, arXiv:2206.13530 [hep-ph].

[242] X. G. He, G. C. Joshi, H. Lew, and R. R. Volkas, "NEW Z-prime PHENOMENOLOGY," *Phys. Rev. D* **43** (1991) 22–24.

[243] S. Baek, N. G. Deshpande, X. G. He, and P. Ko, "Muon anomalous g-2 and gauged L(muon) - L(tau) models," *Phys. Rev. D* **64** (2001) 055006, arXiv:hep-ph/0104141.

[244] E. Ma, D. P. Roy, and S. Roy, "Gauged L(mu) - L(tau) with large muon anomalous magnetic moment and the bimaximal mixing of neutrinos," *Phys. Lett. B* **525** (2002) 101–106, arXiv:hep-ph/0110146.

[245] J. Heeck and W. Rodejohann, "Gauged $L_\mu - L_\tau$ Symmetry at the Electroweak Scale," *Phys. Rev. D* **84** (2011) 075007, arXiv:1107.5238 [hep-ph].

[246] W. Altmannshofer, S. Gori, M. Pospelov, and I. Yavin, "Neutrino Trident Production: A Powerful Probe of New Physics with Neutrino Beams," *Phys. Rev. Lett.* **113** (2014) 091801, arXiv:1406.2332 [hep-ph].

[247] W. Altmannshofer, M. Carena, and A. Crivellin, "$L_\mu - L_\tau$ theory of Higgs flavor violation and $(g-2)_\mu$," *Phys. Rev. D* **94** no. 9, (2016) 095026, arXiv:1604.08221 [hep-ph].

[248] J. C. Montero and V. Pleitez, "Gauging U(1) symmetries and the number of right-handed neutrinos," *Phys. Lett. B* **675** (2009) 64–68, arXiv:0706.0473 [hep-ph].

[249] E. Ma and R. Srivastava, "Dirac or inverse seesaw neutrino masses with $B - L$ gauge symmetry and S_3 flavor symmetry," *Phys. Lett. B* **741** (2015) 217–222, arXiv:1411.5042 [hep-ph].

[250] E. Ma, N. Pollard, R. Srivastava, and M. Zakeri, "Gauge $B - L$ Model with Residual Z_3 Symmetry," *Phys. Lett. B* **750** (2015) 135–138, arXiv:1507.03943 [hep-ph].

[251] C. Bonilla, S. Centelles-Chuliá, R. Cepedello, E. Peinado, and R. Srivastava, "Dark matter stability and Dirac neutrinos using only Standard Model symmetries," *Phys. Rev. D* **101** no. 3, (2020) 033011, arXiv:1812.01599 [hep-ph].

[252] W. Liu and K.-P. Xie, "Probing radiative electroweak symmetry breaking with colliders and gravitational waves," *Phys. Rev. D* **110** no. 11, (2024) 115001, arXiv:2408.03649 [hep-ph].

[253] G. Arcadi, F. Costa, A. Goudelis, and O. Lebedev, "Higgs portal dark matter freeze-in at stronger coupling: observational benchmarks," *JHEP* **07** (2024) 044, arXiv:2405.03760 [hep-ph].

[254] J. C. Pati and A. Salam, "Lepton Number as the Fourth Color," *Phys. Rev. D* **10** (1974) 275–289. [Erratum: Phys.Rev.D 11, 703–703 (1975)].

[255] S. Iso, N. Okada, and Y. Orikasa, "Resonant Leptogenesis in the Minimal B-L Extended Standard Model at TeV," *Phys. Rev. D* **83** (2011) 093011, arXiv:1011.4769 [hep-ph].

[256] V. V. Khoze and G. Ro, "Leptogenesis and Neutrino Oscillations in the Classically Conformal Standard Model with the Higgs Portal," *JHEP* **10** (2013) 075, arXiv:1307.3764 [hep-ph].

[257] A. Azatov, M. Vanvlasselaer, and W. Yin, "Baryogenesis via relativistic bubble walls," *JHEP* **10** (2021) 043, arXiv:2106.14913 [hep-ph].

[258] I. Baldes, S. Blasi, A. Mariotti, A. Sevrin, and K. Turbang, "Baryogenesis via relativistic bubble expansion," *Phys. Rev. D* **104** no. 11, (2021) 115029, arXiv:2106.15602 [hep-ph].

[259] A. Das and Y. Orikasa, "Resonant leptogenesis in minimal $U(1)_X$ extensions of the Standard Model," arXiv:2407.05644 [hep-ph].

[260] G. Chauhan, "Collider Tests of Flavored Resonant Leptogenesis in the $U(1)_X$ Model," arXiv:2407.09460 [hep-ph].

[261] T. Hambye, A. Strumia, and D. Teresi, "Super-cool Dark Matter," *JHEP* **08** (2018) 188, arXiv:1805.01473 [hep-ph].

[262] N. Okada and Q. Shafi, "Observable Gravity Waves From U(1)$\_B - L$ Higgs and Coleman-Weinberg Inflation," arXiv:1311.0921 [hep-ph].

[263] S. Oda, N. Okada, D. Raut, and D.-s. Takahashi, "Nonminimal quartic inflation in classically conformal U(1)$_X$ extended standard model," *Phys. Rev. D* **97** no. 5, (2018) 055001, arXiv:1711.09850 [hep-ph].

[264] P. Olver, *Applications of Lie Groups to Differential Equations*. Graduate Texts in Mathematics.

[265] F. Feruglio, C. Hagedorn, and R. Ziegler, "Lepton Mixing Parameters from Discrete and CP Symmetries," *JHEP* **07** (2013) 027, arXiv:1211.5560 [hep-ph].

[266] J. S. R. Chisholm, "Change of variables in quantum field theories," *Nucl. Phys.* **26** no. 3, (1961) 469–479.

[267] S. Kamefuchi, L. O'Raifeartaigh, and A. Salam, "Change of variables and equivalence theorems in quantum field theories," *Nucl. Phys.* **28** (1961) 529–549.

[268] A. V. Manohar, "Introduction to Effective Field Theories," arXiv:1804.05863 [hep-ph].

[269] I. P. Ivanov, "Two-Higgs-doublet model from the group-theoretic perspective," *Phys. Lett. B* **632** (2006) 360–365, arXiv:hep-ph/0507132.

[270] A. V. Bednyakov, "On three-loop RGE for the Higgs sector of 2HDM," *JHEP* **11** (2018) 154, arXiv:1809.04527 [hep-ph].

[271] A. V. Bednyakov, "On the scalar sector of 2HDM: ring of basis invariants, syzygies, and six-loop renormalization-group equations," arXiv:2501.14087 [hep-ph].

[272] A. Bednyakov and A. Pikelner, "Six-loop beta functions in general scalar theory," *JHEP* **04** (2021) 233, arXiv:2102.12832 [hep-ph].